

Electronic Thesis and Dissertation Repository

4-18-2019 3:00 PM

Growth Characteristics and Lipid Metabolism of Cultured Migratory Bird Skeletal Muscle Cells

Kevin G. Young, *The University of Western Ontario*

Supervisor: Guglielmo, Christopher G., *The University of Western Ontario*

Co-Supervisor: Regnault, Timothy RH, *The University of Western Ontario*

A thesis submitted in partial fulfillment of the requirements for the Master of Science degree in Biology

© Kevin G. Young 2019

Follow this and additional works at: <https://ir.lib.uwo.ca/etd>



Part of the [Comparative and Evolutionary Physiology Commons](#)

Recommended Citation

Young, Kevin G., "Growth Characteristics and Lipid Metabolism of Cultured Migratory Bird Skeletal Muscle Cells" (2019). *Electronic Thesis and Dissertation Repository*. 6154.

<https://ir.lib.uwo.ca/etd/6154>

This Dissertation/Thesis is brought to you for free and open access by Scholarship@Western. It has been accepted for inclusion in Electronic Thesis and Dissertation Repository by an authorized administrator of Scholarship@Western. For more information, please contact wlsadmin@uwo.ca.

Abstract

Diets rich in n-3 polyunsaturated fatty acids (PUFA) may alter the muscle metabolism of migratory birds, improving their endurance performance. I established and validated for the first time *in vitro* muscle models of a migratory songbird (yellow-rumped warbler, *Setophaga coronata coronata*) and shorebird (sanderling, *Calidris alba*). To evaluate the role of n-3 PUFA in improving fatty acid metabolism in migratory bird muscle, I measured metabolic outcomes following n-3 PUFA supplementation in these two avian cell types and a murine (*Mus musculus*, C₂C₁₂) cell line. PUFA supplementation in C₂C₁₂ cells increased metabolic transcription factor expression and increased mitochondrial respiratory chain efficiency. Migrant bird muscle cells did not display the same changes in transcriptional signaling, but sanderling cells increased basal and maximal oxygen consumption with n-3 PUFA supplementation. This research provides support for the hypothesis that n-3 PUFA increase aerobic capacity of a migrant sandpiper and efficiency in mammalian skeletal muscle.

Keywords

Migration, avian, cell culture, satellite cell, lipid metabolism, muscle metabolism, polyunsaturated fatty acid

Co-Authorship Statement

I conducted this study under the supervision of Dr. Christopher Guglielmo and Dr. Timothy Regnault. The primary cell culture isolation procedures were developed with the help of Dr. Christina Vanderboor. Dr. Vanderboor provided additional support optimizing fluorescent immunocytochemistry and flow cytometry preparations. I conducted all of the experiments, collected and analyzed all data and wrote this thesis. Dr. Guglielmo and Dr. Regnault assisted with experimental design, data analysis and interpretation and editing of this thesis. I will publish this thesis with Drs. Vanderboor, Regnault and Guglielmo.

Acknowledgments

While every graduate student needs the support of their supervisors, I feel that my project and successes would not have been possible without the perfect storm of vision and support from my supervisors Dr. Christopher Guglielmo and Dr. Timothy Regnault. Their combined perspectives and mentorship afforded me ample room to explore research topics while leading me to success and growth as a student. Chris has always provided me with the clarity of his perspective and a constant sense of excitement about the work and results which has kept me motivated and excited about research throughout the process. Chris' receptiveness to my ideas has helped me learn the value of confidence and stubbornness in my work.

I am incredibly grateful to Tim for allowing me the opportunity to work with him and his lab. Tim maintained confidence in my abilities from the beginning despite my protests and has made me feel welcome in his research group in the DDT lab. Tim has taught me to think more critically, to question my work and others' and to maintain my style throughout the process. I very much appreciate Tim's integrative approach to research and feel very lucky to be a beneficiary of his openness and enthusiasm for collaboration.

Dr. Christina Vanderboor provided me with critical professional and personal support throughout my work in the lab and I am very grateful for all her help. Throughout my time in the lab, Christie offered me patient guidance and a healthy outlook on the trials of grad school. Christie's vast expertise motivates me to improve myself in all aspects of life and I hope to continue learning from her in the future.

I want to thank my advisors, Dr. Brent Sinclair and Dr. Sashko Damjanovski for their invaluable feedback and advice throughout the research process. My experience at Western has taught me that the more eyes and minds contributing to the research, the better the result will be, and I thank them for their contributions to help me as a student and my work.

I am very grateful for the diverse research communities I have been lucky enough to be a part of at Western. I want to thank all the staff and my fellow students in the Department

of Biology for their solidarity and support. I would also like to thank my colleagues in the P&B stream for their support, critiques and interest that has inspired me and given me confidence. I would also like to thank all of the staff and students at AFAR for their encouragement. I am very thankful to everyone there and especially those who have supported me with bird care, chatted with me about science, and for teaching me about how ‘smart’ birds are. My fellow Gug lab mates have been an incredible support. I am very thankful for their feedback on my presentations, writing, ideas, and for fostering a culture of positivity that allows us all to progress towards our goals. I would also like to thank all members of the Regnault and DDT lab that I have been lucky enough to work alongside. I have learned a tremendous amount and gained skills I didn’t know were possible in the lab from them all and I have thoroughly enjoyed our time working together.

I would finally like to thank the Department of Biology, NSERC, and the Ontario graduate scholarship program for their funding and support of this research.

Table of Contents

Abstract.....	ii
Co-Authorship Statement.....	iii
Acknowledgments.....	iv
Table of Contents.....	vi
List of Tables.....	ix
List of Figures.....	x
List of Appendices.....	xii
List of Abbreviations.....	xiii
1 Introduction.....	1
1.1 Bird Migration.....	3
1.1.1 Physiological Adaptations for Endurance Flight.....	4
1.2 Dietary Fatty Acids.....	11
1.2.1 Polyunsaturated Fatty Acids.....	12
1.3 Experimental Models.....	15
1.3.1 Mouse (<i>Mus musculus</i>) - C ₂ C ₁₂ cell line.....	15
1.3.2 Yellow-rumped Warbler (<i>Setophaga coronata coronata</i>).....	15
1.3.3 Sanderling (<i>Calidris alba</i>).....	16
1.4 Muscle Cell Culture.....	17
1.5 Thesis Objectives.....	18
2 Methods.....	19
2.1 Study Birds.....	19
2.2 Primary Culture of Adult Avian Satellite Cells.....	19
2.3 Cell Culture.....	21
2.3.1 C ₂ C ₁₂ Murine Myoblasts.....	21

2.3.2	Avian Satellite Cells	21
2.4	Cell Counting.....	22
2.5	Immunocytochemistry	23
2.6	Fatty Acid Treatments.....	24
2.7	RT-qPCR.....	24
2.8	Enzyme Assays	27
2.9	Aerobic Profile Assays	30
2.10	Statistical Analysis.....	34
3	Results	35
3.1	Primary Muscle Cell Culture Characteristics	35
3.1.1	Proliferation Rate of Adult Avian Satellite Cells	37
3.1.2	Muscle-specific Protein Expression.....	40
3.2	Responses to PUFA Supplementation	46
3.2.1	Expression of PPARs and Fatty Acid Transporters	46
3.2.2	Enzyme Activities.....	50
3.2.3	Aerobic Profile.....	53
4	Discussion	57
4.1	Avian Myocyte Characteristics <i>in vitro</i>	57
4.2	Comparative Influence of n-3 PUFA on Muscle Cell Metabolism	60
4.2.1	The Differential Effects of n-3 PUFAs on mRNA Expression.....	62
4.2.2	Effects of n-3 PUFA on Metabolic Enzyme Activities	64
4.2.3	Effects of n-3 PUFA on the Aerobic Profiles of Sanderling and C ₂ C ₁₂ (Mouse) Muscle Cells.....	66
4.3	Implications and Future Directions.....	71
4.4	Conclusions.....	73
	References.....	75

Appendices.....	87
Appendix A.....	87
Appendix B.....	94
Appendix C.....	97
Curriculum Vitae.....	98

List of Tables

Table 1. mRNA targets, the associated primer sequences and annealing temperatures used for RT-qPCR.....	26
Table 2. Volumes and dilutions used during kinetic enzyme activity assays for C ₂ C ₁₂ , yellow-rumped warbler, and sanderling myotubes (ndil = not diluted).....	29
Table 3. Definitions and equations of OCR (oxygen consumption rate) ratio-based measurements of cellular aerobic profiles using a Seahorse XFe24 Analyzer.....	33

List of Figures

Figure 1. Summary of fatty acid transport and oxidation pathway adapted from McWilliams et al. 2004.....	8
Figure 2. Example of an individual OCR (oxygen consumption rate) trace produced by the XF24e Seahorse	32
Figure 3. Phase contrast microscope images of yellow-rumped warbler (left) and sanderling (right) satellite cells (top row) and differentiated myotubes (middle and bottom rows).	36
Figure 4. Growth curves of sanderling (gray; SAND) and yellow-rumped warbler (black; YRWA) satellite cells counted using a hemocytometer.	38
Figure 5. Total number of sanderling (top, n = 3; SAND) and yellow-rumped warbler (bottom, n = 5; YRWA) satellite cells at specified timepoints with or without basic fibroblast growth factor (bFGF).....	39
Figure 6. Representative images of yellow-rumped warbler satellite cells expressing Pax7 prior to, 3 and 6 days following differentiation into myotubes.	41
Figure 7. Representative images of sanderling satellite cells expressing Pax7 prior to, 3 and 6 days following differentiation into myotubes.	42
Figure 8. Representative images of yellow-rumped warbler satellite cells expressing myosin prior to, 3 and 6 days following differentiation into myotubes.....	43
Figure 9. Representative images of sanderling satellite cells expressing myosin prior to, 3 and 6 days following differentiation into myotubes	44
Figure 10. Representative images of yellow-rumped warbler satellite cells expressing desmin 3 days after differentiation into myotubes.....	45

Figure 11. Representative images of sanderling satellite cells expressing desmin 3 days after differentiation into myotubes.....	45
Figure 12. Relative expression of PPARs in C ₂ C ₁₂ (mouse), yellow-rumped warbler and sanderling myotubes supplemented with carrier (BSA), oleic acid (OA), eicosapentaenoic acid (EPA) or docosahexaenoic acid (DHA).....	47
Figure 13. Relative expression of <i>CD36</i> (A-C) and <i>FABP3</i> (D-F) in C ₂ C ₁₂ (mouse), yellow-rumped warbler and sanderling myotubes supplemented with carrier (BSA), oleic acid (OA), eicosapentaenoic acid (EPA) or docosahexaenoic acid (DHA).....	49
Figure 14. Maximum activity of citrate synthase (CS) in mU/mg protein (A-C) and lactate dehydrogenase (LDH) in U/mg protein (D-F) from C ₂ C ₁₂ (mouse), yellow-rumped warbler and sanderling myotubes supplemented with carrier (BSA), oleic acid (OA), eicosapentaenoic acid (EPA) or docosahexaenoic acid (DHA).....	51
Figure 15. Maximum activity of β -hydroxyacyl-CoA dehydrogenase (HOAD) (A-C) and carnitine palmitoyltransferase (CPT) in mU/mg protein (D-F) from C ₂ C ₁₂ (mouse), yellow-rumped warbler and sanderling myotubes supplemented with carrier (BSA), oleic acid (OA), eicosapentaenoic acid (EPA) or docosahexaenoic acid (DHA).....	52
Figure 16. Oxygen consumption rate (OCR) proportions of C ₂ C ₁₂ (mouse) and sanderling myotubes measured during a modified mito-stress test using an XFe24 Seahorse following treatment with fatty acids: oleic acid (OA), eicosapentaenoic acid (EPA), docosahexaenoic acid (DHA) or carrier alone (BSA).	54
Figure 17. Oxygen consumption rate (OCR) fold changes of C ₂ C ₁₂ (mouse) and sanderling myotubes measured during a modified mito-stress test using an XFe24 Seahorse following treatment with fatty acids: oleic acid (OA), eicosapentaenoic acid (EPA), docosahexaenoic acid (DHA) or carrier alone (BSA).	56
Figure 18. Summary of the effects of n-3 PUFA supplementation on C ₂ C ₁₂ (mouse) and sanderling muscle cells.	61

List of Appendices

Appendix A. Summary of H-FABP knockdown experiments in yellow-rumped warbler and C ₂ C ₁₂ myotubes.....	87
Appendix B. Environment and Climate Change Canada scientific capture permits issued to Dr. Christopher Guglielmo and Dr. Christy Morrisey.....	94
Appendix C. University of Western Ontario, Animal Use and Care Committee protocol approval letter. Protocol 2010-020 issued to Dr. Christopher Guglielmo.	97

List of Abbreviations

<i>ACTB</i>	Beta-actin
AHY	After hatch-year
Alb	Albumin
ATCC	American type culture collection
ATP	Adenosine triphosphate
ATPase	ATP synthase
BCA	Bicinchonic acid
bFGF	Basic fibroblast growth factor
BSA	Bovine serum albumin
CD36	Cluster of differentiation 36
cDNA	Complimentary DNA
CPT	Carnitine palmitoyl transferase
CS	Citrate synthase
Ct	Cycle threshold
DAPI	4',6-diamidino-2-phenylindole
DEPC	Diethyl pyrocarbonate
DHA	Docosahexaenoic acid
DMEM	Dulbecco's modified Eagle media
DMSO	Dimethyl sulfoxide
DNP	2,4-Dinitrophenol
DNTB	5,5'-dithiobis-(2-nitrobenzoic acid) or Ellman's reagent
EDTA	Ethylenediaminetetraacetic acid
EPA	Eicosapentaenoic acid
ETC	Electron transport chain
FA	Fatty acid
<i>FABP3</i>	Fatty acid binding protein 3 (transcribes H-FABP)
FABPpm	Plasma membrane fatty acid binding protein
<i>GAPDH</i>	Glyceraldehyde 3-phosphate dehydrogenase

HBSS	Hanks' balanced salt solution
HEPES	4-(2-hydroxyethyl)-1-piperazineethanesulfonic acid
H-FABP	Heart-type fatty acid binding protein
HOAD	β -hydroxyacyl-CoA dehydrogenase
HY	Hatch-year
LDH	Lactate dehydrogenase
mRNA	Messenger RNA
MUFA	Monounsaturated fatty acid
NAD ⁺	Nicotinamide adenine dinucleotide
NADH	Nicotinamide adenine dinucleotide, reduced
OA	Oleic acid
OCR	Oxygen consumption rate
Pax7	Paired box protein 7
PBS	Phosphate buffered saline
PCR	Polymerase chain reaction
PMR	Peak metabolic rate
PPAR	Peroxisome proliferator-activated receptor
<i>PPIB</i>	Peptidyl-prolyl cis-trans isomerase B
PPRE	Peroxisome proliferator response element
PUFA	Polyunsaturated fatty acid
ROS	Reactive oxygen species
RXR	Retinoid X receptor
TAG	Triacylglycerol
TNB	2-nitro-5-chlorobenzaldehyde
UCP	Uncoupling protein
VLDL	Very low density lipoprotein

1 Introduction

Spatial and temporal variation of resources drives the evolution of migration in many different taxa across the Earth. Migration is a unique category of movement in which organisms engage in directed movement to capitalize on available resources or escape resource scarcity allowing them to occupy a broader range of habitats/niches than are available to more sedentary life history strategies (Shaw, 2016). Migrations are triggered by surrogate cues that indicate coming resource scarcity, involve specialized behaviour at departure and arrival, contain persistent locomotion and straightened out pathways, inhibit typical responses to resources during movement and are associated with changes in resource and energy allocation to support migratory movement (Dingle, 2014). Animal migrations span as little distance as a few hundred meters as in the case of the black-and-red-bug (*Lygaeus equestris*) or can be tens of thousands of kilometers including the migrations undertaken by many neotropical migrant birds (Dingle, 2014). Furthermore, in some species, individuals may complete many migration events in a lifetime, whereas in others a complete migratory journey may require multiple generations (Holland et al., 2006). These diverse migratory strategies are all driven by variation in resource availability. Consequently, the basic principles driving the seasonal migration of caribou (*Rangifer tarandus*) from the boreal forest to the Arctic tundra are similar to those inciting the multigenerational journey of Monarch butterflies (*Danaus plexippus*) across North and South America (Dingle, 2014). Regardless of their physical distance or strategy, migrations contain significant costs in terms of time, energy, and mortality risk to the organisms that undertake them. The risks associated with migratory movements are mitigated in part by substantial preparations, and the onset of this preparatory stage represents the beginning of migration.

The preparatory stage of migration is critical because of the significant energetic cost associated with undertaking a migratory journey. Different species cope with the costs of migration in slightly different ways. However, there are parallels among species in their strategies. Perhaps one of the most apparent ways an animal may prepare is by changing its morphology to better suit locomotion for migration. Animals undergo

varying degrees of body remodelling to successfully migrate (Dingle, 2014; McGuire et al., 2013; Piersma, 1998). In the case of some insects, the instar in which they migrate may be the only phase of life during which they have wings and can fly (Dingle and Winchell, 1997). In shorebirds, a common strategy involves reducing the size of the digestive system, permitting more space for fuel storage and reduced metabolic demand from digestive tissue (Dietz and Piersma, 2007; Landys-Ciannelli et al., 2003). These adaptations are centered around changing locomotory ability which improves migratory efficiency. However, enhanced movement capabilities intuitively also require improved locomotory muscle endurance. Migratory birds, for example, exhibit increased locomotory muscle mass and expression of molecular machinery involved in oxidative metabolism during the migratory period (McFarlan et al., 2009; Zhang et al., 2015). In concert with changes to locomotion ability, migrants must also prepare to fuel their travel. Fuel loading also contributes to significant body remodelling as these energy stores comprise an increased proportion of body mass during migration (Guglielmo, 2018).

One hallmark of an organism in the first stage of its migration is the hyperphagia associated with its expected energetic demands (Ramenofsky and Wingfield, 2006). The majority of migrants also increase fat deposition because fat is the ideal fuel for migration (Dingle, 2014). To briefly consider the alternatives, carbohydrates provide valuable “fast” fuel and represent a principal fuel source for short periods of activity while proteins are a secondary source of energy in all states of activity (Weber, 2011). However, neither carbohydrates or proteins are efficiently stored in the body for migration because they are necessarily associated with water, increasing storage mass significantly. By weight, fat is the preferred fuel given that wet carbohydrates contain only four kJ, protein only five kJ, whereas fat provides 38 kJ per gram (Jenni and Jenni-Eiermann, 1998).

Among vertebrates, birds are fat burning champions and migrants are especially recognized for their ability to use fat as fuel during extended flight (Guglielmo, 2018). Whether specific fats provide an advantage to migrants is currently debated. In my thesis, I investigate characteristics of muscle physiology from migrant birds as they relate to

muscle growth during migration and use a comparative approach to assess the effects of n-3 polyunsaturated fatty acid supplementation in mammalian and migrant bird skeletal muscle metabolism. To complete these studies, I establish an *in vitro* skeletal muscle model from the muscle of migrant birds. Bird migration physiology is an important topic for my thesis, and I describe its primary considerations as they relate to my research herein.

1.1 Bird Migration

In North America, many birds complete poleward and equatorward migrations as they fly from their southern wintering grounds to their northern breeding habitats in the spring and returning in the fall. The total distance individuals migrate varies among species from a few hundred to thousands of kilometers (Dingle, 2014). Despite most species being diurnal for most of the year, many birds become nocturnal during migration (Alerstam, 2009; Komal et al., 2017). Nocturnal migrants remain active during the day as they refuel at stopover sites for multiple days before departing in the evening. Even short distance migrants complete their migrations as a series of flights punctuated by these stopovers. A consequence of this stop-and-go strategy is that the majority of a bird's total time and energy during migration is spent at these sites (Wikelski et al., 2003). Extended stopovers are necessary because birds need to refuel before continuing their next bout of flight, given the high acute energetic cost of flying.

The per-unit distance energy cost of flying is intermediate to terrestrial (cursorial) and aquatic (swimming) locomotion (Schmidt-Nielsen, 1972). However, flying provides the advantage of greater speed over the absolute 'fuel range' benefit of swimming, which is a key consideration given the long distances some migrants must cover in a relatively short period. Flapping flight, relative to soaring, is most advantageous for small birds (<1kg) allowing them to fly faster, at lower cost, and with smaller body size conferring a reduction in the time required for refueling at stopover (Hedenström, 2003). However, flight—especially flapping flight—is acutely energetically demanding; metabolic rates of birds during flapping flight are elevated to roughly twice that of similar-sized running mammals (Butler, 1991).

Birds have many adaptations allowing them to fly, from the obvious (i.e. feathers and wings) to the less-easily-observed (i.e. large flight muscles, reduced genome size, efficient pulmonary system) (Kapusta et al., 2017; Vágási et al., 2016). These adaptations are common to flying birds, but migratory birds are distinct because they fly for extended durations. Flapping flight does not have a low energy cost alternative, as running does to walking, which results in flapping migrants exercising at extremely high rates for the duration of their flights. The energetic challenges associated with bird migration including the acute costs of flying, when extended over multi-hour or multi-day flights and long stopovers for refueling, necessitate adaptations specific to migratory birds.

1.1.1 Physiological Adaptations for Endurance Flight

Birds change the sizes of organs and muscle tissue during different phases of migration to cope with the energetic demands of the journey (Jehl, 1997; Landys-Ciannelli et al., 2003; Lindström et al., 2000; Piersma et al., 2002). Organ system remodelling corresponds with the pattern of intermittent feeding/refueling and flight during migration with birds increasing mass of energy storage systems (stomach, intestines, liver) early during refueling and decreasing before flight (Landys-Ciannelli et al., 2003; Piersma et al., 2002). These mass changes coincide with increases in overall body mass during the migratory period, contributed to primarily by increases in adipose tissue and flight muscle (King et al., 2015; Price et al., 2011a). However, gains in flight muscle mass are independent of increased activity or exercise during the migratory period (Gaunt et al., 1990; Hawkes et al., 2017; Lindström et al., 2000; Price et al., 2011a).

Skeletal muscle growth in adult animals occurs by hypertrophy: the increase in the size of individual muscle cells. During hypertrophy, myogenic precursor ‘satellite’ cells contribute to muscle growth by mitotic division and fusing to existing myocytes, contributing additional nuclei and volume (Rehfeldt, 2007; Tajbakhsh, 2009; Yoseph and Soker, 2015). Additionally, because training is necessary for inducing hypertrophy, it has been suggested that wild animals engage in exercise to some degree to maintain or improve skeletal muscle condition (Halsey, 2016). Wild mice provided the opportunity to run on a wheel voluntarily engage in this exercise activity (Meijer and Robbers, 2014). Migratory birds exhibit hypertrophy similar to mammals but achieve muscle growth

without training (Dietz et al., 1999; Evans et al., 1992; Hawkes et al., 2017; Marsh, 1984; Price et al., 2011a). Indeed, migratory birds are sometimes referred to as couch potato athletes for their ability to complete endurance flights apparently without exercise training.

Bar-headed geese (*Anser indicus*) are an excellent example of a migratory bird that does not appear to require exercise training. This species is a long-distance and high-altitude migrant that flies over the Tibetan Plateau without changing daily activity before flight (Hawkes et al., 2017). Bar-headed geese fly only a few minutes per day before taking off for their multi-day journey. Similarly, captive white-throated sparrows (*Zonotrichia albicollis*) stimulated to enter a migratory condition by lengthening daylight hours increase pectoral muscle mass coincident with muscle growth associated growth factors without any exercise training (Price et al., 2011a).

The muscle growth rate of some migrants provide dramatic illustrations of the adaptations associated with endurance flights. Migrant red knots (*Calidris canutus islandica*) preparing for long distance flights from Iceland gained pectoral muscle mass at a rate of 1.7% per day from starting mass over the course of a week (Piersma et al., 2002). This rate of muscle growth is in stark contrast to the 0.2% per day growth in muscle volume in human subjects during a resistance exercise regime (Seynnes et al., 2006). These studies demonstrate the ability of migrants to rapidly gain mass prior to a long flight and in the apparent absence of training.

During flight, long-distance migrants catabolize significant amounts of lean mass, including flight muscle, in addition to their fat stores (Dietz and Piersma, 2007). Lean mass catabolism contributes ~10-15% of the energy required for flight in migrants (Jenni and Jenni-Eiermann, 1998). This fuel source likely contributes to the physiological homeostasis of individuals during flight in several ways. In low humidity conditions, birds catabolize a greater proportion of lean mass to free the water bound by proteins (Gerson and Guglielmo, 2011). Catabolizing proteins also generates intermediate molecules required for the Krebs cycle (Jenni and Jenni-Eiermann, 1998). Furthermore, as long-duration flights progress and stored fuel is consumed, the weight lost in stored

energy by respiration alleviates the physical weight load during flight reducing the power required to continue flying. This type of body remodeling results in the reduction of organ and skeletal muscle mass by the end of a long flight (Battley et al., 2000; Bauchinger et al., 2005; Piersma, 1998).

However, most of the energy birds use during flight is in the form of stored fat. Like migrants from other taxa, birds store and catabolize fat to fuel their migratory movements (Dingle, 2014). The majority of fat is stored in discrete subcutaneous deposits visible beneath their translucent skin, including the large furcular hollow (Deppe et al., 2015). The ability of birds to mobilize and catabolize extracellular fat stores at rates that can meet the energetic demands of muscles during flight is of interest to physiologists given our understanding of metabolic fuel use in mammals. The relationship between fuel use and exercise intensity in mammals is well studied and intuitive for anyone who has sprinted and walked before (McClelland, 2004). With increasing exercise intensity, mammals use a greater proportion of carbohydrates for fuel and are increasingly anaerobic. Conversely, with decreasing exercise intensity, a greater proportion of fats contribute to energy production and animals metabolize fuel more aerobically (McClelland, 2004). This relationship does not account for birds engaging in extended flapping flight, which are estimated to meet 90% of their energetic demands using circulating fats while exercising at estimated 70-90% of the maximal aerobic capacity (Guglielmo et al., 2002a; Jenni and Jenni-Eiermann, 1998). Considering these components of bird migration together: the acute metabolic demand of flight, the macronutrients used to fuel it, and the endurance component of migrations leads to the question of how these birds can use fat to fuel high intensity aerobic activity while running mammals cannot (Guglielmo, 2010; Guglielmo, 2018).

The shared evolutionary history of birds and mammals suggest that these taxa did not innovate new biochemical processes to overcome migration but instead that they have optimized existing processes to fit their life histories (Hochachka and Somero, 1984). During activity, fatty acids (FA) stored as triacylglycerol (TAG) in adipocytes are hydrolyzed and enter circulation as FA bound to albumin. Circulating FA are then transported to and taken up at the muscle or delivered to the liver where they are

incorporated back into TAG in very low density lipoproteins (VLDL) and re-enter circulation. Fatty acids are transported into myocytes by membrane-bound transporters (CD36, FABPpm) and are transferred to the heart-type fatty acid binding protein (H-FABP). Fatty acids are then transported to mitochondria where they are transported across both mitochondrial membranes as acyl-carnitines by carnitine palmitoyl-transferases (CPT). After reconversion to acyl-CoAs within the mitochondrial matrix fatty acids can then enter the β -oxidation pathway reducing them to acetyl-CoA which can then enter the Krebs cycle and complete the process of ATP production in the electron transport chain (ETC) (McClelland, 2004; McWilliams et al., 2004; Figure 1). This system that transports fatty acids across membranes, in circulation, and in the cytosol is entirely protein-mediated and thus costly to maintain.

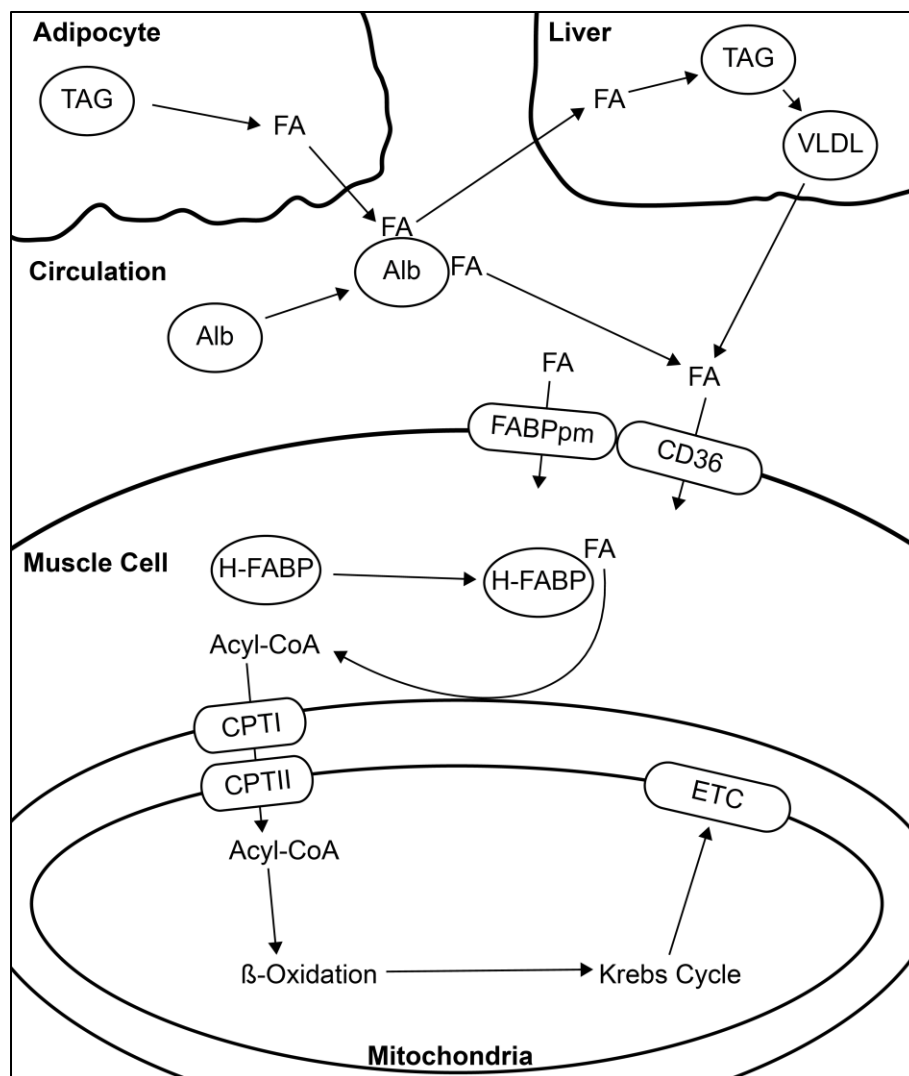


Figure 1. Summary of fatty acid transport and oxidation pathway adapted from McWilliams et al. 2004. Fatty acids (FA) stored in adipocytes as triacylglycerol (TAG) are hydrolyzed and enter circulation bound to albumin (Alb). Circulating FAs transported to the liver are converted into TAG and re-enter circulation as very low density lipoproteins (VLDL). Circulating FA and VLDL converted to FA are transported into muscle cells through membrane-bound transporters CD36 and FABPpm and bound intracellularly by the heart-type fatty acid binding protein (H-FABP). FAs converted to acyl-CoAs are transported into mitochondria by carnitine palmitoyl transferases (CPT) where β -oxidation converts acyl-CoAs to acetyl-CoAs which enter the Krebs cycle and contribute to ATP production in the electron transport chain (ETC).

Migratory birds increase the expression of fat transporting proteins and enzymes involved in FA metabolism during migration (Guglielmo, 2010; Guglielmo, 2018; McFarlan et al., 2009; Zajac et al., 2011). Birds incur the energetic costs associated with expressing these extra proteins during this period and it likely contributes to energy expenditure throughout the migratory period. The enlarged livers of birds during the preparatory stages of migration may synthesize lipoproteins at high rates in addition to the FA released from adipose stores in order to maintain ample fats in circulation (Guglielmo, 2018). Expression of fat transporters in muscle increases dramatically during migration, especially H-FABP which increases 70% in migrant western sandpipers (*Calidris mauri*) until it comprises ~13% of total cytosolic protein (Guglielmo et al., 2002a). The increased capacity for mobilizing FA coincides with changes in the expression of metabolic enzymes to support increased flight capacity. The activity of CPT increases in the muscle of birds during migration (Banerjee and Chaturvedi, 2016; Driedzic et al., 1993; Guglielmo et al., 2002a; McFarlan et al., 2009; Zajac et al., 2011). The activity of other enzymes involved in aerobic metabolism and FA oxidation also increases. Specifically, citrate synthase (CS), the first enzyme in the Krebs cycle, and β -hydroxyacyl-CoA dehydrogenase (HOAD), which catalyzes the third step in β -oxidation, increase in activity in the muscle of migrants, likely to support the aerobic demands of extended flight (Banerjee and Chaturvedi, 2016; McFarlan et al., 2009; Zajac et al., 2011). Conversely, lactate dehydrogenase (LDH), which catalyzes the interconversion of pyruvate and lactate, exhibits decreased activity during the migratory period indicating that birds decrease their reliance on anaerobic metabolism (Banerjee and Chaturvedi, 2016; McFarlan et al., 2009; Zajac et al., 2011). The upregulation of molecular machinery that promotes high rates of lipid metabolism in birds during migration highlights the focal role that fats play in the migratory strategy of birds.

The seasonal migratory phenotype in birds is also characterized in part by increased adiposity and rapid catabolism of those same adipose stores. These conflicting metabolic outcomes have motivated studies on the regulation of lipid metabolism in migrants with growing interest in the role of peroxisome proliferator-activated receptors (PPARs) (Dick and Guglielmo, 2019; Guglielmo, 2018; Hamilton et al., 2018; Nagahuedi et al., 2009). PPARs are a group of three distinct nuclear receptor transcription factors:

PPAR- α , PPAR- β (or PPAR- δ), and PPAR- γ . These transcription factors play a critical role in the regulation of lipid metabolism and whole animal energy homeostasis (Poulsen et al., 2012). PPARs function by coactivation with retinoid X receptor (RXR) and activating ligands to bind peroxisome proliferator response elements (PPREs) in the promoter regions of target genes (Berger and Moller, 2002). FAs are natural ligands of PPARs and promote binding to PPREs. PPARs are widely studied, with each member of the family having distinct but overlapping expression patterns across cell types and roles in regulating metabolism and energy homeostasis (Poulsen et al., 2012). PPAR- α is abundant in highly metabolic tissues including skeletal muscle and plays a central role in the regulation of lipid metabolism. PPAR- α drives the upregulation of lipid transport and oxidation in muscle with the concomitant downregulation of carbohydrate metabolism (Hamilton et al., 2018; Han et al., 2017a). PPAR- β is more ubiquitously expressed across tissues and its expression can be induced by exercise in skeletal muscle (Russell et al., 2005). PPAR- β also plays a focal role in regulating lipid metabolism in skeletal muscle, upregulating genes involved in lipid catabolism and transport (Holst et al., 2003). Unlike PPAR- α , PPAR- β concomitantly upregulates carbohydrate metabolism, resulting in increased glycogen stores, enhanced transport of carbohydrates and pyruvate oxidation (Gan et al., 2011; Han et al., 2017b). PPAR- γ is well-studied for its role in regulating whole animal energy homeostasis by adipocytes (Janani and Ranjitha Kumari, 2015). In skeletal muscle, PPAR- γ plays a role in regulating intracellular fat storage and energy expenditure (Han et al., 2017b).

PPARs change in their relative expression in various tissues with the migratory phenotype. Migrant gray catbirds (*Dumetella carolinensis*) increase expression of PPAR- α and γ in liver tissue implicating their role in regulating adiposity and lipid catabolism in migrants (Corder et al., 2016). Yellow-rumped warblers (*Setophaga coronata coronata*) also upregulate expression of PPAR- β during flight in their pectoral muscles (Dick and Guglielmo, 2019). These studies implicate PPARs in the upregulated fat transport and oxidation pathways in the migratory phenotype. Consequently, the upstream regulation of FA metabolism by PPARs is of interest when examining the migratory phenotype.

1.2 Dietary Fatty Acids

Diet composition is an effector of metabolic phenotypes and dysregulation. Because of their importance in the metabolism of birds, dietary FAs are of interest when studying fat metabolism in these animals. FAs are categorized by their length and degree of saturation (number of double bonds). FAs with one double bond are denoted mono-unsaturated fatty acids (MUFA) whereas FAs with multiple double bonds are polyunsaturated fatty acids (PUFA). Furthermore, when describing the characteristics of unsaturated FAs, the position of the first double bond is usually specified. For example, n-3 PUFA denotes that the first double bond occurs on the third carbon from the methyl terminus. Vertebrates can produce saturated FAs and MUFAs *de novo*, but must consume dietary PUFAs. Generally, terrestrial and freshwater feeding animals are able to produce long chain PUFAs from dietary short chain PUFAs, whereas some marine feeding fish are unable to endogenously elongate PUFAs (Castro et al., 2012; Vagner and Santigosa, 2011). The proportion of PUFAs in vertebrates tissues is consequently a reflection of diet and the proportion of long chain PUFAs specifically is strongly influenced by their abundance in animal diets (Arnold et al., 2015; Gladyshev et al., 2011; Hixson et al., 2015).

Dietary fatty acid composition can influence the metabolism of migrants in their roles as signaling molecules, the primary component of lipid bilayer membranes, and as metabolic fuel (Pierce and McWilliams, 2014). FAs act as ligands to signaling proteins including G-coupled protein receptors and nuclear receptors such as PPARs (Wahli and Michalik, 2012). PPARs have different binding affinities for different FAs (Bordoni et al., 2008). Long-chain PUFAs and their derived eicosanoids are strong ligands for all three PPARs (Wahli and Michalik, 2012; Xu et al., 2002).

Fatty acids are the non-polar component of phospholipids. The composition of FAs in phospholipid membranes influences permeability, fluidity and the function of membrane-bound proteins (Hulbert and Else, 2005). Greater proportions of unsaturated FAs in phospholipids result in increased fluidity of membranes and are characteristic of animals living in cold, typically marine, environments (Hazel, 1984). Permeability is associated with membrane fluidity with high amounts of unsaturated fatty acids also

leading to increased mitochondrial proton leak (Porter et al., 1996). Membrane FA composition can also change the activity of oxidative enzymes or other proteins (Hulbert and Else, 2005; Nagahuedi et al., 2009; Wu et al., 2004).

In their role as fuel, more unsaturated FAs, including PUFAs, can be oxidized more quickly than saturated FAs by whole muscle (Price and Guglielmo, 2009; Price et al., 2011b). However, adipose tissues store and preferentially mobilize predominantly shorter, more saturated FAs for catabolism (Price et al., 2008). These points suggest that the oxidation rate of FAs is not limiting in migrant birds and that the improved storage capacity and mobilization from adipocytes of MUFAs and saturated FAs provide more benefit than the greater oxidation rate associated with PUFAs (Price et al., 2011b). The role of dietary FAs in altering metabolic outcomes is apparent through these mechanisms, and the repeated mention of unsaturated FAs highlights their importance with n-3 PUFAs having an especially prominent role as essential FAs.

1.2.1 Polyunsaturated Fatty Acids

Animals cannot produce PUFAs *de novo*, and consequently, their abundance in the tissues of animals is a direct reflection of diet (Arnold et al., 2015). In particular, long-chain n-3 PUFAS including eicosapentaenoic (20:5 n-3; EPA) and docosahexaenoic (22:6 n-3; DHA) and the n-6 PUFA arachidonic acid (20:4 n-6; ARA), are widely-studied for their benefits to human health, exercise, and in the ecophysiology of cold-adapted animals (Hixson et al., 2015). PUFAs vary in abundance across habitats with marine environments having a greater proportion of n-3 PUFA and less n-6 PUFA than freshwater and terrestrial habitats (Hixson et al., 2015).

Research on the metabolic impacts of dietary PUFA supplementation indicates that these FAs can improve exercise performance (Philpott et al., 2018). Mammals improve running speed and endurance in association with n-6 PUFA abundance (Ruf et al., 2006). Furthermore, endurance exercise in humans increases the proportion of n-3 PUFA in muscle phospholipids (Willer et al., 2001). Peak metabolic rates (PMR) of Red-eyed Vireos (*Vireo olivaceus*) are higher with more n-6 PUFA intake (Pierce et al., 2005). White-throated sparrows (*Zonotrichia albicollis*) also exhibit increased PMR

when fed high n-6 PUFA diet but not with high n-3 PUFA intake (Price and Guglielmo, 2009). These differences in metabolic outcomes for animals engaged in endurance and high-intensity exercise suggest a differential role for n-3 and n-6 PUFAs. Within individual species, this is certainly the case and humans are a well-studied example. Most notably human health is affected by different PUFAs with n-3 PUFAs typically causing an anti-inflammatory response and n-6 promoting downstream pro-inflammatory responses and as noted above, improved exercise performance (Ruf et al., 2006; Schmitz and Ecker, 2008).

While n-6 PUFA supplementation is associated with improved performance, there has been much debate on the influence that dietary n-3 PUFAs may have in long distance migrants (Guglielmo, 2018; Maillet, 2006; Price, 2010). Research on the muscle phospholipid composition of migrating western sandpipers (*Calidris mauri*) demonstrated that these birds have elevated long-chain n-3 PUFA relative to wintering birds (Guglielmo et al., 2002b). Subsequent studies of migrating semipalmated sandpipers (*Calidris pusilla*) in addition to analyses of western sandpiper muscle, demonstrated that long-chain n-3 PUFA accumulation in muscle tissue is associated with increases in metabolic enzyme activities in these birds (Guglielmo, 2010; Maillet, 2006; Maillet and Weber, 2007). These positive relationships between enzyme activities and long-chain n-3 PUFA accumulation were postulated to influence whole animal metabolism and improve endurance performance, suggesting that long-chain n-3 PUFAs are ‘naturally doping’ these birds for endurance flight. Experimental manipulations of long-chain n-3 PUFA supplementation in sedentary bobwhite quail (*Colinus virginianus*) elicited the same relationships between muscle long-chain n-3 PUFA content and aerobic enzyme activities as in the migrant sandpipers providing further support for the role of long-chain n-3 PUFAs in improving oxidative metabolism and performance in muscle (Nagahuedi et al., 2009).

While the relationship between aerobic enzyme activities and greater long-chain n-3 PUFA content as demonstrated in migrant sandpipers and sedentary bobwhite quail implicate n-3 PUFAs in improving FA oxidation, subsequent studies have not demonstrated that metabolic performance is improved by n-3 PUFA supplementation.

Price and Guglielmo (2009) measured increased PMR in a songbird fed high n-6 PUFA but found no effect of n-3 PUFA on aerobic performance. Similarly, Dick and Guglielmo (2019) found decreased activities of some aerobic enzymes following dietary PUFA treatments but no difference in performance during extended wind tunnel flights in migratory yellow-rumped warblers. Together, these results indicate that n-3 PUFAs do not confer a benefit to aerobic performance in migrants. However, it is important to note that these experiments used terrestrial feeding birds which may have different physiological constraints than their marine associated counterparts.

Terrestrial food webs contain a lower abundance of n-3 PUFA in comparison to aquatic and marine environments (Hixson et al., 2015). Consequently, terrestrial animals, including most migrant songbirds naturally have less exposure to dietary n-3 PUFAs and in the wild must meet their PUFA requirements through other means. Terrestrial animals that maintain relatively high levels of long-chain n-3 PUFA in their tissues must feed in aquatic habitats, endogenously upregulate elongases and desaturases to produce long-chain PUFAs from precursor medium-chain PUFA, accumulate and retain PUFA, or engage in some combination of strategies (Cordain et al., 2002; Crawford et al., 1976; Hixson et al., 2015). The proportion of n-3 PUFA found in the tissues of animals in terrestrial habitats is lower than in freshwater or marine animals (Hixson et al., 2015). While this pattern may simply reflect the abundance of PUFAs in these habitat types, differences in the proportion of n-3 PUFAs in the tissues of animals may coincide with differences in PUFA requirements. Studies of marine and freshwater fish deprived of dietary long-chain n-3 PUFA upregulate enzymes to produce long-chain PUFAs from their medium-chain precursors to compensate for the dietary deficiency (Murray et al., 2014; Xue et al., 2015). Wild whale sharks (*Rhincodon typus*) and reef manta rays (*Manta alfredi*) feeding on high n-3 PUFA prey have high proportions of n-6 PUFA in their tissues indicating that they have unknown dietary items or other means of maintaining their FA requirements (Marshall et al., 2013).

If PUFAs are essential, fine-tuning of physiological systems based on evolutionary and life history strategies and behaviour in relation to dietary PUFA abundance has necessarily taken place allowing animals to fill available niches. Because

the underlying systems are homologous, we would not expect that an animal's response to dietary PUFA is fundamentally different, but that differences in how animals fulfill the biological requirements for certain PUFAs may result in different physiological outcomes under the same experimental dietary regime. In my thesis, I use an *in vitro* culture system to compare the influence of n-3 PUFA supplementation on metabolic characteristics of muscle from a terrestrial songbird, a marine shorebird and a terrestrial mammal.

1.3 Experimental Models

1.3.1 Mouse (*Mus musculus*) - C₂C₁₂ cell line

Mice are likely the most widely studied model organism in biological and health science research. C₂C₁₂ cells are an immortalized myoblast (muscle cell) cell line, sub-cloned originally from mouse muscle (Yaffe and Saxel 1977, Blau et al. 1987; ATCC CAT#: CRL-1772). Immortalized cell lines like C₂C₁₂ proliferate without senescing and are indexed and can be purchased for research from the American Type Culture Collection (ATCC). C₂C₁₂ myoblasts are muscle precursors that can be induced to differentiate into myotubes (myocytes *in vitro*) by reducing media serum levels. Differentiation of C₂C₁₂ cells into myotubes is characterized by the sequential expression of muscle specific proteins (i.e. Pax7, MyoD, Myogenin, Desmin, Myosin) and is representative of both *in vivo* and cultured primary muscle cell growth and differentiation (Zammit et al., 2006). Primary cell cultures are similar to immortalized cells in how they are managed within laboratories but must be isolated directly from animals and have limited proliferative lifespans in culture. Immortalized cell lines have similar characteristics to primary cell cultures because both cell types express tissue specific proteins (Blau et al., 1987). Immortalized cell lines are an advantageous alternative to primary cultures because they proliferate indefinitely.

1.3.2 Yellow-rumped Warbler (*Setophaga coronata coronata*)

The yellow-rumped warbler (*Setophaga coronata*) is an abundant North American passerine (of the order Passeriformes). There are two subspecies: the western Audubon's (*S. coronata auduboni*) and eastern myrtle (*S. coronata coronata*). The myrtle warbler is the subspecies used in this research, and from here forward yellow-rumped warbler refers

to this subspecies. Yellow-rumped warblers are relatively small migrants with masses of ~12 grams reaching up to ~15 grams during migration. Yellow-rumped warblers are medium-distance (~2,000km) nocturnal migrants that winter in the mid-United States to Central America and breed in the boreal forest (Hunt and Flaspohler, 1998). Yellow-rumped warblers are omnivorous and opportunistic foragers with seasonal foraging patterns of insects in the summer and fall and fruits in the winter and spring. Yellow-rumped warblers preferentially select foods high in sugars to assimilate into their fat stores but notably feed on high-fat fruits including bay berries during spring migration (Marshall et al., 2016). Yellow-rumped warblers are an excellent model for studying migration physiology of small birds because they adapt well to captivity, fly readily in wind tunnels, can be photo-manipulated to enter a migratory state and have some sequencing data available (Dick, 2017; Marshall et al., 2016; Toews et al., 2016).

1.3.3 Sanderling (*Calidris alba*)

The sanderling (*Calidris alba*) is a globally widespread, non-passerine migrant sandpiper belonging to the order Charadriiformes. Sanderlings range from 45-60 grams during the non-migratory period and can double in mass during migration to reach over 100 grams. Sanderlings are long-distance migrants with total migratory distances of up to 10,000km with populations wintering in coastal areas as far North as Maine and as far south as Chile, migrating to the high Arctic in the summer (Macwhirter et al., 2002; Myers et al., 1990). Sanderlings feed primarily on invertebrates in ponds and lakeshores inland and intertidal mudflats and beaches on the coasts; algal biofilm, mosses and other plant matter may compose some of their diet (Macwhirter et al., 2002; Tsipoura and Burger, 1999). The sanderling is in the same genus as the semipalmated sandpiper mentioned above, and they occupy similar breeding, wintering, and stopover habitats. During migration, both sanderlings and semipalmated sandpipers stopover in many of the same sites including inland lakes in Saskatchewan and coastal areas such as the Bay of Fundy (Howell, 2018; Macwhirter et al., 2002; Maillet, 2006). Consequently, the sanderling is an appropriate model shorebird species for assessing the effects of n-3 PUFA supplementation on muscle metabolism.

1.4 Muscle Cell Culture

Culture systems, including explant tissue cultures and cultured cells permit the use of an expanded toolkit to address molecular based research questions. However, explant culturing has inherent limitations to study design because of the relatively short durations that tissue can be kept alive and cannot be sampled repeatedly because they do not regenerate (Price et al., 2011b). Primary cell culture lines of muscle allow for studies conducted over a longer period of time by using cryopreservation to store cells but require the isolation of muscle progenitor cells.

In vitro culture methods have been optimized in research using embryonic and neonatal tissues of domestic birds (Carrel, 1912; Yao and Asayama, 2017). Embryonic and neonatal muscle tissues differ from those of adults muscle progenitor cell abundance declines with age. Myoblasts are mononucleated cells that can fuse to form new multinucleated muscle cells (myocytes) or divide to maintain the pool of muscle progenitors (Tajbakhsh, 2009). During development, myoblasts are abundant in embryonic muscle tissues and their population is maintained to support the growth rate required in embryonic and neonatal vertebrates (Chen-Ming et al., 2012; Tajbakhsh, 2009). In adult skeletal muscle, most nuclei are in myocytes, with <5% of muscle nuclei in progenitor satellite cells (García-Prat et al., 2013). Satellite cells are adult muscle stem cells that are located between the basal lamina and sarcolemma of skeletal muscle. Satellite cells are typically quiescent but become activated during muscle growth and damage, dividing and fusing to contribute to myocyte growth and repair (Tajbakhsh, 2009). Myogenic satellite cells can be identified by their expression of paired box protein 7 (Pax7) and are identified as myoblasts in this state (Zammit et al., 2006). Satellite cells can be coerced *in vitro* to differentiate into myotubes, a cell type homologous to *in vivo* myocytes (Aas et al., 2013). When satellite cells fuse to myocytes or other satellite cells, they express desmin, a structural protein required for sarcomere function, and myosin, the contractile unit of muscle fibers (Baquero-Perez et al., 2012).

Despite not originating directly from living tissue, differentiated myotubes function similarly to myocytes *in vivo* (Aas et al., 2013). Phenotypic characteristics of individuals from which satellite cells are isolated are subsequently retained in culture

(Aas et al., 2013; Pääsuke et al., 2016; Rosenblatt et al., 1996). Muscle cell culture provides a means to investigate biological questions that would be logistically challenging or impossible in whole animal studies. Methods for the isolation of myoblasts and satellite cells are well-established in mammalian models, however current methods for the isolation of avian muscle progenitors are limited to embryonic and young birds (Baquero-Perez et al., 2012; Yablonka-Reuveni and Nameroff, 1990).

1.5 Thesis Objectives

I had three main objectives in my thesis research. The first was to develop methods to establish primary muscle satellite cell culture systems from adult birds for the first time. To confirm that the cells isolated from two bird species (yellow-rumped warbler and sanderling) in culture were muscle satellite cells, I confirmed that they respond to media conditions in agreement with established satellite cell physiology, and verified that the cells differentiate into myotubes. My second objective was to use short interfering RNA (siRNA) to knock down expression of the H-FABP protein to determine its importance in fatty acid oxidation in these birds and mammalian skeletal muscle cell culture. This objective was successful in C₂C₁₂ cells but not in the avian cells and details are reported in Appendix A. My third objective was to test the hypothesis that supplementary n-3 PUFA alter muscle metabolism in a way that is consistent with improved performance and use of FA as fuel. To test this hypothesis, I evaluated the response of muscle cells from a terrestrial mammal, a terrestrial migrant songbird, and a marine-associated migrant shorebird to supplementation with n-3 PUFA. I measured transcriptional changes in PPARs and selected downstream target genes (fatty acid transporters), activities of key metabolic enzymes, and aerobic performance *in vitro*. I predicted that muscle cells would increase expression of PPARs and fat transporters and exhibit increased activity of aerobic enzymes. I also predicted that cells would increase metabolic rate, elevating their oxygen consumption rate in culture.

2 Methods

2.1 Study Birds

Approval for the capture of birds in these studies was obtained from the Canadian Wildlife Service (Permit #CA0256, 15-SK-SC004; Appendix B) and the University of Western Ontario Animal Care Sub-Committee (Protocol #2010-216; Appendix C). Yellow-rumped warblers were captured using mist-nets at Long Point, Ontario in October 2016 during fall migration. Sanderling were captured at Chaplin Lake, Saskatchewan in May 2017 during spring migration. All birds were transported to the Advanced Facility for Avian Research at the University of Western Ontario (London Ontario) where they were housed. All birds were aged by wing moult pattern upon capture and categorically assigned to either hatch year (HY) or after hatch-year (AHY) in the case of yellow-rumped warblers and only AHY for sanderlings in the spring. These age designations mean that HY yellow-rumped warblers caught in fall were ~2-4 months and AHY individuals 14+ months whereas all sanderlings were a minimum 9-10 months of age at capture (Hunt and Flaspohler, 1998; Macwhirter et al., 2002).

2.2 Primary Culture of Adult Avian Satellite Cells

Methods for the isolation of muscle progenitor cells were adapted from those used by Bacquero-Perez et al. and Cooper-Mullin et al. (Bacquero-Perez et al., 2012; Cooper-Mullin et al., 2015). Birds were euthanized by decapitation under isoflurane anesthesia with minimum ages of individuals at that time of 12 or 21 months for yellow-rumped warblers and sanderlings respectively. All reagents used during the isolation process were pre-warmed in a 37 °C water bath. Left and right pectoralis major muscles were immediately excised and washed twice in Hanks Balanced Salt Solution (HBSS; Gibco, Burlington, Ontario). Visible fat and connective tissues were removed from the muscle before a final rinse in HBSS. I then minced the pectoral muscle into small pieces ~1 mm³ in collection media (DMEM supplemented with 1% antibiotic-antimycotic; Gibco) using surgical scissors in a sterile cell culture plate. This physical digestion process was conducted rapidly to limit satellite cell death from prolonged exposure to *ex vivo* conditions. Minced tissue was then transferred to a 50 mL conical tube and the collection

media was siphoned from the tissue layer and replaced with 7.5 mL digestion solution (1.4 mg/mL Pronase; Millipore-Sigma, Oakville, Ontario, 15 mM HEPES, 1% Antibiotic-Antimycotic; Gibco) per gram of tissue. The digestion solution was then transferred to a 37 °C water bath for one hour with gentle rocking at 10-minute intervals.

Digested tissue was then centrifuged at 300 ×g for six minutes, pelleting the digested tissue. I aspirated the digestion media and washed the tissue in phosphate buffered saline (PBS) and centrifuged the tissue again. The PBS was then removed and the tissue was resuspended in 7.5 mL collection media per gram tissue and triturated vigorously using a 10 mL pipette for 5-10 minutes to release live satellite cells from their native position. The tissue solution was then centrifuged for six minutes at 300 ×g and the supernatant was retained. The remaining muscle tissue was digested further in fresh digestion media for an additional 30 minutes following the methods described above before continuing as follows with the second fraction of digested tissue. I passed the retained supernatant through a 40 µm cell strainer and diluted it to 40 mL total volume with PBS and centrifuged the diluted solution for ten minutes at 800 ×g. The cell pellet was resuspended in growth media (10% chicken serum; Millipore-Sigma, 10% horse serum, 1% Antibiotic-Antimycotic, 0.1% Gentamycin; Gibco, 20 ng/mL bFGF; Millipore-Sigma in McCoy's 5A culture media; Gibco) and preplated onto an uncoated 150 mm cell culture dish and placed in an incubator set to 38.5 °C and 5% CO₂ for two hours to adhere fibroblasts that may contaminate the satellite cell population. The supernatant was then removed and the cell isolation was added directly to a collagen I (Gibco) coated 150 mm cell culture plate and placed in the incubator.

Following initial isolation, I washed primary cells daily three times with warm PBS and maintained them in growth media until reaching ~85% confluency. Upon reaching the desired confluency, primary cells were lifted from the plate using 0.25% trypsin and plated evenly across three collagen-coated dishes for the first passage. Once the first passage of cells reached ~85% confluency, cell plates were trypsinized again, centrifuged for 10 minutes at 800 ×g and resuspended in 3 mL 10% DMSO (Millipore-Sigma) in horse serum per plate and frozen slowly (~1°C min⁻¹) to -80 °C in 1.5 mL aliquots for 48h before depositing in liquid nitrogen for long term storage. Primary cells

used in the studies described below were frozen in liquid nitrogen for up to seven months before thawing and plating for experiments.

2.3 Cell Culture

Immortalized and primary cell culture lines were kept in liquid nitrogen for long term storage. Cells were thawed rapidly in a 37 °C water bath and quickly diluted in cell type specific growth media (see sections 2.3.1-2.). I centrifuged diluted cells for 10 min at 800 ×g and resuspended in growth media before plating.

2.3.1 C₂C₁₂ Murine Myoblasts

C₂C₁₂ cells were obtained from the American Type Culture Collection (ATCC; Catalog Number: CRL-1772; Manassas, VA, USA). I plated C₂C₁₂ murine myoblasts onto sterile uncoated adherent cell culture dishes. Myoblasts were maintained in DMEM (Gibco) containing 10% fetal bovine serum (Gibco) and 1% penicillin-streptomycin (Gibco). Myoblasts were trypsinized and plated upon reaching ~ 80% confluency. All experiments were conducted using C₂C₁₂ cells below passage 20. For experiments involving differentiated myotubes, the culture media was replaced with DMEM containing 2% horse serum and 1% penicillin-streptomycin when myoblasts reached ~90% confluency.

2.3.2 Avian Satellite Cells

I plated avian satellite cells from liquid nitrogen storage onto sterile collagen I (Gibco, Burlington, ON) coated adherent cell culture dishes. Cells were maintained in growth media until reaching ~80% confluency when they were trypsinized and plated for experiments. Cells plated for experiments on differentiated myotubes were switched to differentiation media (yellow-rumped warbler: 10% chicken serum (Millipore-Sigma, Oakville, ON), 10% horse serum (Gibco), 1% Antibiotic-Antimycotic (Gibco), 0.1% Gentamycin (Gibco) in McCoy's 5A culture media (Gibco); sanderling: 5% chicken serum, 5% horse serum, 1% Antibiotic-Antimycotic, 0.1% Gentamycin in McCoy's 5A culture media) upon reaching ~90% confluency. I changed growth media every other day and changed differentiation media daily. I plated yellow-rump warbler and sanderling satellite cells up to passage three for experiments.

2.4 Cell Counting

I plated approximately 20,000 cells for cell counting experiments onto 35 mm cell culture dishes. I plated yellow-rumped warbler satellite cells for counting 24, 48, 96, 144, and 192 h after plating and sanderling satellite cells for counting 6, 12, 18, 24, 36, 48, 72, and 96 h after plating. Cells were plated in duplicate for each time point. At each timepoint, I thoroughly trypsinized cells following a single wash in PBS and physically struck the sides of the dishes repeatedly to dislodge adhered cells. Upon lifting the cells from the plate surface, I added four volumes of growth media to the cell suspension and removed an aliquot of the solution placing it into a 1.5 mL microtube. I mixed the aliquot thoroughly before adding an equal volume of the cell suspension and 0.4% trypan blue in a fresh microtube. I counted cells using an Improved Double Neubauer Hemocytometer (W.E. Saunders Ltd., Germany) by adding 10 μ L of trypan blue cell suspension and counting the total number of cells in four corner squares and the center. From the calculated cell concentration using the hemocytometer, I calculated the total number of cells in each 35 mm dish using the known volume of trypsin and media added at each timepoint.

I validated the accuracy of cell counts by comparing the doubling time of sanderling cells by hemocytometer counts and by cell concentration measurements using a BD Accuri flow cytometer (BD Biosciences, San Jose CA, USA). I plated sanderling cells for only two timepoints (48 and 72 h) following the procedure described above. These time points were selected to ensure enough cells could be collected to run the flow cytometer and capture the exponential growth phase accurately. Cells were trypsinized as described, pelleted and washed twice in PBS before fixation in ice-cold 70% ethanol and overnight incubation at 4 °C. I then pelleted, and resuspended them in suspension buffer (0.1% Triton-100X, 0.5 mM MgCl₂, 1 mM CaCl₂, 150 mM NaCl, and 100 mM Tris, pH 7.4). I diluted aliquoted samples with 25 μ L of CountBright Absolute counting beads (Invitrogen, Burlington ON) to a final volume of 300 μ L. Samples were pooled for negative controls of sonicated cell suspension, cell suspension, and cell suspension with counting beads to identify debris, cells, and beads respectively. I retained the first 20,000 counted cell events for analysis based on gated populations of forward and side scatter

area. Gates and data organization was conducted in R version 3.5.1 using the package flowCore (Ellis et al., 2018; R Core Team, 2018). Cell concentration was determined based on the lot number of beads. Doubling times of cells counted by hemocytometer and flow cytometer were calculated using equation 1.

$$dt = t \times \ln(2)/\ln(Xe/Xb) \quad (1)$$

Where t is the number of hours between time points, with Xb representing the number of counted cells at the first time point and Xe representing the second time point.

2.5 Immunocytochemistry

I grew cells on collagen I coated Nunc Lab-Tek II permanox chamber slides for immunocytochemistry (Thermo Scientific). Cells were then plated and differentiated following the procedure described in section 2.3.2. I fixed cells 24 h after plating to stain initial cell populations and fixed additional sets of differentiating cells three and six days after differentiation. I fixed cells in 4% paraformaldehyde for 1 h to stain cells for paired box factor 7 (Pax7) and sarcomeric myosin. Cells stained for desmin were fixed in ice-cold methanol at -20 °C for 5 min. Fixed cells were washed with PBS, permeabilized in 0.25% Triton x-100 and blocked using background sniper (Biocare Medical, Pacheco, CA, USA). I incubated fixed cells in primary antibody overnight at 4 °C at the specified concentration for each target: anti-Pax7 (Developmental Studies Hybridoma Bank (DSHB), Iowa City IA, USA: Pax7, 0.5 µg/mL), anti-sarcomeric myosin (DSHB: MF20, 2.5 ug/mL) and anti-desmin (DSHB: D3, 0.5µg/mL). Following primary antibody incubation, I washed cells in PBS and incubated in Alexa Fluor goat anti-mouse 568 secondary antibody (Invitrogen) for 2 h. Cells were then washed 3 times in PBS and fixed in ProLong Gold mountant (Invitrogen) before mounting a coverslip. Slides were set to cure in mountant at 4 °C for at least 24 h before imaging. Stained cells were qualitatively assessed at each time point using a Zeiss Imager Z1 compound light microscope (Zeiss) to confirm expression of muscle-specific proteins and differentiation.

2.6 Fatty Acid Treatments

Stock solutions of eicosapentaenoic acid (EPA, 20:5n-3; Sigma-Aldrich, Oakville, ON), docosahexaenoic acid (DHA, 22:6n-3; Sigma-Aldrich), and oleic acid (OA, 18:1n-9; Sigma-Aldrich) were solubilized in anhydrous ethanol and stored at -20 °C. I diluted fatty acids in cell type specific differentiation media to 10x final concentration, conjugated to fatty acid free bovine serum albumin (BSA; Sigma-Aldrich) in a 2:1 molar ratio. I conjugated FAs to BSA by briefly vortexing the solutions and incubating them in a 37 °C water bath for 45 min. Conjugated FAs were stored at 4 °C for up to four days and prewarmed before adding to cell media. The control treatment of BSA alone was prepared following the same protocol and replacing the volume of solubilized FA with ethanol.

Avian satellite cells and C₂C₁₂ myoblasts were plated and differentiated as described above. I plated all cells in duplicate for each set of independent assays. I differentiated avian satellite cells for 4 d and C₂C₁₂ myoblasts for 5 d before applying treatments. FA and control treatments were then added to a final concentration of 100 µM FA in cell type specific differentiation media. Cells were treated for 48 h with fresh media and FA:BSA or BSA control added at 24 h.

2.7 RT-qPCR

I collected mRNA from adherent myotubes by washing cells twice in PBS and adding TRIzol (Invitrogen, Burlington, ON) and following the manufacturer's instructions to isolate total mRNA. Briefly, cells grown in 35 mm dishes were incubated in 1 mL TRIzol for 5 min at room temperature before adding 200 µL of chloroform and intermittently vortexing for 3 min. The Trizol solution was then centrifuged for 15 min at 12000 ×g and 4 °C before I transferred the colourless supernatant to a sterile tube. I added 500 µL of isopropanol to the transferred supernatant, briefly vortexing the mixture and incubating it at 4°C for 1 h. The mixture was then centrifuged for 10 min at 12,000 ×g and 4 °C before aspirating the supernatant. I then added 1 mL of 70% ethanol to the remaining RNA pellet and centrifuged for 10 min at 12000 ×g and 4 °C. I aspirated the supernatant again and added 1 mL of 70% ethanol to wash the RNA pellet, and centrifuged it for 10 min at

1200 $\times g$ and 4°C. I then carefully removed the remaining supernatant before adding 20 μL of DEPC treated water and storing the dissolved RNA solution at -80 °C.

RNA yield and purity were measured using a NanoDrop 2000 spectrophotometer (Thermo Scientific, Burlington, ON). All retained RNA samples had an A260/A280 between 1.8 and 2.0. I also evaluated RNA quality by visually assessing the degradation of ribosomal 28S/18S bands separated on a 1.5% agarose denaturing gel using redsafe nucleic acid staining solution (iNtRON Biotechnology, Jungwon-gu, Korea). I only retained samples without degradation for analysis. I reverse-transcribed mRNA to cDNA using the High Capacity RNA-to-cDNA kit (Applied Biosystems, Burlington, ON) following the manufacturer's instructions and I diluted cDNA samples 1:100 in water.

I designed primer sets using the NIH NCBI Primer-BLAST service. Primers optimized for C₂C₁₂ were taken from previously published work and I designed some primers based on published mRNA sequences of *Mus musculus* using NCBI's primer-BLAST (Agarwala et al., 2018; Zhang, 2012). Primers optimized for sanderling and yellow-rumped warbler were taken from unpublished and published primers for yellow-rumped warbler based on a *de novo* transcriptome assembly and I designed primers for sanderling and yellow-rumped warbler based on mRNA sequences of closely related species' sequences available through NCBI (Bradley et al. 2017, Agarwala et al. 2018, M. Dick. personal communication). Primer sets for genes of interest: *FABP3* (coding the H-FABP protein), *CD36*, *PPAR- α* , *PPAR- β* , *PPAR- γ* and for reference genes *PP1B* and *ACTB* were used for all three species; an additional reference gene, *GAPDH*, was used for yellow-rumped warbler and C₂C₁₂. Quantitative real-time PCR and Ct value determination was completed using a CFX384 thermal cycler (Bio-Rad, Mississauga, Ontario). All PCR reactions were in 8 μL final volume containing 0.2 μM primer set, 3 μL of 1:100 diluted cDNA, 4 μL Sensifast SYBER (Bioline). Amplification efficiencies for each primer set were determined by standard curves and were within 90-100%. The reaction conditions for primer sets were: 95 °C for 10 min, 45 cycles of 95 °C for 20 sec, 59-65 °C for 20 sec, 72 °C for 10 sec. Primer sequences, their source, and annealing temperatures are listed in Table 1.

Table 1. mRNA targets, the associated primer sequences and annealing temperatures used for RT-qPCR. The source of primer sequences used from publications are listed.

Species	mRNA Target	Annealing t (°C)	Primer Sequence	Primer Source	
Mouse - C ₂ C ₁₂ (<i>Mus musculus</i>)	ACTB	60	F: TATCGCTGCGCTGGTCTG R: CATCCCCACCATCACACCCCT	NCBI Primer blast (Agarwala et al. 2018)	
			F: ATTGGTGCAGTCCTGGCTGT R: TCTTTGCCACGTCATCTGGGT	(Zhang 2012)	
	H-FABP	60	F: TGCTCATGGTTTCCCTC R: CCTGGAGCACCCCTTTGGAT	NCBI Primer blast	
	GAPDH	62	F: AGGTCGGTGTGAACGGATTTG R: TGTAGACCATGTAGTTGAGGTCA	(Zhang et al. 2010)	
	PPAR- α	60	F: AACCGGAACAAATGCCAGTA R: CCGAATCTTTCAGGTCGTGT	(Zhang 2012)	
	PPAR- β	60	F: ACATCGAGACACTGTGGCAG R: CGGTAGAACACGTGCACACT	NCBI Primer blast	
	PPAR- γ	61	F: CCAACTTCGGAATCAGCTCT R: CAACCATTGGGTCAGCTCTT	(Zhang 2012)	
	PPIB	60	F: TCGGAGCGCAATATGAAGGT R: TTATCGTTGGCCACGGAGG	NCBI Primer blast	
	Sanderling (<i>Calidris alba</i>)	ACTB	61	F: CCCTGAAGTACCCATTGAA R: GGGGTGTTGAAGGTCTCAA	NCBI Primer blast
F: AGAGACCTCTCGTGCCTACA R: GCCATAGGACTCTAGGGATGC				NCBI Primer blast	
H-FABP		60	F: AAGACCCAGAGCACCTTCAAGA R: ACTTCTGCACGTGGACGAGTT	NCBI Primer blast	
PPAR- α		63	F: CACTCAGCCAGGAGCATGAA R: AACCCATTGTAAGACACGTTGTG	NCBI Primer blast	
PPAR- β		60	F: GACTCTGCTCAAGTACGGGG R: AGGATGATGGCAGCCACAAA	(Dick and Guglielmo 2019)	
PPAR- γ		63	F: TCGTGCCCTCCATAACAAGG R: ATGGCACCTGATTGCTCAGT	NCBI Primer blast	
PPIB		60	F: GGCTCTTTGGCAAGACAGTG R: CCTTGATCACACGGTGGAACT	NCBI Primer blast	
Yellow-rumped warbler (<i>Setophaga coronata coronata</i>)		ACTB	61	F: CCCTGAAGTACCCATTGAA R: GGGGTGTTGAAGGTCTCAA	NCBI Primer blast
				F: GGTGCATCAGCTTGTAGACAGA R: TGGAAAGAGACGCAGCAACA	NCBI Primer blast
	H-FABP	60	F: AAGACCCAGAGCACCTTCAAGA R: ACTTCTGCACGTGGACGAGTT	NCBI Primer blast	
	GAPD	60	F: TCCCGAAGCGGTAAAGATGG R: CCGGAAGTGGCCATGAGTAG	(Bradley et al. 2017)	
	PPAR- α	60	F: ATGGCTGGTTTGAGACACCC R: TACCTGTGACACTTCCCCGA	(Dick and Guglielmo 2019)	
	PPAR- β	60	F: GACTCTGCTCAAGTACGGGG R: AGGATGATGGCAGCCACAAA	(Dick and Guglielmo 2019)	
	PPAR- γ	63	F: TCGTGCCCTCCATAACAAGG R: ATGGCACCTGATTGCTCAGT	(Dick and Guglielmo 2019)	
	PPIB	60	F: GGCTCTTTGGCAAGACAGTG R: CCTTGATCACACGGTGGAACT	NCBI Primer blast	

Relative expression values were calculated using the $\Delta\Delta C_q$ method in the CFX maestro software package (Bio-Rad). Relative expression was determined for C₂C₁₂ and yellow-rumped warbler by normalizing mRNA of interest expression to the arithmetic mean of reference transcripts *ACTB*, *PPIB* and *GAPDH*; mRNA expression for sanderling was normalized to *ACTB* and *PPIB*.

2.8 Enzyme Assays

Treated myotubes were collected for enzyme assays by trypsinization, centrifuged at 800 $\times g$, 4 °C and washed three times with ice-cold PBS. After the final spin, I aspirated the PBS and flash froze the cell pellets in LN and stored them at -80 °C. I carried out enzyme assays following methods adapted from Price et al. (2010). Briefly, frozen cell pellets were resuspended in 100 μ L of ice-cold homogenization buffer (20 mM Na₂HPO₄, 0.5 mM EDTA, 0.2% fatty acid free BSA, 0.1% Triton X-100) and ground within 1.5 mL microtubes using a plastic pestle.

Enzyme activities were measured in duplicate wells of 96-well plates using a SpectraMax M5 plate reader (Molecular Devices, San Jose CA, USA). The temperature was set to 37 °C for assays of C₂C₁₂ and 39 °C for avian samples; the final reaction volume for all assays was 300 μ L.

Citrate synthase (CS) converts oxaloacetate to citrate by consuming acetyl-CoA. I measured the rate of this reaction by the increase in absorbance at 412 nm as free CoA converts DTNB (5,5'-dithiobis-(2-nitrobenzoic acid) or Ellman's reagent) to TNB ($\lambda = 412$ nm). CS rate was measured with 150 μ M acetyl-CoA, 150 μ M DTNB, and 330 μ M oxaloacetate in 50 mM Tris buffer (pH 8.0). Similarly, CPT activity was measured by the increase in absorbance at 412 nm with the production of TNB from DTNB. CPT facilitates the conversion of acyl-CoA to acyl-carnitine producing a free CoA. CPT activity rate was measured with 5 mM carnitine, 35 μ M palmitoyl-CoA, and 150 μ M DTNB in 50 mM Tris buffer (pH 8.0) by measuring the increase in absorbance at 412 nm. LDH catalyzes the interconversion of pyruvate and lactate. The rate at which pyruvate is converted to lactate can be monitored by the coincidental oxidation of NADH ($\lambda = 340$ nm). I measured LDH activity with 1 mM pyruvate, 1 mM EDTA and 200 μ M

NADH in 50 mM imidazole buffer (pH 7.4) by measuring the reduction of absorbance at 340 nm. The third step of fatty acid oxidation is catalyzed by HOAD, which converts hydroxyacyl-CoA to ketoacyl-CoA through the reduction of NAD⁺. HOAD activity is measured *in vitro* by forcing this reaction to run in reverse, wherein acetoacetyl-CoA is converted to β -hydroxybutyryl-CoA coinciding with the reduction of NADH. HOAD activity rate was measured with the same imidazole buffer, replacing the pyruvate with 100 μ M acetoacetyl-CoA and measuring the reduction of absorbance at 340 nm. Table 2 lists the volumes and dilutions of species-specific samples for each assay described. I normalized all activity rates to total protein by completing BCA assays (Thermo Scientific, Burlington, ON) following the manufacturer's instructions. Activities were calculated using equation 2.

$$mU/mg_{protein} = \frac{\Delta Abs \cdot V \cdot DF}{V_{sample} \cdot PL \cdot \epsilon \cdot C_{protein}} \quad (2)$$

Where ΔAbs is the change in absorbance, PL is the path length in cm, V is the total volume in μ L, DF is the dilution factor, V_{sample} is the sample volume in μ L, ϵ is the molar attenuation coefficient in $mM^{-1}cm^{-1}$ and $C_{protein}$ is the protein concentration of the sample in mg/mL. DTNB has an ϵ of $13.6 mM^{-1}cm^{-1}$ the ϵ of NADH is $6.22 mM^{-1}cm^{-1}$. The path length is 0.81 cm and the total volume of all reactions is 300 μ l.

Table 2. Volumes and dilutions used during kinetic enzyme activity assays for C₂C₁₂, yellow-rumped warbler, and sanderling myotubes (ndil = not diluted).

	C ₂ C ₁₂	Sanderling	Yellow-rumped warbler
CS Volume / Dilution	10 μ l / 1:10	10 μ l / 1:10	10 μ l / 1:2
CPT Volume / Dilution	10 μ l / 1:2	10 μ l / 1:2	10 μ l / ndil
LDH Volume / Dilution	2.5 μ l / 1:40	2.5 μ l / 1:20	2.5 μ l / 1:10
HOAD Volume / Dilution	10 μ l / 1:4	10 μ l / 1:2	10 μ l / ndil

2.9 Aerobic Profile Assays

The Seahorse XFe24 Analyzer (Agilent Technologies, Mississauga, ON) uses solid-state probes to measure the decline in the oxygen concentration of cell media at programmed intervals providing measures of oxygen consumption rate (OCR) in pmol/min under experimental conditions. During a Seahorse assay, aerobic metabolism can be manipulated by injecting reagents to inhibit components of the electron transport chain (ETC) altering OCR from the 'resting' basal conditions. Oligomycin inhibits the activity of ATP synthase (ATPase) providing a measure of OCR not contributing to ATP production. 2,4-Dinitrophenol (DNP) is a protonophore that acts to uncouple the established proton gradient across the mitochondrial membrane. DNP uncoupling causes the ETC complexes to consume oxygen at a maximal rate to provide maximal OCR capacity measurements. Rotenone and antimycin A inhibit the activity of complex I and complex III respectively and ultimately stop ETC mediated OCR in cells to allow measurement of non-ETC mediated OCR.

I attempted to optimize Seahorse XF assays to be conducted with both avian species, however yellow-rumped warbler cells did not exhibit a dose-dependent response to the reagents described above and frequently failed to elicit changes in OCR in the prescribed direction. Consequently, I conducted Seahorse XF assays using sanderling and C₂C₁₂ cells only. I plated 2,000 sanderling satellite cells or C₂C₁₂ myoblasts onto XF24 cell culture microplates (Agilent Technologies) and followed the differentiation and FA treatment procedure described in section 2.6. XFe24 sensor cartridges (Agilent Technologies) were prepared overnight by incubating in Seahorse XF Calibrant Solution (Agilent Technologies) overnight in a CO₂ free incubator set to the cell type specific temperature. Following FA treatments, I changed the differentiation media with FA treatments to starvation media (500 μM dextrose, 500 μM carnitine, 1 mM glutamine, in Seahorse XF base media (Agilent Technologies), pH = 7.4 with 0.5% chicken serum and 0.5% horse serum for sanderling and 1% fetal bovine serum for C₂C₁₂) and placed cells into a CO₂ free incubator for 2 h. Before running the assay, I loaded Xfe24 sensor cartridges with 56 μL of 10 μg/mL oligomycin for sanderling or 80 μg/mL for C₂C₁₂, 62 μL of 2 mM DNP for sanderling or 2.5 mM for C₂C₁₂, and 69 μL of 20 μM rotenone and

antimycin A in ports A, B and C respectively. I replaced the starvation media with assay media (500 μ L carnitine, 5 mM HEPES, and 200 μ M OA conjugated to BSA in a 1:4 molecular ratio following the procedure described in section 2.6, in Seahorse XF base media pH = 7.4) and placed the microplate immediately into a Seahorse XFe24 Analyzer (Agilent) set to the cell type specific temperature to run the assay.

I designed this assay protocol to follow closely the Mito Stress Test kit prescribed by Agilent but adapted it for a FA oxidation stress test (Agilent). Briefly, 12 cycles of 3 min mix, 2 min wait, and 3 min measure were included following equilibration. Oligomycin was injected after the 4th cycle, DNP was injected after the 7th cycle and rotenone and antimycin A after the 9th cycle (Figure 2).

I calculated OCR ratio-based differences as defined by Yépez et al. (2018) using the manufacturer's default extreme differences method. OCR ratios provide a means to account for inter-well variation and are represented as unitless proportions of oxygen consumption or fold changes. Table 3, adapted from Yépez et al. (2018) lists the OCR ratios and equations used to calculate them. Figure 1 displays an example OCR trace from the FA oxidation tests I conducted with the metrics used to calculate OCR ratios.

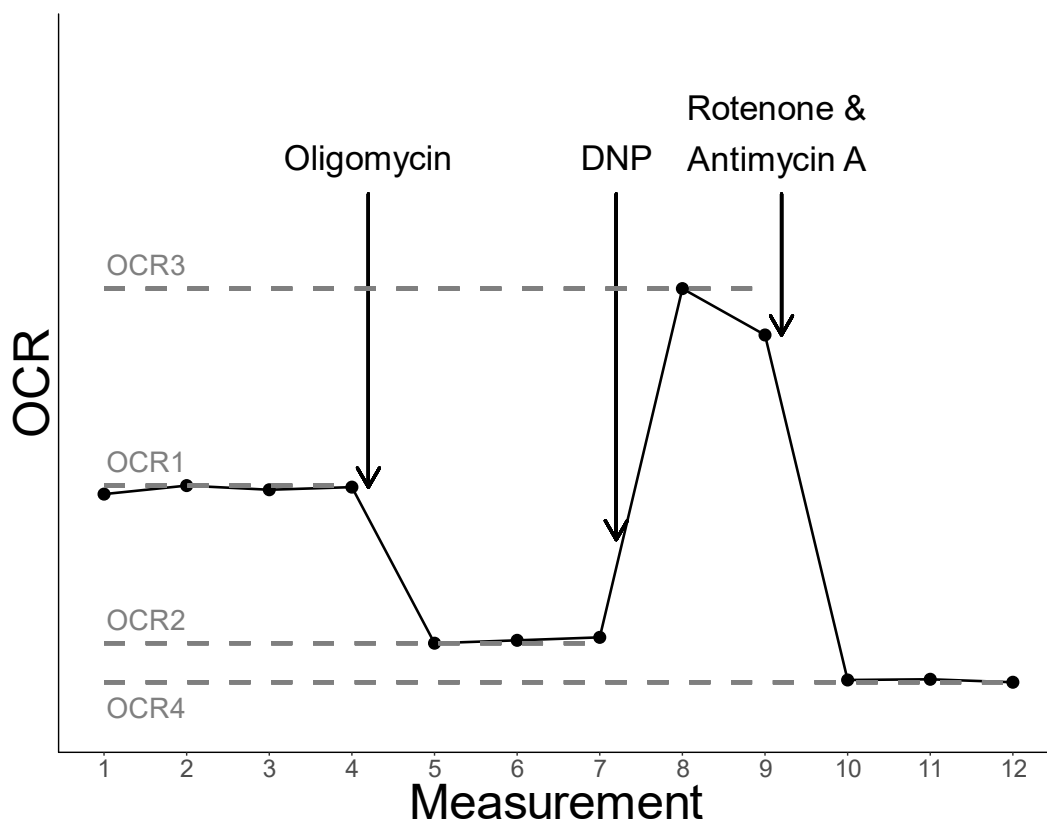


Figure 2. Example of an individual OCR (oxygen consumption rate) trace produced by the XF24e Seahorse based on the methods described. Individual measurements of OCR are taken at discrete timepoints throughout the assay in pmol/min indicated by the black points. Oligomycin injection inhibits ATPase activity reducing OCR. DNP uncouples the mitochondrial membrane, forcing complexes I-IV to consume O₂ at a maximal capacity. Rotenone and antimycin A inhibit complexes I and III respectively to inhibit ETC based respiration. OCR1-4 designate the timepoints from which OCR values are used to calculate OCR ratios (Table 3).

Table 3. Definitions and equations of OCR (oxygen consumption rate) ratio-based measurements of cellular aerobic profiles using a Seahorse XFe24 Analyzer. The first column indicates the notation used in this thesis and their associated definitions and equations from Yépez et al. (2018). The number notations in the equations column indicate the interval at which the OCR measurements were taken: 1. pre-oligomycin injection, 2. post-oligomycin injection, 3. post-DNP injection, 4. post rotenone & antimycin-A injection (Figure 2).

Bioenergetic Measurement	Definition	Equations
ETC OCR Proportion	Proportion of OCR in the ETC with respect to the initial OCR	$(OCR1-OCR4)/OCR1$
ATPase OCR Proportion	Proportion of OCR driven from ATPase proton pumping with respect to the initial OCR	$(OCR1-OCR2)/OCR1$
Proton Leak OCR Proportion	Proportion of OCR in the ETC, but not driven from ATPase proton pumping, with respect to all non ATPase driven OCR	$(OCR2-OCR4)/OCR2$
Spare Capacity OCR	Ratio between maximal OCR and initial OCR	$OCR3/OCR1$
Maximal Capacity OCR	Ratio between maximal OCR and non-ETC driven OCR	$OCR3/OCR4$

2.10 Statistical Analysis

C₂C₁₂ cells grown at independent passage numbers under individual treatments were considered experimental units for analyses. Similarly, for primary cultures of yellow-rumped warbler and sanderling cells, individual bird id from which the cells were isolated in combination with treatment were considered experimental units. Consequently, all experiments described follow a randomized complete block design with individual or passage as the blocking units for avian and C₂C₁₂ cells respectively.

I analyzed cell counting data for each species using general linear models with individual as the blocking variable and timepoint in hours and bFGF treatment as independent variables to determine the effect of bFGF on proliferation rate. To assess the accuracy of manual cell counts of sanderling satellite cells by comparison to flow cytometry, doubling times calculated by each method were contrasted using paired t-test under each bFGF treatment.

I analyzed all measurements taken after FA treatment experiments within species by ANOVA, blocking for individual or passage in avian and C₂C₁₂ cells respectively. To determine if there were differences among treatments, I included planned contrasts in these ANOVAs for comparisons between BSA-OA, BSA-DHA, BSA-EPA and pooled comparison of PUFA groups against the pooled BSA and OA treatments (BSA+OA vs DHA+EPA). Because these contrasts are not orthogonal, p-values were adjusted using the ‘free’ method (Hothorn et al., 2008). Assumptions of all general linear models were assessed graphically prior to generating ANOVA tables. Where assumptions were not met, data were transformed appropriately before proceeding. All analyses were conducted in R version 3.5.1 and the packages dplyr, multcomp, ggplot2, and ggsignif were used for data organization, analyses and generating plots (Ahlmann-Eltze, 2017; Hothorn et al., 2008; R Core Team, 2018; Wickham, 2016; Wickham et al., 2018).

3 Results

3.1 Primary Muscle Cell Culture Characteristics

I isolated satellite cells from the pectoral muscle of three adult sanderlings and five adult yellow-rumped warblers for the experiments described herein. Following initial isolation, satellite cells were difficult to find and usually not resolved until ~48h after plating. In growth media, most isolated satellite cells appear fusiform (typical myoblast morphology) with a minority of spherical shaped cells. Cells isolated from yellow-rumped warbler reached 80% confluency after ~ two weeks whereas cells isolated from sanderling took only one week. I observed these spherical satellite cells actively dividing under light microscope and when trypsinizing satellite cells, all cells on the plate retracted to this spherical shape. Cryopreservation of these satellite cells did not apparently affect growth characteristics, and thawed cells were successfully grown in culture up to seven months following preservation. Under differentiation conditions, avian satellite cells aligned in fusiform shapes end-to-end prior to fusing. After three days of differentiation, avian satellite cells/myotubes formed apparently fused cellular swirls (Figure 3). I observed myotubes spontaneously contracting after three days of differentiation providing strong evidence that I had isolated and differentiated muscle cell progenitors and myotubes from adult avian muscle.

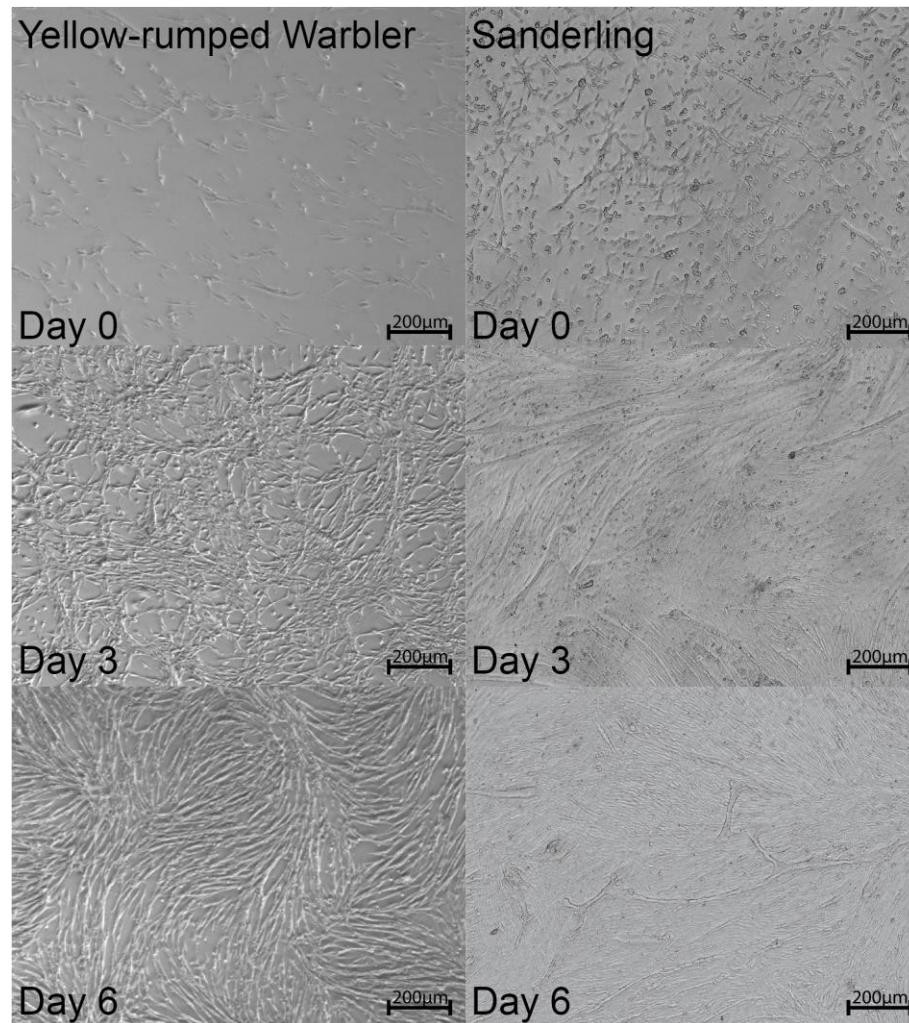


Figure 3. Phase contrast microscope images of yellow-rumped warbler (left) and sanderling (right) satellite cells (top row) and differentiated myotubes (middle and bottom rows). Individual muscle satellite cells (top) fuse together during differentiation to form multinucleated myotubes visible as elongated fused cells by day 3 and 6 (middle and bottom rows).

3.1.1 Proliferation Rate of Adult Avian Satellite Cells

Satellite cells isolated from the muscle of sanderlings rapidly proliferated in growth media compared to those isolated from yellow-rumped warblers (Figure 4). Figure 5 shows the growth rate of satellite cells with and without bFGF in the growth media of sanderling and yellow-rumped warbler cells. Both sanderlings ($F_{1,43} = 39.09$, $P < 0.001$) and yellow-rumped warblers ($F_{1,43} = 6.81$, $P = 0.012$) responded to bFGF in the growth media with more rapid growth (Figure 5). Based on these count data, population doubling times of yellow-rumped warbler cells ranged from $23.1 \pm 8.2\text{h}$ (SD) to $39.4 \pm 10.8\text{h}$ (SD) between 96-144h and 144-192h respectively. Doubling times for sanderling cells ranged from $7.6 \pm 1.4\text{h}$ (SD) to $44.9 \pm 16.1\text{h}$ (SD) between 12-18h and 72-96h respectively. Validation of sanderling cell doubling times by comparing hemocytometer count to flow cytometry data of cells grown with or without bFGF indicates that there is no difference in the calculated doubling time between these methods (with bFGF: $t = 0.09$, $df = 2$, $P = 0.937$; without bFGF: $t = 1.60$, $df = 2$, $P = 0.251$). The rapid doubling time of sanderling cells was also validated by examining the isolation timeline of these cells which revealed that sanderling cells reached confluency ~7 days earlier than isolated yellow-rumped warbler cells, additionally confirming their measured growth rates.

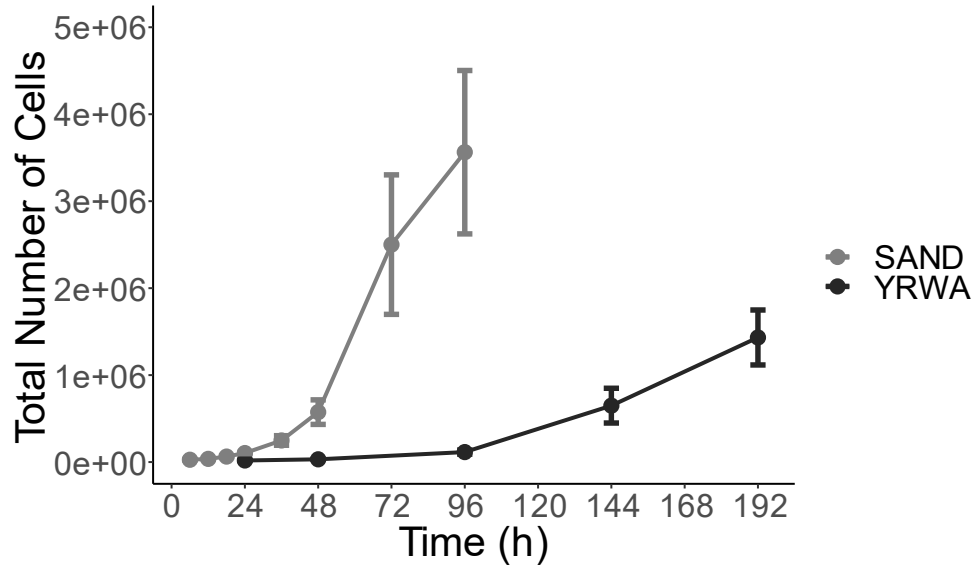


Figure 4. Growth curves of sanderling (gray; SAND) and yellow-rumped warbler (black; YRWA) satellite cells counted using a hemocytometer. At 0 h, 20,000 cells were plated in individual 35 mm plates and subsequently sampled and counted at specified timepoints to calculate total cells for yellow-rumped warbler (24, 48, 96, 144, 192 h) and sanderling (6, 12, 18, 24, 36, 48, 72, 96 h). Error bars represent standard error.

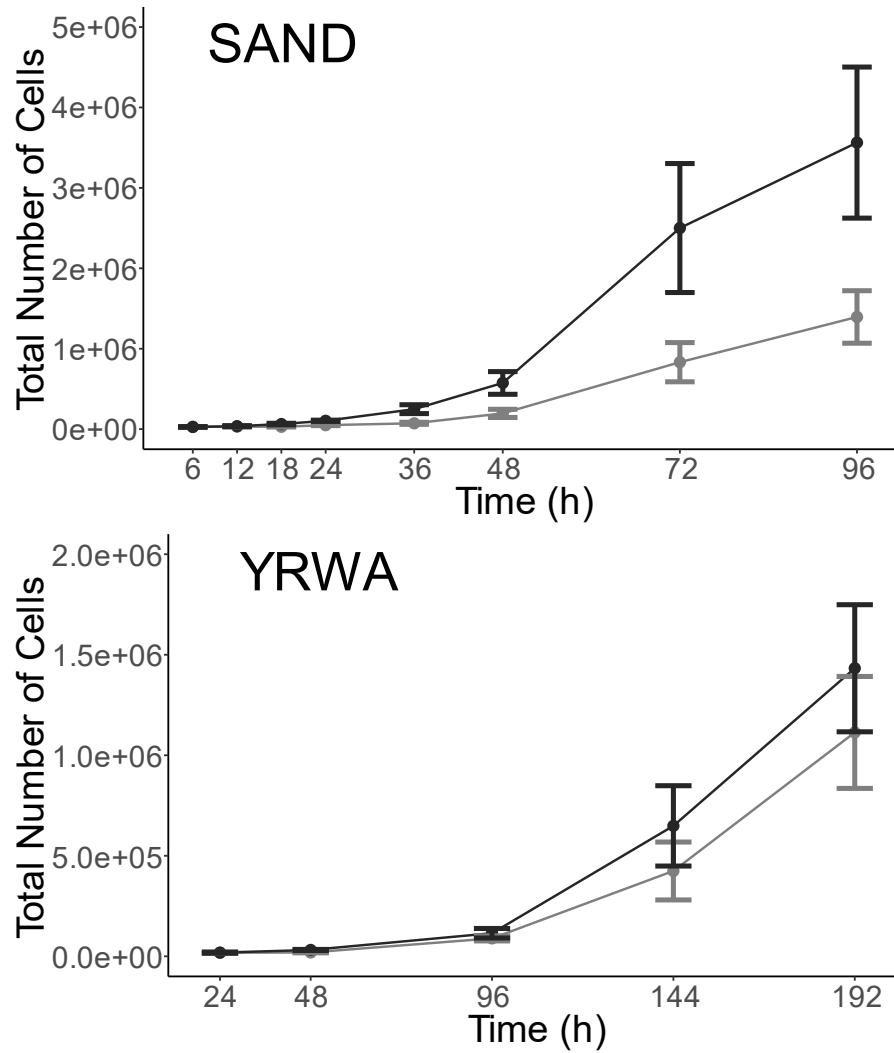


Figure 5. Total number of sanderling (top, n = 3; SAND) and yellow-rumped warbler (bottom, n = 5; YRWA) satellite cells at specified timepoints with or without basic fibroblast growth factor (bFGF). Cells without bFGF are represented in gray and cells with bFGF are shown in black. Cells were manually counted using a hemocytometer. Both sanderling and yellow-rumped warbler had improved growth rates with bFGF supplementation ($P < 0.05$). Error bars represent standard error.

3.1.2 Muscle-specific Protein Expression

Muscle-specific protein expression was qualitatively assessed by immunocytochemistry in cells fixed 1 d after plating, 3 and 6 d into differentiation. Pax7 expressing cells were present at each timepoint and appeared similarly abundant in both yellow-rumped warblers and sanderlings (Figures 6 and 7). Myosin was not expressed in the first timepoint, before differentiation, but was present at 3 and 6 d differentiation timepoints in both yellow-rumped warblers and sanderlings (Figures 8 and 9). Desmin expression was only assessed on day 3 of differentiation. Both yellow-rumped warbler and sanderling cells expressed desmin at this timepoint supporting the differentiation observed through myosin expression at this timepoint (Figures 10 and 11).

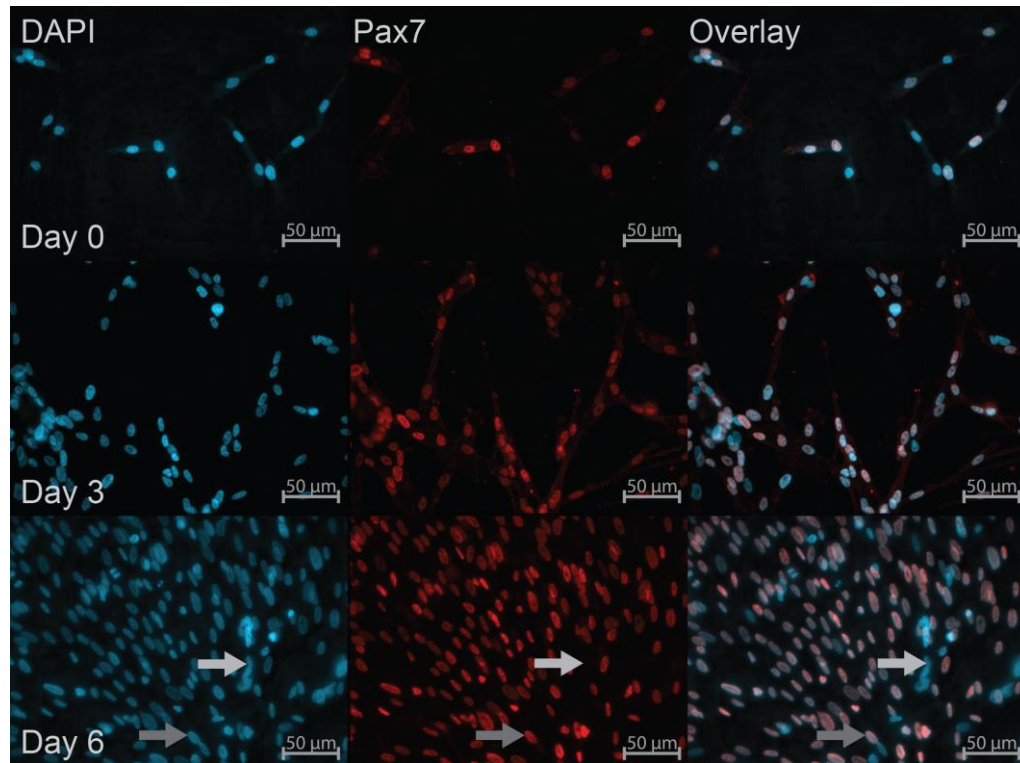


Figure 6. Representative images of yellow-rumped warbler satellite cells expressing Pax7 prior to, 3 and 6 days following differentiation into myotubes. Images on the left show DAPI stained nuclei in blue, center column images show nuclei stained for Pax7 in red, and the right panels are the overlaid images. Dark gray arrows indicate a cell expressing Pax7 and light gray arrows indicate a cell not expressing Pax7.

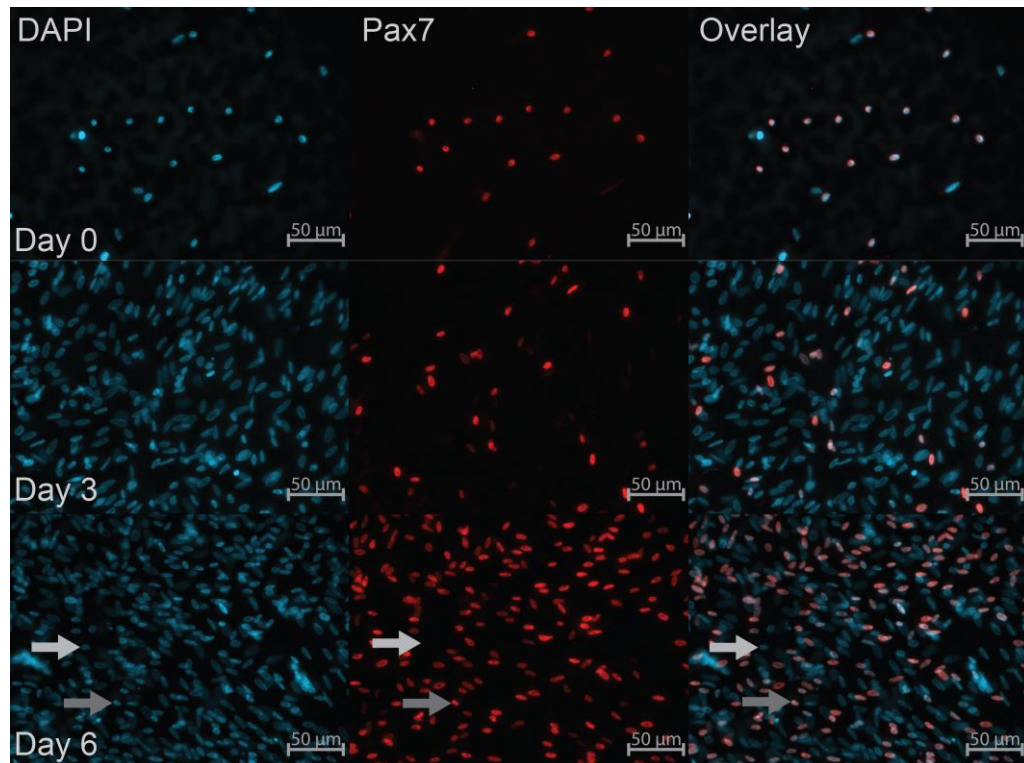


Figure 7. Representative images of sanderling satellite cells expressing Pax7 prior to, 3 and 6 days following differentiation into myotubes. Images on the left show DAPI stained nuclei in blue, center column images show nuclei stained for Pax7 in red, and the right panels are the overlaid images. Dark gray arrows indicate a cell expressing Pax7 and light gray arrows indicate a cell not expressing Pax7.

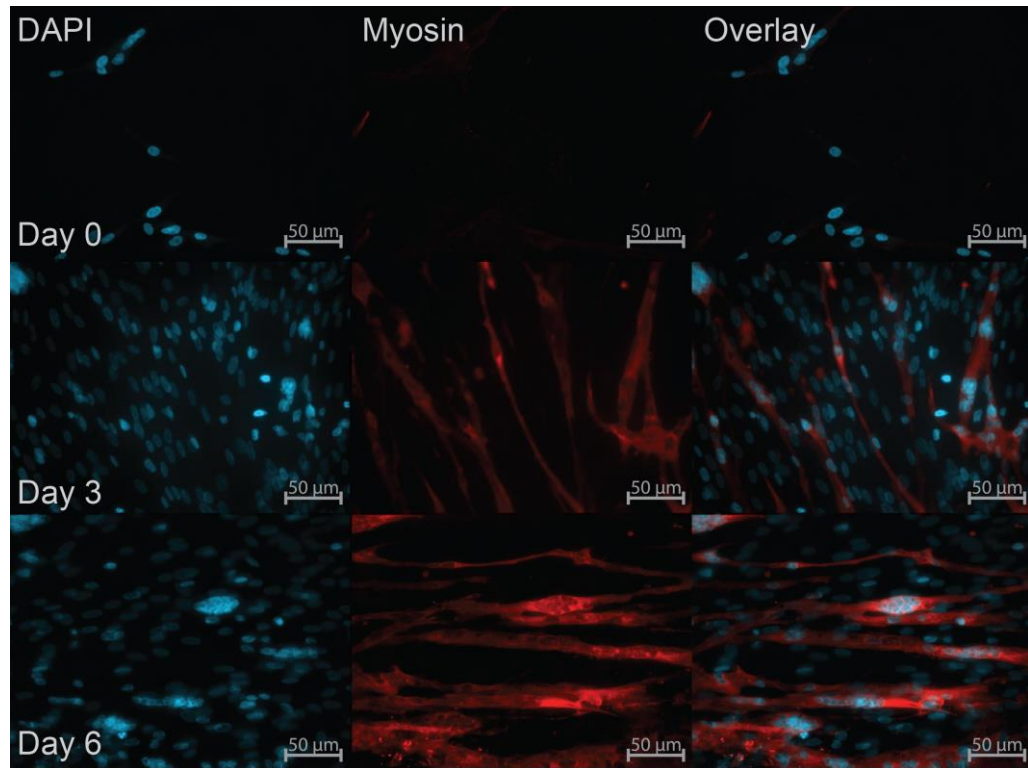


Figure 8. Representative images of yellow-rumped warbler satellite cells expressing myosin prior to, 3 and 6 days following differentiation into myotubes. Images on the left show DAPI stained nuclei in blue, center column images show cells stained for myosin in red, and the right panels are the overlaid images.

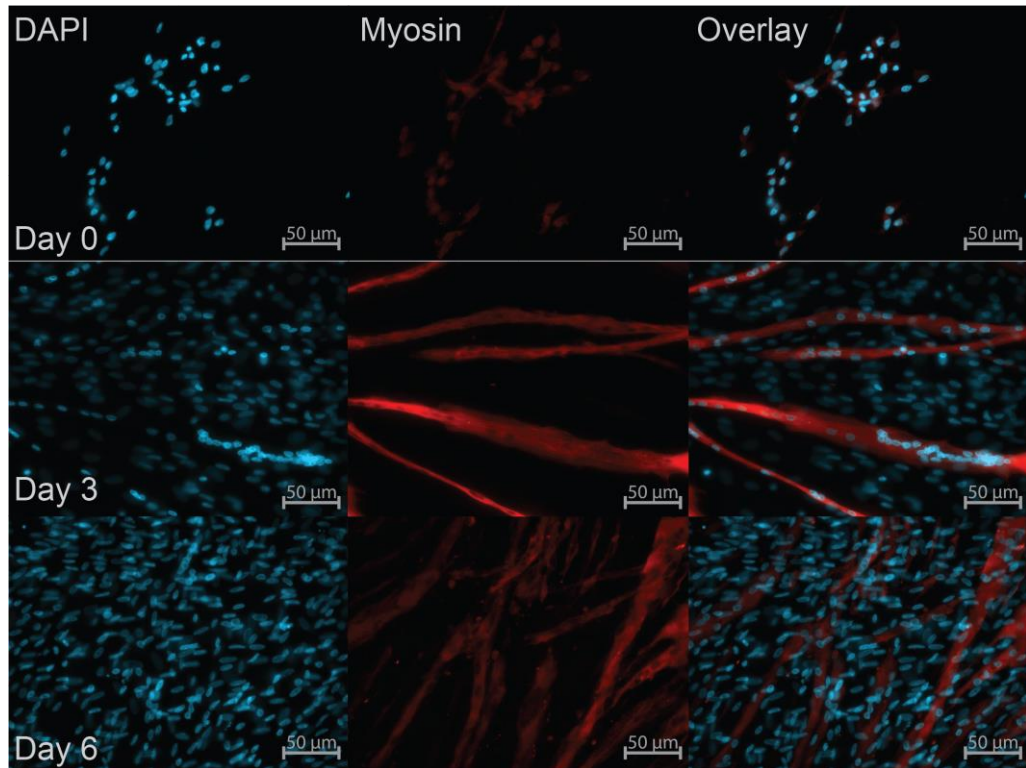


Figure 9. Representative images of sanderling satellite cells expressing myosin prior to, 3 and 6 days following differentiation into myotubes. Images on the left show DAPI stained nuclei in blue, center images show cells stained for myosin in red, and the right panels are the overlaid images.

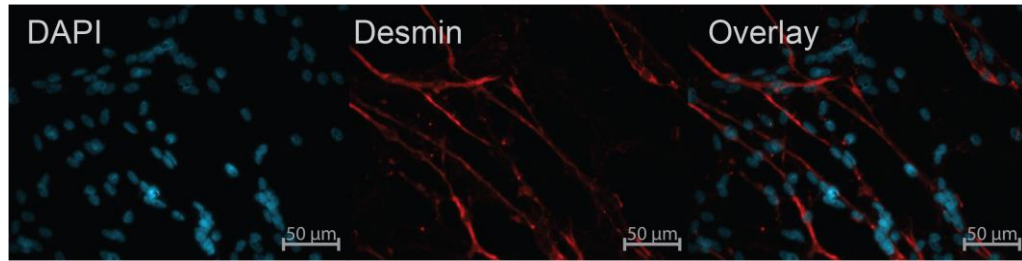


Figure 10. Representative images of yellow-rumped warbler satellite cells expressing desmin 3 days after differentiation into myotubes. Images on the left show DAPI stained nuclei in blue, center images show cells stained for desmin in red, and the right panels are the overlaid images.

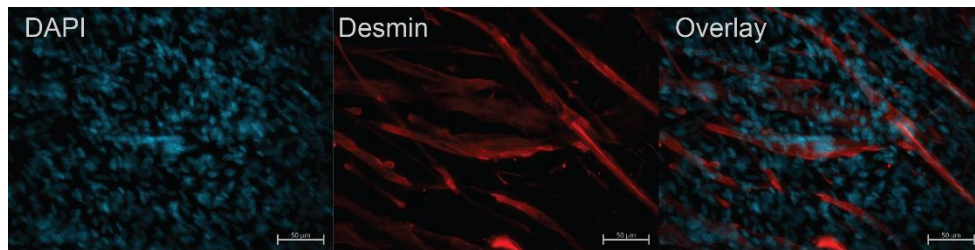


Figure 11. Representative images of sanderling satellite cells expressing desmin 3 days after differentiation into myotubes. Images on the left show DAPI stained nuclei in blue, center images show cells stained for desmin in red, and the right panels are the overlaid images.

3.2 Responses to PUFA Supplementation

3.2.1 Expression of PPARs and Fatty Acid Transporters

I measured differences in expression of *PPARs* α , β , and γ across treatments within each species. Expression of PPARs was less varied across treatments within yellow-rumped warblers and sanderlings compared to C₂C₁₂. *PPAR- α* expression was only different within sanderlings wherein pooled PUFA treated cells had greater expression than pooled BSA and OA treated cells ($F_{3,6} = 3.88$, $P = 0.074$; Contrast: $P = 0.042$; Figure 12C). *PPAR- α* expression was not different among treatments within C₂C₁₂ ($F_{3,9} = 0.71$, $P = 0.569$; Figure 12A) or yellow-rumped warblers ($F_{3,12} = 2.18$, $P = 0.144$; Figure 12B).

PPAR- β expression in C₂C₁₂ myotubes increased in DHA ($F_{3,9} = 15.13$, $P < 0.001$; Contrast: $P < 0.001$) and in pooled PUFA ($P < 0.001$) treated groups in comparison to BSA and BSA & OA pooled treatments respectively (Figure 12D). There was no difference in *PPAR- β* expression among treatments in yellow-rumped warbler ($F_{3,12} = 0.17$, $P = 0.917$; Figure 12E) or sanderling myotubes ($F_{3,6} = 2.73$, $P = 0.136$; Figure 12F).

PPAR- γ mRNA expression was greater in all FA treatments compared to BSA within C₂C₁₂ cells ($F_{3,9} = 23.10$, $P < 0.001$; OA: $P = 0.033$; DHA: $P < 0.001$; EPA: $P < 0.001$; Figure 12G). Additionally, *PPAR- γ* expression was greater in the pooled PUFA treatment groups compared to pooled BSA and OA ($P < 0.001$). However, no differences were found among treatments within yellow-rumped warbler ($F_{3,12} = 3.23$, $P = 0.061$; Figure 12H) or sanderling cells ($F_{3,6} = 0.78$, $P = 0.547$; Figure 12I). The comparison of *PPAR- γ* expression between BSA and DHA treated cells approached but did not reach significance in yellow-rumped warbler myotubes ($P = 0.056$).

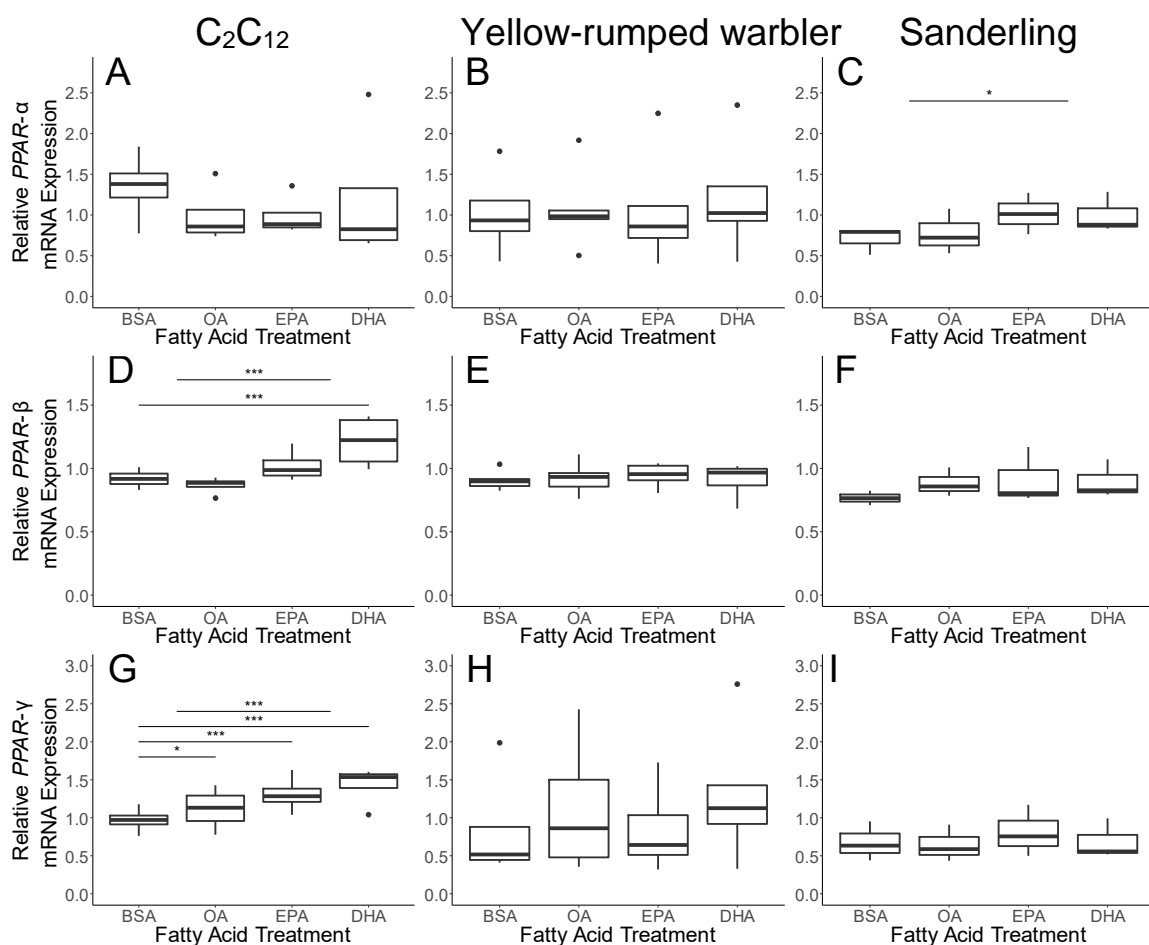


Figure 12. Relative expression of PPARs in *C2C12* (mouse), yellow-rumped warbler and sanderling myotubes supplemented with carrier (BSA), oleic acid (OA), eicosapentaenoic acid (EPA) or docosahexaenoic acid (DHA). Myotubes were supplemented with 100 μ M fatty acid conjugated to 50 μ M BSA or BSA only for 48 h prior to measurements. Boxplots represent the interquartile range with the thick line indicating the median value. Boxplot whiskers extend to 1.5 times beyond the interquartile range with individual points indicating values outside of that range. *PPAR- α* expression is shown in the top row (A-C), *PPAR- β* in the middle (D-F), and *PPAR- γ* on the bottom row (G-I). From left to right columns are *C2C12* (A, D, G, $n = 4$), yellow-rumped warbler (B, E, H, $n = 5$), and sanderling (C, F, I, $n = 3$) myotubes. Significant differences between treatments are denoted by lines at the top of individual plots. Contrasts were made between each treatment and the control (BSA) and a pooled comparison between BSA+OA and EPA+DHA. (* $P < 0.05$, ** $P < 0.01$, *** $P < 0.001$).

The expression of fatty acid transporters *CD36* and *FABP3* were more varied across treatments within all species. C₂C₁₂ myotubes treated with EPA had reduced *CD36* expression compared to the control group ($F_{3,9} = 6.37$, $P = 0.013$; Contrast: $P = 0.011$; Figure 13A) and PUFA treated cells had reduced expression compared to control and OA treated cells ($P = 0.020$). Conversely, *CD36* expression in yellow-rumped warblers was greater in EPA ($F_{3,12} = 6.16$, $P = 0.009$; Contrast: $P = 0.007$; Figure 13B) and DHA ($P = 0.009$) compared to BSA. Additionally, yellow-rumped warbler PUFA treated cells had greater expression of *CD36* in comparison to control and OA groups ($P = 0.005$). Sanderlings exhibited a similar *CD36* expression pattern to yellow-rumped warblers across treatments with EPA ($F_{3,6} = 14.52$, $P = 0.004$; Contrast: $P = 0.003$; Figure 13C) and DHA ($P = 0.006$), having greater expression compared to BSA and pooled PUFA ($P = 0.002$) treatments having greater expression compared to pooled BSA and OA treatments.

The expression pattern of *FABP3* was similar to *CD36* across species and treatments. C₂C₁₂ *FABP3* mRNA was less abundant in EPA compared to BSA treated cells ($F_{3,9} = 4.26$, $P = 0.039$; Contrast: $P = 0.028$; Figure 13D) and in the pooled PUFA treatments compared to pooled BSA and OA treatments ($P = 0.037$). Yellow-rumped warbler cells treated with DHA had greater *FABP3* expression compared to BSA ($F_{3,12} = 4.18$, $P = 0.003$; Contrast: $P = 0.027$; Figure 13E) and in PUFA treated groups compared to BSA and OA ($P = 0.041$). In sanderling myotubes, cells treated with EPA ($F_{3,6} = 7.66$, $P = 0.018$; Contrast: $P = 0.016$; Figure 13F) and DHA ($P = 0.014$) had greater *FABP3* expression compared to BSA and pooled PUFA treatments had greater expression in comparison to pooled control BSA and OA treatments ($P = 0.014$).

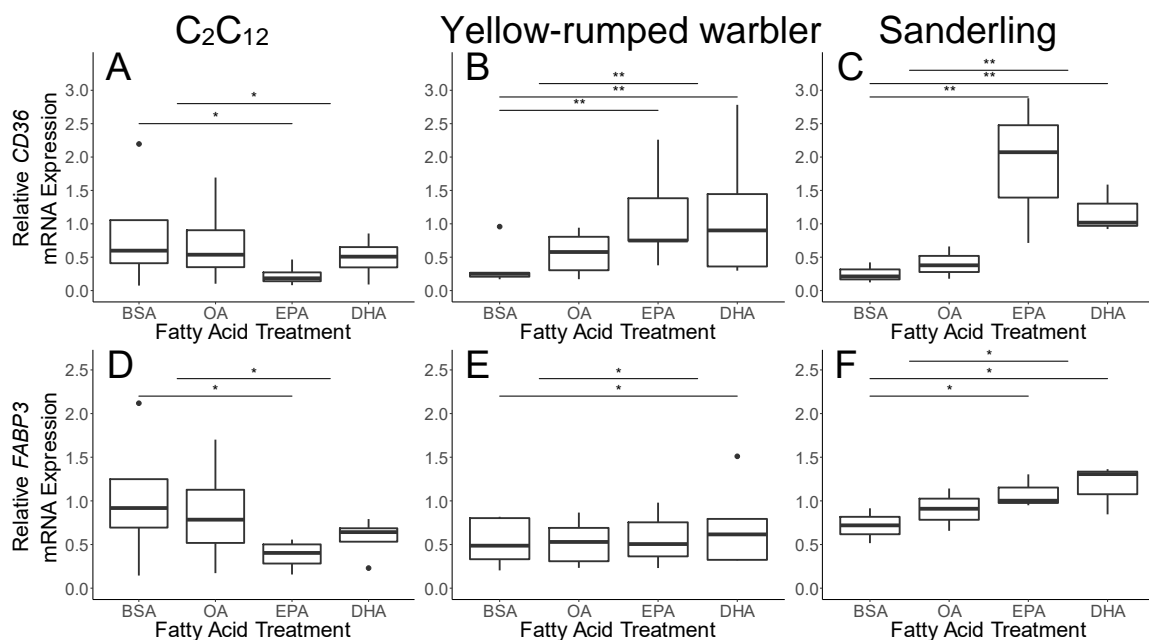


Figure 13. Relative expression of *CD36* (A-C) and *FABP3* (D-F) in C₂C₁₂ (mouse), yellow-rumped warbler and sanderling myotubes supplemented with carrier (BSA), oleic acid (OA), eicosapentaenoic acid (EPA) or docosahexaenoic acid (DHA).

Myotubes were supplemented with 100 μ M fatty acid conjugated to 50 μ M BSA or BSA only for 48 h prior to measurements. Boxplots represent the interquartile range with the thick line indicating the median value. Boxplot whiskers extend to 1.5 times beyond the interquartile range with individual points indicating values outside of that range. From left to right columns are C₂C₁₂ (A, D, n = 4), yellow-rumped warblers (B, E, n = 5), and sanderlings (C, F, n = 3). Significant differences between treatments are denoted by lines at the top of individual plots. Contrasts were made between each treatment and the control (BSA) and a pooled comparison between BSA+OA and EPA+DHA. (* P<0.05, ** P<0.01, *** P<0.001).

3.2.2 Enzyme Activities

Citrate synthase activity was similar across all FA treatments within each species (C₂C₁₂: $F_{3,9} = 1.73$, $P = 0.230$; yellow-rumped warbler: $F_{3,12} = 0.43$, $P = 0.739$; sanderling: $F_{3,6} = 2.07$, $P = 0.206$; Figure 14A-C). These results were paralleled by LDH activity, which exhibited no differences across treatments within each species (C₂C₁₂: $F_{3,9} = 0.31$, $P = 0.817$; yellow-rumped warbler: $F_{3,12} = 1.35$, $P = 0.304$; sanderling: $F_{3,6} = 2.11$, $P = 0.200$; Figure 14D-F). HOAD activity was similar among treatments in C₂C₁₂ and sanderling cells (C₂C₁₂: $F_{3,9} = 0.30$, $P = 0.822$; sanderling: $F_{3,6} = 0.71$, $P = 0.583$; Figure 15A,C). Yellow-rumped warblers exhibited increased HOAD activity in the pooled PUFA treatments in comparison to pooled BSA and OA ($F_{3,12} = 3.69$, $P = 0.043$; Contrast: $P = 0.026$; Figure 15B). C₂C₁₂ CPT activity was greater in EPA treated cells compared to BSA ($F_{3,9} = 4.92$, $P = 0.027$; Contrast: $P = 0.049$; Figure 15D) and pooled PUFA treated cell groups had greater activity than pooled BSA and OA treatments ($P = 0.030$). Conversely, yellow-rumped warbler CPT activity was greater in DHA treated cells ($F_{3,12} = 10.33$, $P = 0.001$; Contrast: $P = 0.038$; Figure 15E) but also had greater activity in the pooled PUFA cell groups in comparison to the pooled BSA and OA groups ($P < 0.001$). Yellow-rumped warbler OA treated cells had lower CPT activity relative to BSA ($P = 0.034$). Similar to the HOAD results in sanderling cells, there were no differences in CPT activity among any of the treatment groups ($F_{3,6} = 0.78$, $p = 0.545$; Figure 15F).

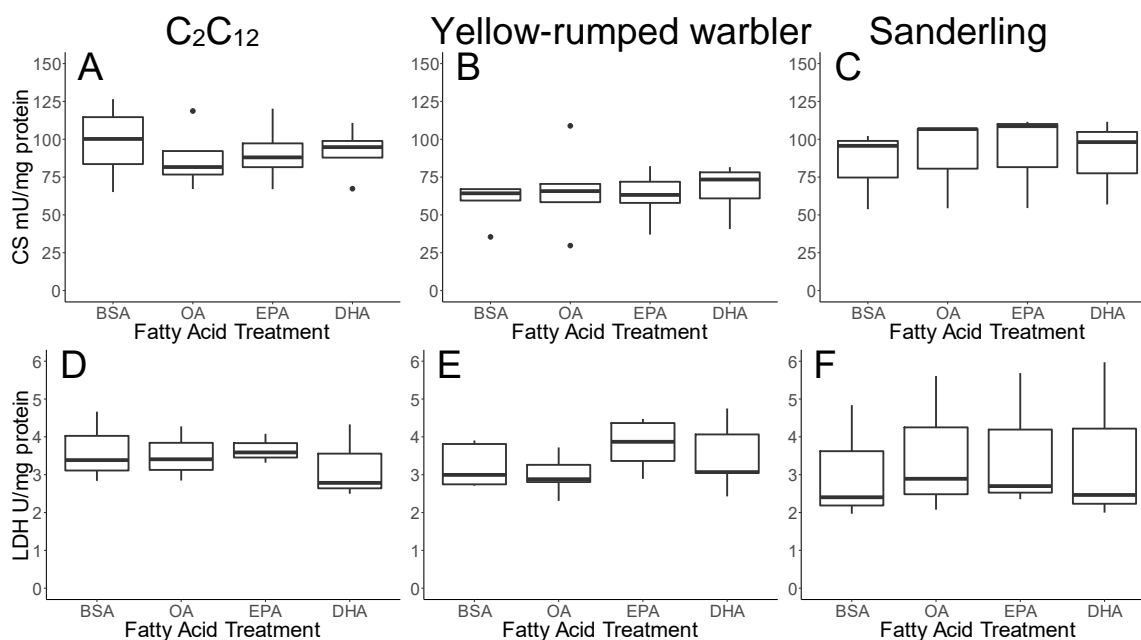


Figure 14. Maximum activity of citrate synthase (CS) in mU/mg protein (A-C) and lactate dehydrogenase (LDH) in U/mg protein (D-F) from C₂C₁₂ (mouse), yellow-rumped warbler and sanderling myotubes supplemented with carrier (BSA), oleic acid (OA), eicosapentaenoic acid (EPA) or docosahexaenoic acid (DHA). Myotubes were supplemented with 100 μ M fatty acid conjugated to 50 μ M BSA or BSA only for 48 h prior to measurements. Boxplots represent the interquartile range with the thick line indicating the median value. Boxplot whiskers extend to 1.5 times beyond the interquartile range with individual points indicating values outside of that range. Columns from left to right represent C₂C₁₂ (A, D, n = 4), yellow-rumped warbler (B, E, n = 5), and sanderling (C, F, n = 3) activity. Significant differences between treatments are denoted by lines at the top of individual plots. Comparisons were made between each treatment and the control (BSA) and a pooled comparison between BSA+OA and EPA+DHA. (* P<0.05, ** P<0.01, *** P<0.001).

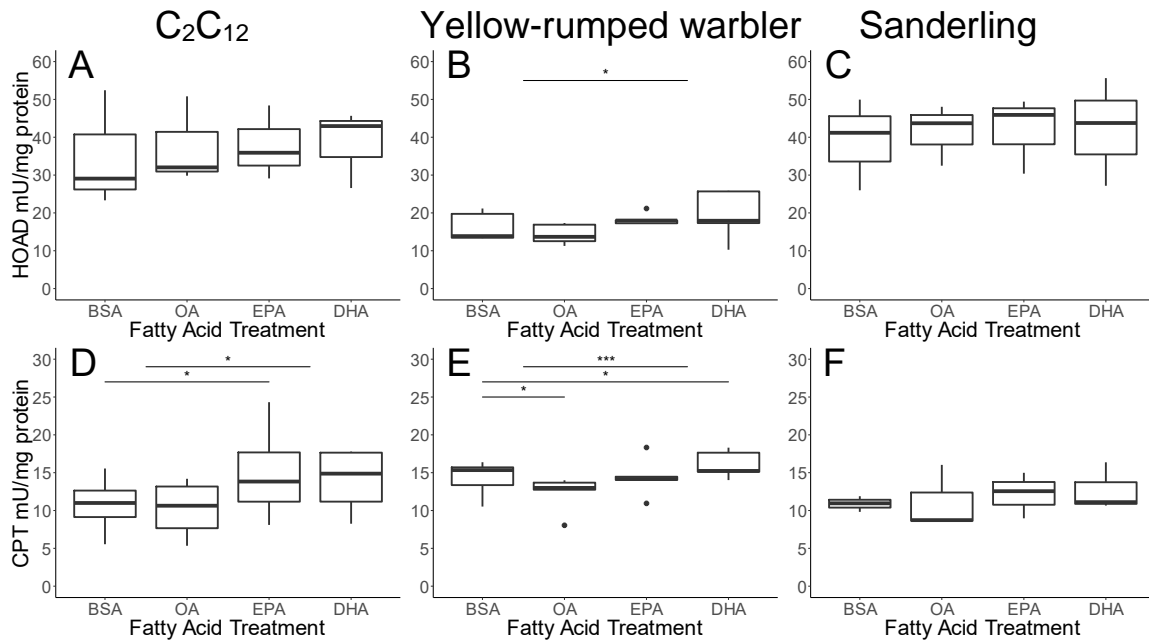


Figure 15. Maximum activity of β -hydroxyacyl-CoA dehydrogenase (HOAD) (A-C) and carnitine palmitoyltransferase (CPT) in mU/mg protein (D-F) from C₂C₁₂ (mouse), yellow-rumped warbler and sanderling myotubes supplemented with carrier (BSA), oleic acid (OA), eicosapentaenoic acid (EPA) or docosahexaenoic acid (DHA). Myotubes were supplemented with 100 μ M fatty acid conjugated to 50 μ M BSA or BSA only for 48 h prior to measurements. Boxplots represent the interquartile range with the thick line indicating the median value. Boxplot whiskers extend to 1.5 times beyond the interquartile range with individual points indicating values outside of that range. Columns from left to right represent C₂C₁₂ (A, D, n = 4), yellow-rumped warbler (B, E, n = 5), and sanderling (C, F, n = 3) activity. Significant differences between treatments are denoted by lines at the top of individual plots. Comparisons were made between each treatment and the control (BSA) and a pooled comparison between BSA+OA and EPA+DHA. (* P<0.05, ** P<0.01, * P<0.001).**

3.2.3 Aerobic Profile

Baseline measurements of ETC OCR (Table 3) were similar among treatments within C₂C₁₂ cells ($F_{3,9} = 2.52$, $P = 0.124$; Figure 16A). Sanderling cells had elevated ETC OCR proportion in the EPA treatment group compared to BSA ($F_{3,6} = 7.82$, $P = 0.017$; Contrast: $P = 0.010$; Figure 16B) and pooled PUFA groups had greater ETC OCR compared to pooled BSA and OA treatments ($P = 0.015$). Conversely, ATP production measured through ATPase OCR proportion was greater in OA ($F_{3,9} = 7.98$, $P = 0.007$; Contrast: $P = 0.011$; Figure 16C) and DHA treated cells ($P = 0.024$) relative to BSA in C₂C₁₂ myotubes. Sanderling cells exhibited no differences in ATPase OCR among treatments ($F_{3,6} = 1.88$, $P = 0.235$; Figure 16D). Basal measurements of proton leak OCR were similar among treatments in C₂C₁₂ cells ($F_{3,9} = 2.64$, $P = 0.113$; Figure 16E), but differences among treatments were present in FA supplemented sanderling cells ($F_{3,6} = 6.79$, $P = 0.023$; Figure 16F). EPA treated sanderling cells had greater proton leak OCR relative to BSA ($P = 0.023$), and PUFA treated cells had greater proton leak compared to pooled BSA and OA treatments ($P = 0.027$).

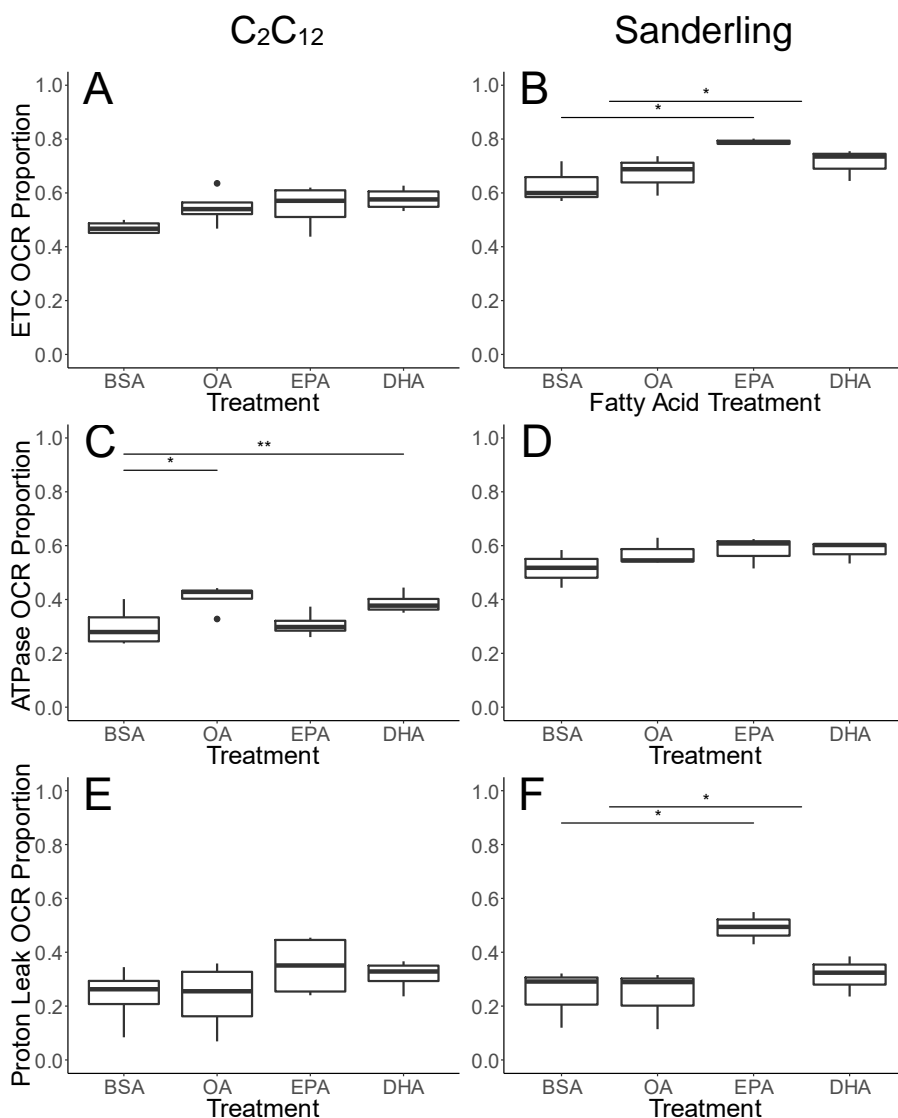


Figure 16. Oxygen consumption rate (OCR) proportions of C_2C_{12} (mouse) and sanderling myotubes measured during a modified mito-stress test using an XFe24 Seahorse following treatment with fatty acids: oleic acid (OA), eicosapentaenoic acid (EPA), docosahexaenoic acid (DHA) or carrier alone (BSA). Myotubes were supplemented with 100 μ M fatty acid conjugated to 50 μ M BSA or BSA only for 48 h prior to measurements and provided OA during the assay. Boxplots represent the interquartile range with the thick line indicating the median value. Boxplot whiskers extend to 1.5 times beyond the interquartile range with individual points indicating values outside of that range. The left column represents C_2C_{12} (A, C, E, $n = 4$) and the right represents sanderling (B, D, F, $n = 3$) OCR proportions calculated following Yépez et al. (2018; Table 3). The top row represents the ETC dependent OCR under basal conditions, middle row represents the ATPase dependent OCR and the bottom row represents the ETC dependent, non-ATPase linked OCR proportion (proton leak). Significant differences between treatments are denoted by lines at the top of individual plots. Comparisons were made between each treatment and the control (BSA) and a pooled comparison between BSA+OA and EPA+DHA. (* $P < 0.05$, ** $P < 0.01$, *** $P < 0.001$).

Measures of elevated OCR by inhibition of ATPase and mitochondrial membrane uncoupling were similar across treatments within C₂C₁₂ myotubes. Spare capacity OCR was not different among treatments within C₂C₁₂ treated cells ($F_{3,9} = 2.35$, $P = 0.140$; Figure 17A). These results paralleled the maximum respiration fold difference in OCR, which was similar among treatments within C₂C₁₂ ($F_{3,9} = 1.63$, $P = 0.250$; Figure 17C).

Both spare and maximal capacity OCR (Table 3) measured in sanderling cells violated the assumption of equality of variance primarily due to an extreme outlier in the EPA treatment group. I checked this value and the OCR trace throughout the assay was normal and there were no reasons to remove it from the analysis. These data did not fit ANOVA criteria under continuous transformations and were rank transformed before conducting the analysis. Sanderling cells exhibited greater spare capacity OCR in all FA treatments relative to BSA ($F_{3,6} = 11.34$, $P = 0.040$; OA: $P = 0.014$; DHA: $P = 0.004$; EPA: $P = 0.010$; Figure 17B). Pooled PUFA treatments also had greater spare capacity OCR compared to pooled BSA and OA treatments ($P = 0.010$). There were also differences in maximal capacity among treatments within sanderlings with both EPA ($F_{3,6} = 15.62$, $P = 0.003$; Contrast: $P = 0.002$; Figure 17D) and DHA ($P = 0.012$) resulting in greater OCR. However, there was no difference between BSA and OA treatments ($P = 0.091$). In concordance with these results, the PUFA treatment groups had greater maximum OCR than pooled BSA and OA ($P = 0.002$).

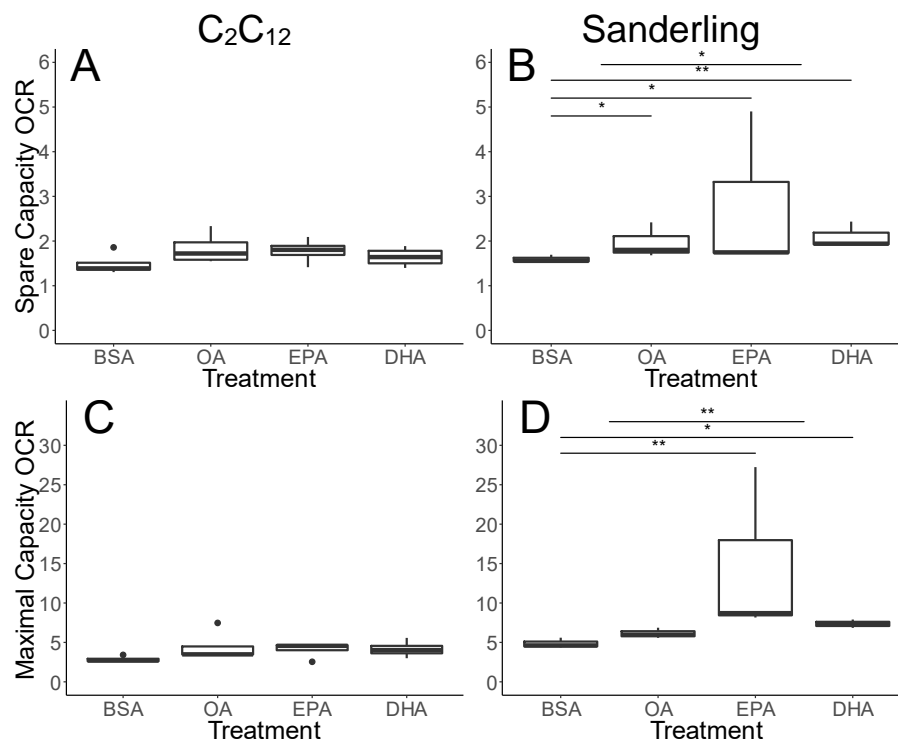


Figure 17. Oxygen consumption rate (OCR) fold changes of C_2C_{12} (mouse) and sanderling myotubes measured during a modified mito-stress test using an XFe24 Seahorse following treatment with fatty acids: oleic acid (OA), eicosapentaenoic acid (EPA), docosahexaenoic acid (DHA) or carrier alone (BSA). Myotubes were supplemented with 100 μ M fatty acid conjugated to 50 μ M BSA or BSA only for 48 h prior to measurements and provided OA during the assay. Boxplots represent the interquartile range with the thick line indicating the median value. Boxplot whiskers extend to 1.5 times beyond the interquartile range with individual points indicating values outside of that range. The left column represents C_2C_{12} (A, C, $n = 4$) and the right represents sanderling (B, D, $n = 3$) OCR fold changes calculated following Yépez et al. (2018; Table 3). The top row (A, B) represents the metabolic spare capacity above basal conditions and the bottom row (C, D) represents the maximal metabolic capacity. Significant differences between treatments are denoted by lines at the top of individual plots. Comparisons were made between each treatment and the control (BSA) and a pooled comparison between BSA+OA and EPA+DHA. (* $P < 0.05$, ** $P < 0.01$, *** $P < 0.001$).

4 Discussion

Cell culture systems permit the examination of biological phenomena that are otherwise inaccessible to whole animal studies. Current methods are well-established for isolating muscle satellite cells from mammals and domesticated embryonic and young birds. However, until now methods for the isolation of adult avian muscle satellite cells had not been successful. As the primary focus of my thesis, I aimed to establish adult avian primary muscle cell culture from wild-sourced migratory birds and to evaluate the response of muscle cells to supplementary n-3 PUFA treatment in the three models described. I was successful in achieving these two aims and my results describe the characteristics of avian muscle cell culture that parallel those of mammalian culture systems. Additionally, I examine the role of n-3 PUFA in a migrant shorebird muscle model with comparisons to a terrestrial migrant songbird and an established mammalian skeletal muscle model.

4.1 Avian Myocyte Characteristics *in vitro*

The skeletal muscle models I established from yellow-rumped warblers and sanderlings adhered well to the general characteristics of mammalian (vertebrate) cell culture. The addition of bFGF to growth media increased the growth rate of both yellow-rumped warbler and sanderling satellite cells (Figure 5). The growth rate of isolated yellow-rumped warbler satellite cells was within the expected range of typical primary cultures or immortalized cell lines with population doubling times of ~24h (Figure 4). Sanderling cells grew very rapidly reaching confluency faster than expected initially and reaching doubling times as low as ~8 h determined by manual counts and ~12 h as measured by both hemocytometer and flow cytometry (Figure 4). Such rapid rates of growth have not been found in primary cultures of other cell types from vertebrates as primary cells are typically expected to proliferate more slowly, especially from adult animals (Chakravarthy et al., 2000; Pääsuke et al., 2016). Some immortalized cell lines display similarly rapid growth rates, but these are characteristic of cancerous cells or similarly transformed mutants (Azmir et al., 2008; Iloki et al., 2013). Given that the very rapid growth rate of sanderling satellite cells is uncharacteristic of muscle progenitors, I speculate that the rapid proliferation rates observed in this culture system may signify

underlying mechanisms that permit similar growth rates in the muscle of sanderlings *in vivo*.

During muscle growth *in vivo*, satellite cells are recruited to contribute nuclei to growing muscle fibers or to differentiate into myocytes directly. Like other migratory birds, sanderlings undergo significant muscle growth during the migratory period before flying (Evans et al., 1992; Piersma et al., 2002). Significant muscle growth has also been measured in other migrant shorebirds and passerines (Akesson et al., 1992; Bauchinger and Biebach, 2006; Piersma, 1998). Relative to their wintering phenotype, migratory red knots (*Calidrus canutus islandica*) increase pectoral muscle mass by 43% with 12% gained in the final week before flight (Dietz et al., 1999; Piersma et al., 2002). During ~3-5 week stopovers both semipalmated sandpipers and bar-tailed godwits (*Limosa lapponica taymyrensis*) have been measured to accumulate a ~25% increase in pectoral muscle mass as they refuel (Driedzic et al., 1993; Landys-Ciannelli et al., 2003). These dramatic muscle mass increases in long-distance migrants are not unique to shorebirds as similar increases in flight muscle sizes have been measured in small passerines as well. Garden warblers (*Sylvia borin*) increase flight muscle mass 13% in advance of the migratory flights over the Saharan desert (Bauchinger and Biebach, 2006). Migrant yellow-rumped warbler and warbling vireos have pectoral muscle mass increases of 24 and 10% during spring migration relative to fall migration and summer respectively (King et al., 2015).

This pattern of increased muscle mass is consistent among migrant shorebirds and passerines; however, birds that undergo long, multi-day migratory flights catabolize significant amounts of lean mass including flight muscle (Akesson et al., 1992; Battley et al., 2000; Bauchinger et al., 2005; Piersma, 1998). Muscle catabolism occurs in long-distance migrant shorebirds during very long flights and garden warblers when flying over the Saharan desert (Battley et al., 2000; Bauchinger et al., 2005; Piersma, 1998). Although muscle catabolism may occur to some degree in all birds during flight, it is most significant in birds flying over ecological barriers during extended non-stop flights (Akesson et al., 1992; Battley et al., 2000). Consequently, these birds must rapidly rebuild muscle tissue at stopovers whereas birds that undertake relatively shorter

nocturnal flights may not require muscle growth and repair at stopover to the same degree. Sanderlings and yellow-rumped warblers are exemplary species for this migratory strategy contrast because sanderlings undertake multi-day flights whereas yellow-rumped warbler fly only for multiple hours during their migratory flights (Dunn et al., 2006; Hunt and Flaspohler, 1998; Macwhirter et al., 2002; Myers et al., 1990). I suspect then that the growth rate of satellite cells observed *in vitro* is indicative of the muscle growth rates of sanderlings during migration. As sanderlings rebuild muscle during stopover, their muscle satellite cells may necessarily proliferate rapidly to facilitate the muscle growth required for a successful migration. This warrants further research to determine if satellite cells of other long-distance migrants have similarly high proliferation rates.

Muscle satellite cells are multipotent stem cells that can differentiate into different cell types *in vitro* (Asakura et al., 2001). Myogenic satellite cells can be identified by their expression of Pax7 (Zammit et al., 2006). Similarly, muscle-specific proteins including desmin and sarcomeric myosin can be used to identify differentiating myotubes (Baquero-Perez et al., 2012). I confirmed the identity of isolated cells by staining for Pax7, desmin and sarcomeric myosin. Pax7 was expressed in yellow-rumped warbler and sanderling cell populations both before and after differentiation commenced (Figure 6 and 7). The retention of Pax7 expressing cells throughout differentiation is consistent with the maintenance of a 'reserve' population of mononucleated myogenic cells. Myosin was only expressed after differentiation was induced by switching media in both sanderling and yellow-rumped warbler cells (Figure 8 and 9). Desmin was also expressed abundantly in fused cells from both yellow-rumped warbler and sanderling cells (Figure 10 and 11). Furthermore, I observed cells contracting in culture as early as three days into differentiation. The expression of these muscle-specific markers and the physical contraction of myotubes in culture provide strong evidence that I isolated myogenic progenitor cells and differentiated them in culture.

These presence of satellite and muscle cell specific markers at specific developmental time points allowed me to identify these cell types and the results are consistent with work conducted in mammalian cell culture (Baquero-Perez et al., 2012).

Together, the growth and differentiation characteristics of these isolated muscle progenitor cells validated their use as an experimental muscle model for adult birds.

4.2 Comparative Influence of n-3 PUFA on Muscle Cell Metabolism

Studies of migrant shorebirds consuming diets abundant in n-3 PUFAs have proposed that n-3 PUFA condition their muscles for flight by increasing metabolic enzyme activities and improving their aerobic capacity (Maillet, 2006; Maillet and Weber, 2007). Subsequent research has provided mixed support for the role of n-3 PUFA in promoting endurance performance, where aerobic enzyme activities have been analyzed in relation to tissue PUFA content or dietary PUFAs fed to captive birds (Dick and Guglielmo, 2019; Guglielmo, 2010; Nagahuedi et al., 2009; Price and Guglielmo, 2009). However, only some of these studies have evaluated exercise performance metrics and those that have did not provide support for natural doping (Dick and Guglielmo, 2019; Price and Guglielmo, 2009). Additionally, only observational studies have measured the correlative relationship between n-3 PUFA and aerobic enzyme activity in marine feeding shorebird migrants (Guglielmo, 2010; Maillet, 2006; Maillet and Weber, 2007).

Previous research has necessarily assumed that n-3 PUFA supplementation affects species similarly, however differences in the natural availability of n-3 PUFA to animals may influence their responses (Hixson et al., 2015). In my thesis I examined the role of n-3 PUFA supplementation in altering muscle metabolism specifically, isolating the influence that other organ systems may play in altering metabolism through dietary n-3 PUFA. Additionally, by using a comparative approach, my thesis examines the differential responses of three models to n-3 PUFA supplementation to test the hypothesis that n-3 PUFA alter muscle metabolism in a way that is consistent with improved performance and use of FA as fuel. Here I discuss the results of a comparative study examining the impact that n-3 PUFA supplementation has on the muscle of a terrestrial mammal, migrant songbird, and marine shorebird *in vitro*. The resultant differences in metabolic pathways and aerobic performance in sanderling and C₂C₁₂ cells are summarized in figure 18.

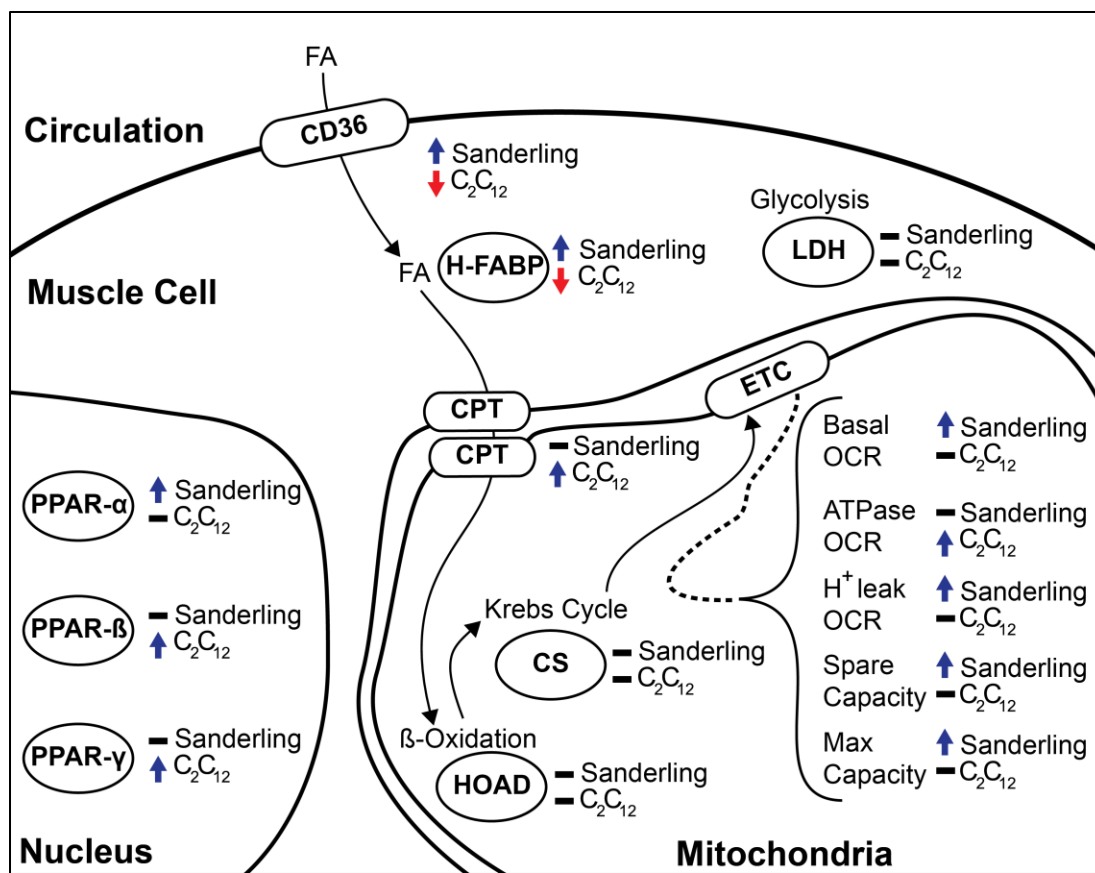


Figure 18. Summary of the effects of n-3 PUFA supplementation on C₂C₁₂ (mouse) and sanderling muscle cells. The depicted fatty acid (FA) transport and oxidation pathway is simplified from Figure 1. The effects of n-3 PUFA supplementation on mRNA expression of peroxisome proliferator-activated receptors (PPAR) α , β and γ are indicated in the nucleus and FA transporters cluster of differentiation 36 (CD36) and the heart-type fatty acid binding protein (H-FABP coded by *FABP3* gene) are indicated in the muscle cell. n-3 PUFA induced changes to enzyme activities are indicated for citrate synthase (CS), lactate dehydrogenase (LDH), β -hydroxyacyl-CoA dehydrogenase (HOAD) and carnitine palmitoyltransferases (CPT). Aerobic profile oxygen consumption rate (OCR) alterations by n-3 PUFA supplementation are indicated within the open curly bracket associated with the electron transport chain (ETC). Black dashes indicate that no change was induced by n-3 PUFA treatment, blue arrows pointing up indicate an increase in expression, activity, or OCR associated with n-3 PUFA treatment and red arrows pointing down indicate a decrease in the associated measurement with n-3 PUFA treatment.

4.2.1 The Differential Effects of n-3 PUFAs on mRNA Expression

I measured mRNA expression of PPARs and fatty acid transporters of C₂C₁₂, yellow-rumped warbler and sanderling muscle cells after 48 h treatment with FAs. Increases in PPAR expression after n-3 PUFA supplementation in C₂C₁₂ and sanderling but not yellow-rumped warbler cells suggests that n-3 PUFA upregulate FA metabolism in C₂C₁₂ and sanderling through different mechanisms (Figure 12).

PPAR-α upregulates expression of most genes associated with FA transport and oxidation and downregulates the use of alternative fuels (Han et al., 2017a; Huang et al., 2002). Additionally, avian *PPAR-α* expressed in C₂C₁₂ myotubes upregulates FA transport and metabolism (Hamilton et al., 2018). Consequently, the increased expression of *PPAR-α* in n-3 PUFA treated sanderling muscle indicates that these cells are directed towards increasing their FA oxidation potential and use of FA substrates for energy production (Figure 12C).

PPAR-β and *γ* function similarly to *PPAR-α* by increasing FA metabolism but also upregulate the expression of genes not directly associated with FA metabolism resulting in different phenotypes associated with the expression of each (Gan et al., 2011; Han et al., 2017b; Norris et al., 2003). Expression of *PPAR-β* in muscle is associated with increased glucose uptake and metabolism and running endurance performance (Gan et al., 2011; Wang et al., 2004). Whereas the role of *PPAR-γ* in muscle is in maintaining energy balance, insulin sensitivity and uptake of circulating lipids (Han et al., 2017b; Norris et al., 2003). Consequently, the increased expression of *PPAR-β* and *γ* in C₂C₁₂ cells suggests that n-3 PUFAs induce an overall upregulation of aerobic metabolism in C₂C₁₂ cells and not a FA oxidation specific strategy as in the sanderling (Figure 12D and G). Additionally, C₂C₁₂ cells treated with OA increased *PPAR-γ* expression, implicating OA as a positive regulator of energy balance in mammalian skeletal muscle but to a lesser degree than n-3 PUFA.

Increased expression of PPARs after n-3 PUFA treatment in C₂C₁₂ and sanderling cells suggests that n-3 PUFA promote FA metabolism in muscle but through different mechanisms. The differences in PPAR expression between C₂C₁₂ and sanderling may

reflect differences in fuel selection with n-3 PUFA promoting a FA catabolism specific phenotype through increased *PPAR-α* expression in sanderling whereas increased expression of *PPAR-β* and *γ* indicates that FA and aerobic metabolism more broadly is upregulated in C₂C₁₂ cells. However, PPAR expression in yellow-rumped warbler cells was not altered by FA treatments indicating that n-3 PUFAs do not universally promote FA metabolism through changes in PPAR expression in agreement with previous research on yellow-rumped warblers fed n-3 PUFA diets (Dick and Guglielmo, 2019; Figure 12B, E and H).

The expression patterns of fatty acid transporters in muscle cells after n-3 PUFA treatment further indicate that C₂C₁₂ cells promote a different metabolic phenotype in comparison to sanderling. Both n-3 PUFA treated yellow-rumped warbler and sanderling cells increased expression of *CD36* and *FABP3* (Figure 13B, C, E and F). By contrast, n-3 PUFA treated C₂C₁₂ cells exhibited decreased expression of *CD36* and *FABP3* (Figure 13A and D). Both *FABP3* and *CD36* are associated with PPAR expression and are important cellular FA transporters (Hamilton et al., 2018). The decreased expression of these fatty acid transporters in C₂C₁₂ cells concomitant with increases in expression of *PPAR-β* and *γ* further suggest that C₂C₁₂ cells direct metabolic processes to a more generalized aerobic phenotype and maintain energy homeostasis in part by reducing intracellular FA availability through reduced transport (Han et al., 2017b). Conversely, increased expression of fatty acid transporters in sanderling and yellow-rumped warbler cells suggest that n-3 PUFA promote a FA metabolism focused phenotype in these avian cells. Birds are fat specialists in comparison to mammals and the promotion of FA metabolism is consistent with the preferential selection of FA as the primary substrate for mitochondrial energy production in birds whereas mammalian mitochondria predominantly select alternative fuel sources (Kuzmiak-Glancy and Willis, 2014).

The mRNA expression patterns I measured may also be explained in part by standard cell culture conditions, which provide energetic substrates *ad libitum*, simulating a constant ‘fed-state’. When fasted, expression of PPAR-β, H-FABP and CD36 increase in skeletal muscle and decrease when fed and refeeding (Holst et al., 2003). Although I have not presented direct evidence in this thesis, the counterintuitive increase in

expression of PPARs and a concurrent decrease in expression of FA transporters in C₂C₁₂ cells indicate that there may be an interactive effect between the feeding status of cells and the downstream regulation of PPAR targets in mammalian skeletal muscle supplemented with n-3 PUFAs (Hessvik et al., 2010). If elevated PPAR expression by PUFA supplementation differentially affects downstream FA transporters in a fasting state, PUFA supplementation could act to promote fuel switching by increasing sensitivity to PPAR ligands (circulating FAs) in mammalian skeletal muscle (Han et al., 2017b; Hessvik et al., 2010). Consequently, the expression patterns measured in C₂C₁₂ cells may be confounded by a fed-state paradigm that does not affect birds to the same extent. Similar to mammals, birds catabolize available carbohydrates in the fed state (Walsberg and Wolf, 1995). However, birds also have circulating plasma glucose levels that are ~2 times higher than similarly sized mammals, and as a result may not be in a similar 'feeding' state in comparison to cultured mammalian cells (Braun and Sweazea, 2008; Scanes and Braun, 2013). Consequently, n-3 PUFA may influence the expression of mammalian FA transporters differently in comparison to a fasted-state model.

Conversely, n-3 PUFA treated yellow-rumped warbler and sanderling cells exhibited increased expression of fatty acid transporters despite similar culture conditions to C₂C₁₂ cells. Yellow-rumped warbler cells increased expression of fatty acid transporters following n-3 PUFA treatment without changes in PPAR expression suggesting changes in transporter expression may be caused by PPAR activation alone. Similarly, n-3 PUFA induced FA transporter expression in sanderling cells but with coincident increased expression of *PPAR-α* suggesting that sanderling promote a feed-forward cycle effect through increasing PPAR expression with the availability of n-3 PUFAs and increased transport capacity (Glatz and Luiken, 2017).

4.2.2 Effects of n-3 PUFA on Metabolic Enzyme Activities

Enzyme activities provide insight into the functional capacity of key metabolic pathways and permit inferences about organ-specific or whole animal metabolism. I measured similar CS and LDH activities among FA treatments within all three muscle models tested (Figure 14). CS activity is a useful index of aerobic capacity and correlates with mitochondrial content of tissue (Wang et al., 1999). Consequently, a change in CS

activity would have implied a change in mitochondria quantity. Previous research and the current study does not support the hypothesis that n-3 PUFAs stimulate mitochondrial biogenesis (Johnson et al., 2015). Relative changes in CS are often reflected by an inverse relationship with LDH activity (Dick and Guglielmo, 2019; McFarlan et al., 2009; Price et al., 2010; Zajac et al., 2011). The similarity in LDH activity between treatments here follows this pattern.

In contrast to the decreased mRNA expression of FA transporters, C₂C₁₂ myotubes had increased CPT activity with n-3 PUFA supplementation and particularly EPA (Figure 15D). This pattern of FA transporter expression and activity may reflect a coordinated increase in usage of intracellular FAs coincident with a reduction in the capacity to import extracellular FAs. The stable rate of HOAD activity across FA treatments does however suggest that n-3 PUFAs do not promote an increase in FA oxidation capacity under these conditions (Figure 15A).

Activities of HOAD and CPT in yellow-rumped warbler cells reflected a coordinated upregulation of FA metabolism with PUFA treatments and for CPT activity under DHA treatment in particular (Figure 15B and E). These results disagree with *in vivo* muscle enzyme activities in yellow-rumped warbler wherein muscle HOAD and CPT activity decreased following an n-3 PUFA dietary regime (Dick and Guglielmo, 2019). In contrast to the present study, the control diet was designated a monounsaturated FA diet and in the present study I measured a relative reduction in CPT activity in the OA treatment relative to BSA control. Differences in methodology and especially in models can elicit different responses from apparently similar treatments.

Sanderling cells did not exhibit changes in HOAD or CPT activity (Figure 15C and F). I expected the activities of these enzymes to increase under n-3 PUFA treatment in sanderling cells and the lack of change in the activity of HOAD and CPT indicates that n-3 PUFAs do not alter mitochondrial FA oxidation capacity. Although I predicted that n-3 PUFA would have an impact predominantly on sanderlings, yellow-rumped warbler and C₂C₁₂ cells were more affected than sanderlings.

Measuring the maximal activity of key metabolic enzymes provides insight into the potential aerobic and FA metabolism capacity. However, because maximal enzyme activities are not direct indicators of cell or organismal performance, these measurements are most usefully interpreted when paired with functional assays to identify measurable metabolic outcomes at higher levels of organization.

4.2.3 Effects of n-3 PUFA on the Aerobic Profiles of Sanderling and C₂C₁₂ (Mouse) Muscle Cells

It can be challenging to measure metabolic performance metrics, such as exercise capacity, but it is crucial to do so because they are more relevant to fitness outcomes than metabolic indicators such as transcription factors or enzyme activities. In the present study, I measured oxygen consumption rate (OCR) of C₂C₁₂ and sanderling myotubes at a baseline and following manipulation of ETC function to make inferences about the metabolic characteristics and flexibility of these cells under different FA treatments. C₂C₁₂ and sanderling myotubes responded differently to these manipulations, indicating species-specific responses to n-3 PUFA supplementation.

C₂C₁₂ cells had unchanged ETC and proton leak OCR across FA treatments, but both DHA and OA treated cells had a greater proportion of ATPase linked OCR (Figure 16A, C and E). This result is indicative of an increase in the ATP production efficiency of C₂C₁₂ cells under OA and DHA treatments but not EPA. Similarly increased efficiency in oxygen consumption has been measured in rat hearts and in exercising humans following dietary n-3 PUFA supplementation (Peoples et al., 2008; Pepe and McLennan, 2002). DHA specifically is the effector of cardiac benefits, not EPA (Stanley et al., 2012), as I similarly demonstrated in C₂C₁₂ myotubes in the present study. Oleic acid treated cells exhibited a similar effect through increased ATPase linked OCR, which may reflect a difference between mammalian skeletal muscle and cardiac function. C₂C₁₂ cells did not have measurable differences in spare or maximal capacity OCR across any FA treatments (Figure 17A and C). This suggests that the difference in ETC efficiency through increased ATPase linked OCR under basal conditions does not confer a measurable benefit under highly uncoupled conditions in skeletal muscle. Uncoupled respiration of n-3 PUFA supplemented cardiac mitochondria have lower oxygen consumption, matching

the increased efficiency under basal conditions (Stanley et al., 2012). Experimentally isolated mitochondria are often provided highly bioavailable fuel substrates (e.g. pyruvate) whereas in the present study I provided OA to specifically address FA utilization by intact cells (Kuzmiak-Glancy and Willis, 2014; Stanley et al., 2012). FAs are not typically catabolized by mammals during periods of high energy demand and so the similar spare and maximal OCR capacities among treatments within C₂C₁₂ may reflect inability of these cells to increase their use of FAs under uncoupled conditions despite increased efficiency under basal conditions (McClelland, 2004).

I prepared cells for aerobic profile assays by reducing energy substrate availability prior to commencing the assays but they are not depleted of intracellular energy stores required for basal cellular functions. Consequently, the substrate availability conditions present in these assays are most accurately described as a mixture of decreased intracellular energy stores due to the starvation media incubation and abundant extracellular OA. The lack of carry-over efficiency from basal conditions to the uncoupled state may be a result of shifting fuel selection toward depleted intracellular carbohydrate stores due to upstream transport limitations of FAs (Hessvik et al., 2010). Both *FABP3* and *CD36* mRNA expression were reduced in n-3 PUFA treated C₂C₁₂ myotubes and may limit FA mobilization, especially under uncoupled conditions.

In contrast to the basal respiratory characteristics of C₂C₁₂, sanderling cells exhibited an opposing pattern of increased ETC-dependent and proton leak OCR under EPA and pooled PUFA treatments and unchanged ATPase linked OCR (Figure 16B, D and F). Relative to C₂C₁₂ cells, it is apparent that sanderling myotubes responded in an opposite way to n-3 PUFA treatment. This opposing result suggests that sanderlings have a loss of ETC efficiency through increased proton leak (ATPase independent OCR) under EPA treatment. However, this effect is apparently overcome by increased ETC OCR resulting in a stable ATPase linked OCR across all treatments. The apparently positive health outcomes of n-3 PUFA supplementation to cardiac function in mammals, with a similar effect produced in this study, the ETC uncoupling of sanderling myotubes by EPA may be considered an adverse outcome that is necessarily compensated for by an increased basal ETC OCR (Berry et al., 2018; Peoples et al., 2008; Pepe and McLennan,

2002; Stanley et al., 2012). However, mitochondrial proton leak does not necessarily confer negative outcomes to cells and may be a byproduct of n-3 PUFA supplementation mechanistically induced by either the incorporation of n-3 PUFAs into mitochondrial membranes increasing ion leak or by regulating uncoupling proteins through PPAR activation (Berry et al., 2018; Han et al., 2017b; Porter et al., 1996).

Increased proton leak under n-3 PUFA treatment in basal conditions did not translate into a reduced metabolic potential in chemically induced uncoupling conditions. Sanderling myotubes exhibited increased spare capacity across all FA treatments, but to a greater degree in n-3 PUFA treatments, specifically EPA (Figure 17B). Maximal capacity OCR also increased in both n-3 PUFA treatments and the pooled comparison (Figure 17D). Consequently, the relative increase in OCR within n-3 PUFA treatments under both basal and uncoupled conditions indicates that despite the loss in ATP production efficiency by proton leak, sanderling myotubes can compensate by increasing overall OCR. Increased OCR may be a negative outcome of n-3 PUFA and EPA supplementation specifically in sanderling cells, but their ability to compensate by increasing OCR under both conditions suggests there are alternative explanations to consider.

Increased proton leak, or mild uncoupling, may provide some benefit separate from metabolic capacity considerations and I will briefly discuss two mechanisms through which proton leak is facilitated in context of n-3 PUFA supplementation and speculate on the impact increases in proton leak may have on cell and organismal physiology (Berry et al., 2018). Increased proton leak associated with n-3 PUFA supplementation likely occurs through the incorporation of these FAs into mitochondrial membranes, influencing fluidity and increasing permeability to ions including protons (Porter et al., 1996). Additionally, n-3 PUFA induce the expression of uncoupling proteins (UCP) through activation of PPARs or increased ROS production associated with the incorporation of n-3 PUFA into membranes, which induces UCP expression directly (Berry et al., 2018; Han et al., 2017a; Holst et al., 2003).

One potential alternative benefit of increased proton leak is the production of heat. This could be achieved through the expression of uncoupling proteins as triggered by upstream PPAR signaling or by physical changes to membranes through the incorporation of n-3 PUFA into phospholipids increasing viscosity and permeability (Hulbert and Else, 2005; Porter et al., 1996). Uncoupling proteins have a focal role in heat production within brown adipose tissue of mammals and UCP expression in mammalian these tissues is stimulated by n-3 PUFA supplementation (Jiyoung et al., 2016). However, birds do not have brown adipose tissue and are thought to rely primarily on active skeletal muscle shivering for thermogenesis (Vaillancourt et al., 2005). Cold-adapted birds do upregulate the avian UCP isoform in skeletal muscle and it is triggered by lipid signaling (Talbot et al., 2004), although whether specific FAs enhance UCP activity in birds is not known.

A second potential benefit to increased proton leak is the mitigation of reactive oxygen species (ROS) production (Cooper-Mullin and McWilliams, 2016). Reactive oxygen species can negatively impact cell physiology by causing damage to cell components through the formation of free radicals (Berry et al., 2018). Increased mitochondrial membrane uncoupling reduces the potential for ROS production by the ETC. The rate of ETC specific ROS production is influenced mainly by the strength of the proton motive force (pmf) which affects the rate of electron flux through the transport chain. When the pmf is high, ETC flux is low, causing the ETC to remain reduced for longer. Extended residence in the ETC by electrons increase the probability that they will react with oxygen to form ROS. Mild uncoupling of the mitochondrial membrane acts to reduce the pmf, increasing electron flux, and decreasing ROS production (Berry et al., 2018).

Periods of high energy consumption including exercise are known to increase ROS production through increased rates of oxygen flux in mitochondria and ETC activity (Berry et al., 2018). European starling (*Sternus vulgaris*) muscle mitochondria have increased ROS release immediately following flight, but this effect is mitigated in birds consuming high PUFA diets (Gerson, 2012). Although these birds did not fly to exhaustion, Gerson (2012) suggests that ROS accumulation may limit flight duration and

that PUFA supplementation may be one mechanism through which migrants limit ROS production. This argument is particularly compelling when considering long distance migrant sandpipers including sanderlings. The energetic challenge of migration is one of endurance, not acute cost alone (Guglielmo, 2018). Consequently, if endurance exercise capacity is limited by ROS production, then its mitigation through high n-3 PUFA diets may improve exercise endurance. Research on the endurance performance of terrestrial songbirds supplemented with n-3 PUFAs has not demonstrated measurable benefits in these birds (Dick and Guglielmo, 2019; Price and Guglielmo, 2009). However, the gene expression patterns and aerobic profiles of sanderlings I present in this thesis indicate that migrant sandpipers may have different outcomes.

Together these results indicate a species-specific role of n-3 PUFA in altering metabolic characteristics of murine and sandpiper skeletal muscle. The metabolic profile of C₂C₁₂ myotubes reflected that of *in vivo* experimental models that displayed enhanced metabolic efficiency through reduced oxygen consumption for the same amount of work with DHA specific supplementation (Peoples et al., 2008). However, the increased ETC efficiency in C₂C₁₂ myotubes treated with DHA may coincide with cellular damage due to increased ROS production (Berry et al., 2018; Hoffman and Brookes, 2009). DHA has been demonstrated to increase ROS production in C₂C₁₂ myotubes by reducing the activity of endogenous ROS scavenging enzymes (da Silva et al., 2016). The more tightly coupled ETC in the present study may be an additional mechanism through which C₂C₁₂ myotubes increase ROS production when treated with DHA.

The resultant metabolic profile of sanderling myotubes after n-3 PUFA supplementation provides support for the hypothesis that n-3 PUFA improve performance and use of FA as fuel in a migrant shorebird. OCR under chemically uncoupled conditions was greater with n-3 PUFA supplementation and EPA especially indicating an increase in maximal aerobic capacity (Figure 17C and D). Furthermore, the relative increase in proton leak suggests EPA may increase the ability of sanderlings to manage ROS production (Cooper-Mullin and McWilliams, 2016; Figure 16F). Consequently, migrant sanderlings may benefit from high n-3 PUFA diets, and specifically EPA, through increased aerobic capacity and reduced ROS production. The metabolic effects

of n-3 PUFA measured in the current study may translate to improved flight endurance in migrant sanderlings (Gerson, 2012).

4.3 Implications and Future Directions

My thesis represents the first work to successfully isolate skeletal muscle satellite cells from the flight muscle of adult birds and demonstrates that this method can be used to study wild migratory species which cannot be easily bred or obtained as embryos or neonates. This method permits the use of the *in vitro* molecular ‘toolkit’ previously accessible only to other model systems. Applications of both established and emerging molecular techniques provide the opportunity to expand our understanding of molecular signaling, protein function, cell physiology and metabolism in migrant birds. I will focus here on future directions closely related to the work I conducted in my thesis.

One strength of my thesis is its comparative approach. Physiological comparisons across taxa provide valuable insight into the functional responses of animals to the same stimuli or signal as in the present study, however my results must be carefully interpreted to avoid over-generalization. A focal assumption of my work is that the experimental models are representative of the broader taxa being considered. Previous work in this area has been critiqued in part for the selection of inappropriate model systems (Nagahuedi et al., 2009). Early studies on the association between aerobic enzyme activities and assimilated n-3 PUFAs in migrant sandpipers implicate shorebirds as ideal models for studying the role of n-3 PUFA in altering metabolism (Guglielmo et al., 2002b; Maillet, 2006; Maillet and Weber, 2007). Sanderling are closely related to the other *Calidris* sandpipers originally proposed to ‘naturally dope’ on high n-3 PUFA diets, but I cannot exclude the possibility that other species would exhibit differences under the PUFA treatments I used in the present study. However, the close relatedness of *Calidris* sandpipers, and given that the results of my thesis provide some support for the role of n-3 PUFA in promoting FA metabolism and improved performance, my work is assumed to be sufficiently representative of *Calidris* sandpipers in this context. Future research should investigate these differences across a wider diversity of bird species and properly account for phylogeny to determine if there are differences among shorebirds in the physiological effects of n-3 PUFA. Many terrestrial animals can elongate and desaturate

shorter chain n-3 PUFAs to produce n-3 PUFAs endogenously (Castro et al., 2012). Most marine fish are unable to produce n-3 PUFAs from their precursors whereas many freshwater fish can desaturate and elongate shorter chain n-3 PUFA (Vagner and Santigosa, 2011). It is possible then, that marine feeding animals more generally, including shorebirds, have a limited capacity to produce n-3 PUFA from precursors endogenously and must necessarily consume them in their diet. To fully understand the importance of n-3 PUFAs in the diets of birds, future studies should investigate and compare the desaturase and elongase activities of marine, freshwater, and terrestrial feeding birds. If shorebirds including the sanderling have a reduced capacity to elongate and desaturate n-3 PUFA precursors relative to terrestrial birds, then shorebirds will have a greater reliance on dietary n-3 PUFA and the environments they are in to reach their required n-3 PUFA levels.

My results indicate that n-3 PUFAs stimulate mitochondrial membrane uncoupling in sanderling muscle cells (Figure 16F). Mitochondrial membrane uncoupling mitigates ROS production by increasing electron flux through the ETC (Berry et al., 2018). The mechanisms by which migratory birds manage oxidative stress due to elevated ROS production is an important area of current research (Cooper-Mullin and McWilliams, 2016). Oxidative damage is elevated in migrant birds after extended flights, indicating that their elevated respiration rates when they are flying lead to elevated ROS production (Jenni-Eiermann et al., 2014; Skrip et al., 2015). Future studies should investigate the role of mitochondrial membrane uncoupling through the action of n-3 PUFAs in potentially regulating avian UCP and increasing membrane permeability by incorporation into membrane phospholipids (Hulbert and Else, 2005; Jiyoung et al., 2016; Porter et al., 1996). If elevated ROS production limits the flight endurance of migratory birds, n-3 PUFA dependent mitochondrial uncoupling may act to improve flight endurance through reduced ROS production and subsequent oxidative damage.

Lastly, the rapid growth rate of sanderling satellite cells observed in this study warrants future investigation. While it was not the focus of my thesis objectives, the rapid growth of sanderling satellite cells may indicate *in vivo* muscle growth potential. Sanderlings are long-distance migrants that undertake multi-day flights during migration

(Macwhirter et al., 2002; Myers et al., 1990). Multi-day flights like those completed by sanderlings, force birds to catabolize muscle and other lean tissue to fuel their locomotion which must be rebuilt during stopover refueling (Battley et al., 2000; Bauchinger et al., 2005; Piersma, 1998). Consequently, the migratory muscle growth, catabolism and regrowth during stopover necessitates a physiological means to grow muscle rapidly for the time constraining nature of migration (Åkesson and Hedenström, 2007). If the rapid proliferation rates I observed in sanderling satellite cells indicate *in vivo* requirements for rapid muscle growth associated with multi-day flight preparation and recovery, then other migrant species with similar migratory strategies should also exhibit very rapid proliferation rates. Future studies should conduct additional comparisons of isolated muscle satellite cells from shorebirds with similar migratory strategies and in passerines that undertake multi-day flights to cross large ecological barriers such as blackpoll warblers (*Setophaga striata*) and garden warblers (*Sylvia borin*).

4.4 Conclusions

I presented a validated method for the isolation of skeletal muscle progenitor satellite cells from adult migratory birds. I discovered that shorebird muscle cells appear to have extremely fast growth rates, more similar to cancer cells (Azmir et al., 2008; Iloki et al., 2013) than to typical vertebrate skeletal muscles (Pääsuke et al., 2016; Shahini et al., 2018) and this may relate to their unusual capacity to make and recover quickly from extreme non-stop flights lasting several days and covering thousands of kilometers (Macwhirter et al., 2002; Myers et al., 1990). Using my established skeletal muscle models, I examined the impact of n-3 PUFA supplementation on the metabolism of migrant birds and a non-migrant mammal *in vitro*. My research provides some support for the natural doping hypothesis, showing that there are species-specific metabolic responses to n-3 PUFA supplementation in muscle. Following n-3 PUFA supplementation, murine C₂C₁₂ myotubes increased expression of *PPAR-β* and γ suggesting an increased sensitivity to FA signaling and potentially downstream upregulation of FA and glucose metabolism.

Conversely sanderlings only upregulated *PPAR-α* suggesting an increase in FA catabolism downstream. Both sanderling and yellow-rumped warbler cells upregulated

mRNA of FA transporters whereas C₂C₁₂ decreased expression of the same messengers. FA oxidation and transport enzyme activities increased by n-3 PUFA in yellow-rumped warbler myocytes and only transport enzymes were increased in C₂C₁₂, whereas aerobic and FA oxidation enzymes unaffected by n-3 PUFA in sanderling cells. Cellular respirometry indicated that n-3 PUFA, specifically DHA, increase ETC efficiency in C₂C₁₂ but do not improve aerobic, whereas sanderlings exhibited increased basal and maximal aerobic capacities concomitant with evidence of increased proton leak when supplemented with EPA. The effects of n-3 PUFA supplementation on sanderling and C₂C₁₂ cells are summarized in figure 18.

My research suggests that the effects of n-3 PUFA supplementation on muscle metabolism are species-specific. My results indicate that all three species tested had increased FA metabolic capacity, but that mammalian and avian aerobic performance is differently impacted. Future studies should examine the role of n-3 PUFA in whole animals to determine if these effects scale up to performance and fitness and whether n-3 PUFAs improve metabolic capacity, endurance, oxidative damage mitigation, or some combination of these factors in migrant shorebirds.

References

- Aas, V., Bakke, S. S., Feng, Y. Z., Kase, E. T., Jensen, J., Bajpeyi, S., Thoresen, G. H. and Rustan, A. C.** (2013). Are cultured human myotubes far from home? *Cell Tissue Res.* **354**, 671–682.
- Agarwala, R., Barrett, T., Beck, J., Benson, D. A., Bollin, C., Bolton, E., Bourexis, D., Brister, J. R., Bryant, S. H., Canese, K., et al.** (2018). Database resources of the National Center for Biotechnology Information. *Nucleic Acids Res.* **46**, D8–D13.
- Ahlmann-Eltze, C.** (2017). ggsignif: Significance Brackets for “ggplot2.” *R package version 0.4.0*. <https://CRAN.R-project.org/package=ggsignif>.
- Akesson, S., Karlsson, L., Pettersson, J. and Walinder, G.** (1992). Body composition and migration strategies: a comparison between robins (*Erithacus rubecula*) from two stop-over sites in Sweden. *Vogelwarte* **36**, 188–195.
- Åkesson, S. and Hedenström, A.** (2007). How Migrants Get There: Migratory Performance and Orientation. *Bioscience* **57**, 123–133.
- Alerstam, T.** (2009). Flight by night or day? Optimal daily timing of bird migration. *J. Theor. Biol.* **258**, 530–536.
- Arnold, W., Giroud, S., Valencak, T. G. and Ruf, T.** (2015). Ecophysiology of Omega Fatty Acids: A Lid for Every Jar. *Physiology* **30**, 232–240.
- Asakura, A., Komaki, M. and Rudnicki, M.** (2001). Muscle satellite cells are multipotential stem cells that exhibit myogenic, osteogenic, and adipogenic differentiation. *Differentiation.* **68**, 245–253.
- Azmir, M. A., Maizirwan, M., Raha, A. R., Sharifah, S. H. and Aini, I.** (2008). Comparison of Growth Rate and Viability of Df-1 Cell Line in Different Culture Media. **12**, 1–5.
- Banerjee, S. and Chaturvedi, C. M.** (2016). Migratory preparation associated alterations in pectoralis muscle biochemistry and proteome in Palearctic-Indian emberizid migratory finch, red-headed bunting, *Emberiza bruniceps*. *Comp. Biochem. Physiol. Part D* **17**, 9–25.
- Baquero-Perez, B., Kuchipudi, S. V, Nelli, R. K. and Chang, K.-C.** (2012). A simplified but robust method for the isolation of avian and mammalian muscle satellite cells. *BMC Cell Biol.* **13**, 16.
- Battley, P. F., Piersma, T., Dietz, M. W., Tang, S., Dekinga, A. and Hulsman, K.** (2000). Empirical evidence for differential organ reductions during trans-oceanic bird flight. *Proc. R. Soc. London. Ser. B Biol. Sci.* **267**, 191–195.
- Bauchinger, U. and Biebach, H.** (2006). Transition between moult and migration in a long-distance migratory passerine: Organ flexibility in the African wintering area. *J. Ornithol.* **147**, 266–273.

- Bauchinger, U., Wohlmann, A. and Biebach, H.** (2005). Flexible remodeling of organ size during spring migration of the garden warbler (*Sylvia borin*). *Zoology* **108**, 97–106.
- Berger, J. and Moller, D. E.** (2002). The Mechanisms of Action of PPARs. *Annu. Rev. Med.* **53**, 409–435.
- Berry, B. J., Trewin, A. J., Amitrano, A. M., Kim, M. and Wojtovich, A. P.** (2018). Use the Protonmotive Force: Mitochondrial Uncoupling and Reactive Oxygen Species. *J. Mol. Biol.* **430**, 3873–3891.
- Blau, H. M., Pavlath, G. K., Hardeman, E. C., Chiu, C., Silberstein, L., Webster, S. G., Miller, S. C. and Webster, C.** (1987). Plasticity of the Differentiated State. *Science* (80-.). **230**, 758–766.
- Bordoni, A., Di Nunzio, M., Danesi, F. and Biagi, P. L.** (2008). Polyunsaturated fatty acids: From diet to binding to ppars and other nuclear receptors. *Genes Nutr.* **1**, 95–106.
- Bradley, S. S., Dick, M. F., Guglielmo, C. G. and Timoshenko, A. V.** (2017). Seasonal and flight-related variation of galectin expression in heart, liver and flight muscles of yellow-rumped warblers (*Setophaga coronata*). *Glycoconj. J.* **34**, 603–611.
- Braun, E. J. and Sweazea, K. L.** (2008). Glucose regulation in birds. *Comp. Biochem. Physiol. - B Biochem. Mol. Biol.* **151**, 1–9.
- Butler, P. J.** (1991). Exercise in Birds. *J. Exp. Biol.* **160**, 233–262.
- Carrel, A.** (1912). On the permanent life of tissues of the organism. *J. Exp. Med.* **15**, 516–528.
- Castro, L. F. C., Monroig, Ó., Leaver, M. J., Wilson, J., Cunha, I. and Tocher, D. R.** (2012). Functional Desaturase Fads1 ($\Delta 5$) and Fads2 ($\Delta 6$) Orthologues Evolved before the Origin of Jawed Vertebrates. *PLoS One* **7**, e31950.
- Chakravarthy, M. V., Abraha, T. W., Schwartz, R. J., Fiorotto, M. L. and Booth, F. W.** (2000). IGF-I Extends in vitro replicative life span of skeletal muscle satellite cells by enhancing G1/S cell cycle progression via the activation of PI3'-Kinase/Akt signaling pathway. *J. Biol. Chem.* **275**, 35942–52.
- Chen-Ming, F., Li, L., Rozo, M. E. and Lepper, C.** (2012). Making skeletal muscle from progenitor and stem cells: Development versus regeneration. *Wiley Interdiscip. Rev. Dev. Biol.* **1**, 315–327.
- Cooper-Mullin, C. and McWilliams, S. R.** (2016). The role of the antioxidant system during intense endurance exercise: lessons from migrating birds. *J. Exp. Biol.* **219**, 3684–3695.
- Cooper-Mullin, C., Jimenez, A. G., Anthony, N. B., Wortman, M. and Williams, J. B.** (2015). The metabolic rate of cultured muscle cells from hybrid *Coturnix* quail is intermediate to that of muscle cells from fast-growing and slow-growing *Coturnix* quail. *J. Comp. Physiol. B Biochem. Syst. Environ. Physiol.* **185**, 547–557.

- Cordain, L., Watkins, B. A., Florant, G. L., Kelher, M., Rogers, L. and Li, Y.** (2002). Fatty acid analysis of wild ruminant tissues: Evolutionary implications for reducing diet-related chronic disease. *Eur. J. Clin. Nutr.* **56**, 181–191.
- Corder, K. R., DeMoranville, K. J., Russell, D. E., Huss, J. M. and Schaeffer, P. J.** (2016). Annual life-stage regulation of lipid metabolism and storage and association with PPARs in a migrant species: the gray catbird (*Dumetella carolinensis*). *J. Exp. Biol.* **219**, 3391–3398.
- Crawford, M. A., Casperd, N. M. and Sinclair, A. J.** (1976). The long chain metabolites of linoleic and linolenic acids in liver and brain in herbivores and carnivores. *Comp. Biochem. Physiol. -- Part B Biochem.* **54**, 395–401.
- da Silva, E. P., Nachbar, R. T., Levada-Pires, A. C., Hirabara, S. M. and Lambertucci, R. H.** (2016). Omega-3 fatty acids differentially modulate enzymatic anti-oxidant systems in skeletal muscle cells. *Cell Stress Chaperones* **21**, 87–95.
- Deppe, J. L., Ward, M. P., Bolus, R. T., Diehl, R. H., Celis-Murillo, A., Zenzal, T. J. J., Moore, F. R., Benson, T. J., Smolinsky, J. A., Schofield, L. N., et al.** (2015). Fat, weather, and date affect migratory songbirds' departure decisions, routes, and time it takes to cross the Gulf of Mexico. *Proc. Natl. Acad. Sci.* **112**, E6331–E6338.
- Dick, M. F.** (2017). The long haul: migratory flight preparation and performance in songbirds. *Ph.D Thesis*. The University of Western Ontario, London, ON.
- Dick, M. F. and Guglielmo, C. G.** (2019). Dietary polyunsaturated fatty acids influence flight muscle oxidative capacity, but not endurance flight performance in a migratory songbird. *Am. J. Physiol. - Regul. Integr. Comp. Physiol.*
- Dietz, M. W. and Piersma, T.** (2007). Red knots give up flight capacity and defend food processing capacity during winter starvation. *Funct. Ecol.* **21**, 899–904.
- Dietz, M. W., Piersma, T. and Dekinga, A.** (1999). Body-building without power training: Endogenously regulated pectoral muscle hypertrophy in confined shorebirds. *J. Exp. Biol.* **202**, 2831–2837.
- Dingle, H.** (2014). *Migration: The Biology of Life on the Move*. 2nd ed. New York, NY: Oxford University Press.
- Dingle, H. and Winchell, R.** (1997). Juvenile hormone as a mediator of plasticity in insect life histories. *Arch. Insect Biochem. Physiol.* **35**, 359–373.
- Driedzic, W. R., Crowe, H. L., Hicklin, P. W. and Sephton, D. H.** (1993). Adaptations in pectoralis muscle, heart mass, and energy metabolism during premigratory fattening in semipalmated sandpipers (*Calidris pusilla*). *Can. J. Zool.* **71**, 1602–1608.
- Dunn, E. H., Hobson, K. A., Wassenaar, L. I., Hussell, D. J. T. and Allen, M. L.** (2006). Identification of Summer Origins of Songbirds Migrating through Southern Canada in Autumn. *Avian Conserv. Ecol.* **1**, 4.
- Ellis, B., Haaland, P., Hahne, F., Le Meur, N., Gopalakrishnan, N., Spidlen, J., Jiang, M. and Finak, G.** (2018). flowCore: flowCore: Basic structures for flow cytometry data. R. package version 1.48.0.

- Evans, P. R., Davidson, N. C., Uttley, J. D. and Evans, R. D.** (1992). Premigratory Hypertrophy of Flight Muscles: An Ultrastructural Study. *Ornis Scand.* **23**, 238–243.
- Gan, Z., Burkart-Hartman, E. M., Han, D. H., Finck, B., Leone, T. C., Smith, E. Y., Ayala, J. E., Holloszy, J. and Kelly, D. P.** (2011). The nuclear receptor PPAR β/δ programs muscle glucose metabolism in cooperation with AMPK and MEF2. *Genes Dev.* **25**, 2619–2630.
- García-Prat, L., Sousa-Victor, P. and Muñoz-Cánoves, P.** (2013). Functional dysregulation of stem cells during aging: A focus on skeletal muscle stem cells. *FEBS J.* **280**, 4051–4062.
- Gaunt, A. S., Hikida, R. S., Jehl, J. R. and Fenbert, L.** (1990). Rapid atrophy and hypertrophy of an avian flight muscle. *Auk* **107**, 649–659.
- Gerson, A. R.** (2012). Environmental Physiology of Flight in Migratory Birds. *Ph.D Thesis*. The University of Western Ontario, London, ON.
- Gerson, A. R. and Guglielmo, C. G.** (2011). Flight at low ambient humidity increases protein catabolism in migratory birds. *Science* **333**, 1434–1436.
- Gladyshev, M. I., Sushchik, N. N., Anishchenko, O. V., Makhutova, O. N., Kolmakov, V. I., Kalachova, G. S., Kolmakova, A. A. and Dubovskaya, O. P.** (2011). Efficiency of transfer of essential polyunsaturated fatty acids versus organic carbon from producers to consumers in a eutrophic reservoir. *Oecologia* **165**, 521–531.
- Glatz, J. F. C. and Luiken, J.** (2017). From fat to FAT (CD36/SR-B2): Understanding the regulation of cellular fatty acid uptake. *Biochimie* **136**, 21–26.
- Guglielmo, C. G.** (2010). Move that fatty acid: Fuel selection and transport in migratory birds and bats. *Integr. Comp. Biol.* **50**, 336–345.
- Guglielmo, C. G.** (2018). Obese super athletes: fat-fueled migration in birds and bats. *J. Exp. Biol.* **221**, jeb165753.
- Guglielmo, C. G., Haunerland, N. H., Hochachka, P. W. and Williams, T. D.** (2002a). Seasonal dynamics of flight muscle fatty acid binding protein and catabolic enzymes in a migratory shorebird. *Am. J. Physiol. Regul. Integr. Comp. Physiol.* **282**, R1405-13.
- Guglielmo, C. G., Williams, T. D., Zwingelstein, G., Brichon, G. and Weber, J.-M.** (2002b). Plasma and muscle phospholipids are involved in the metabolic response to long-distance migration in a shorebird. *J. Comp. Physiol. B Biochem. Syst. Environ. Physiol.* **172**, 409–417.
- Halsey, L. G.** (2016). Do animals exercise to keep fit? *J. Anim. Ecol.* **85**, 614–620.
- Hamilton, A., Ly, J., Robinson, J. R., Corder, K. R., DeMoranville, K. J., Schaeffer, P. J. and Huss, J. M.** (2018). Conserved transcriptional activity and ligand responsiveness of avian PPARs: Potential role in regulating lipid metabolism in migratory birds. *Gen. Comp. Endocrinol.* **268**, 110–120.

- Han, L., Shen, W.-J., Bittner, S., Kraemer, F. B. and Azhar, S.** (2017a). PPARs: regulators of metabolism and as therapeutic targets in cardiovascular disease. Part I: PPAR- α . *Future Cardiol.* **13**, 259–278.
- Han, L., Shen, W. J., Bittner, S., Kraemer, F. B. and Azhar, S.** (2017b). PPARs: Regulators of metabolism and as therapeutic targets in cardiovascular disease. Part II: PPAR- β/δ and PPAR- γ . *Future Cardiol.* **13**, 279–296.
- Hawkes, L. A., Batbayar, N., Butler, P. J., Chua, B., Frappell, P. B., Meir, J. U., Milsom, W. K., Natsagdorj, T., Parr, N., Scott, G. R., et al.** (2017). Do Bar-Headed Geese Train for High Altitude Flights? *Integr. Comp. Biol.* **57**, 240–251.
- Hazel, J. R.** (1984). Effects of temperature on the structure and metabolism of cell membranes in fish. *Am. J. Physiol. Integr. Comp. Physiol.* **246**, R460–R470.
- Hedenström, A.** (2003). Scaling migration speed in animals that run, swim and fly. *J. Zool.* **259**, 155–160.
- Hessvik, N. P., Bakke, S. S., Fredriksson, K., Boekschoten, M. V., Fjørkenstad, A., Koster, G., Hesselink, M. K., Kersten, S., Kase, E. T., Rustan, A. C., et al.** (2010). Metabolic switching of human myotubes is improved by n-3 fatty acids. *J. Lipid Res.* **51**, 2090–2104.
- Hixson, S. M., Sharma, B., Kainz, M. J., Wacker, A. and Arts, M. T.** (2015). Production, distribution, and abundance of long-chain omega-3 polyunsaturated fatty acids: a fundamental dichotomy between freshwater and terrestrial ecosystems. *Environ. Rev.* **23**, 414–424.
- Hochachka, P. W. and Somero, G. N.** (1984). *Biochemical Adaptation* Princeton University Press. *Princeton, New Jersey* 538.
- Hoffman, D. L. and Brookes, P. S.** (2009). Oxygen sensitivity of mitochondrial reactive oxygen species generation depends on metabolic conditions. *J. Biol. Chem.* **284**, 16236–16245.
- Holland, R. A., Martin Wikelski and David S. Wilcove** (2006). How and Why Do Insects Migrate? *Science* (80-.). **313**, 794–796.
- Holst, D., Luquet, S., Nogueira, V., Kristiansen, K., Leverve, X. and Grimaldi, P. A.** (2003). Nutritional regulation and role of peroxisome proliferator-activated receptor δ in fatty acid catabolism in skeletal muscle. *Biochim. Biophys. Acta - Mol. Cell Biol. Lipids* **1633**, 43–50.
- Hothorn, T., Bretz, F. and Westfall, P.** (2008). Simultaneous Inference in General Parametric Models. *Biometrical J.* **50**, 346–363.
- Howell, J. E.** (2018). Shorebird staging and migratory movements at Chaplin and Reed Lakes, Saskatchewan, with implications for wind energy development. *M.Sc Thesis.* University of Saskatchewan, Saskatoon, SK.
- Huang, B., Wu, P., Bowker-Kinley, M. M. and Harris, R. A.** (2002). Regulation of pyruvate dehydrogenase kinase expression by peroxisome proliferator-activated receptor- α ligands, glucocorticoids, and insulin. *Diabetes* **51**, 276–283.

- Hulbert, A. J. and Else, P. L.** (2005). Membranes and the setting of energy demand. *J. Exp. Biol.* **208**, 1593–1599.
- Hunt, P. D. and Flaspohler, D. J.** (1998). Yellow-rumped Warbler (*Setophaga coronata*). *Birds North Am.* (A. F. Poole F. B. Gill, Ed.)
- Iloki, A., S.B., Gil-Salido, A. A., Lewis Luján, L. M., Rosas-Durazo, A., Acosta-Silva, A. L., Rivera-Castañeda, E. G. and Rubio-Pino, J. L.** (2013). Cell growth curves for different cell lines and their relationship with biological activities. *Int. J. Biotechnol. Mol. Biol. Res.* **4**, 60–70.
- Janani, C. and Ranjitha Kumari, B. D.** (2015). PPAR gamma gene - A review. *Diabetes Metab. Syndr. Clin. Res. Rev.* **9**, 46–50.
- Jehl, J. R.** (1997). Cyclical Changes in Body Composition in the Annual Cycle and Migration of the Eared Grebe *Podiceps nigricollis*. *J. Avian Biol.* **28**, 132–142.
- Jenni-Eiermann, S., Jenni, L., Smith, S. and Costantini, D.** (2014). Oxidative stress in endurance flight: An unconsidered factor in bird migration. *PLoS One* **9**, 1–6.
- Jenni, L. and Jenni-Eiermann, S.** (1998). Fuel Supply and Metabolic Constraints in Migrating Birds. *J. Avian Biol.* **29**, 521–528.
- Jiyoung, K., Meshail, O., Anjeza, E., Timothy, C., Statish, K. N. and Soonkyu, C.** (2016). Eicosapentaenoic acid potentiates brown thermogenesis through FFAR4-dependent up-regulation of miR-30b and miR-378. *J. Biol. Chem.* **291**, 20551–20562.
- Johnson, M. L., Lalia, A. Z., Dasari, S., Pallauf, M., Fitch, M., Hellerstein, M. K. and Lanza, I. R.** (2015). Eicosapentaenoic acid but not docosahexaenoic acid restores skeletal muscle mitochondrial oxidative capacity in old mice. *Aging Cell* **14**, 734–743.
- Kapusta, A., Suh, A. and Feschotte, C.** (2017). Dynamics of genome size evolution in birds and mammals. *Proc. Natl. Acad. Sci.* **114**, E1460–E1469.
- King, M. O., Zhang, Y., Carter, T., Johnson, J., Harmon, E. and Swanson, D. L.** (2015). Phenotypic flexibility of skeletal muscle and heart masses and expression of myostatin and toll-like proteinases in migrating passerine birds. *J. Comp. Physiol. B Biochem. Syst. Environ. Physiol.* **185**, 333–342.
- Komal, R., Khushboo, Dwivedi, A., Vaish, V. and Rani, S.** (2017). Conquering the night: understanding nocturnal migration in birds. *Biol. Rhythm Res.* **48**, 747–755.
- Kuzmiak-Glancy, S. and Willis, W. T.** (2014). Skeletal muscle fuel selection occurs at the mitochondrial level. *J Exp Biol* **217**, 1993–2003.
- Landys-Ciannelli, M. M., Piersma, T. and Jukema, J.** (2003). Strategic size changes of internal organs and muscle tissue in the Bar-tailed Godwit during fat storage on a spring stopover site. *Funct. Ecol.* **17**, 151–159.

- Lindström, A., Kvist, A., Piersma, T., Dekinga, A. and Dietz, M. W.** (2000). Avian pectoral muscle size rapidly tracks body mass changes during flight, fasting and fuelling. *J. Exp. Biol.* **203**, 913–9.
- Macwhirter, R. B., Austin-smith Jr., P. and Kroodsma, D. E.** (2002). Sanderling (*Calidris alba*). *Birds North Am.* (A. F. Poole F. B. Gill, Ed.)
- Maillet, D.** (2006). Performance-enhancing role of dietary fatty acids in a long-distance migrant shorebird: the semipalmated sandpiper. *J. Exp. Biol.* **209**, 2686–2695.
- Maillet, D. and Weber, J.-M.** (2007). Relationship between n-3 PUFA content and energy metabolism in the flight muscles of a migrating shorebird: evidence for natural doping. *J. Exp. Biol.* **210**, 413–420.
- Marsh, R. L.** (1984). Adaptations of the gray catbird *Dumetella carolinensis* to long-distance migration: Flight muscle hypertrophy associated with elevated body mass. *Physiol. Zool.* **57**, 105–117.
- Marshall, A. D., Jaine, F. R. A., Townsend, K. A., Pierce, S. J., Richardson, A. J., Rohner, C. A., Nichols, P. D., Bennett, M. B., Couturier, L. I. E. and Weeks, S. J.** (2013). Unusually High Levels of n-6 Polyunsaturated Fatty Acids in Whale Sharks and Reef Manta Rays. *Lipids* **48**, 1029–1034.
- Marshall, T. J., Dick, M. F. and Guglielmo, C. G.** (2016). Seasonal dietary shifting in yellow-rumped warblers is unrelated to macronutrient targets. *Comp. Biochem. Physiol. Part A* **192**, 57–63.
- McClelland, G. B.** (2004). Fat to the fire: The regulation of lipid oxidation with exercise and environmental stress. *Comp. Biochem. Physiol. Part B* **139**, 443–460.
- McFarlan, J. T., Bonen, A. and Guglielmo, C. G.** (2009). Seasonal upregulation of fatty acid transporters in flight muscles of migratory white-throated sparrows (*Zonotrichia albicollis*). *J. Exp. Biol.* **212**, 2934–2940.
- McGuire, L. P., Fenton, M. B. and Guglielmo, C. G.** (2013). Phenotypic flexibility in migrating bats: seasonal variation in body composition, organ sizes and fatty acid profiles. *J. Exp. Biol.* **216**, 800–808.
- McWilliams, S. R., Guglielmo, C. G., Pierce, B. and Klaassen, M.** (2004). Flying , Fasting , and Feeding in Birds during Migration : A Nutritional and Physiological Ecology Perspective. *J. Avian Biol.* **35**, 377–393.
- Meijer, J. H. and Robbers, Y.** (2014). Wheel running in the wild. *Proc. R. Soc. B Biol. Sci.* **281**.
- Murray, D. S., Hager, H., Tocher, D. R. and Kainz, M. J.** (2014). Effect of partial replacement of dietary fish meal and oil by pumpkin kernel cake and rapeseed oil on fatty acid composition and metabolism in Arctic charr (*Salvelinus alpinus*). *Aquaculture* **431**, 85–91.
- Myers, J. P., Castro, A. E. O. G., Gordon, L., Tabilo, E. and Serena, L.** (1990). Migration routes of New World Sanderlings (*Calidris alba*). *Auk* **107**, 172–180.

- Nagahuedi, S., Popesku, J. T., Trudeau, V. L. and Weber, J.-M.** (2009). Mimicking the natural doping of migrant sandpipers in sedentary quails: effects of dietary n-3 fatty acids on muscle membranes and PPAR expression. *J. Exp. Biol.* **212**, 1106–1114.
- Norris, A. W., Chen, L., Fisher, S. J., Szanto, I., Ristow, M., Jozsi, A. C., Hirshman, M. F., Rosen, E. D., Goodyear, L. J., Gonzalez, F. J., et al.** (2003). Muscle-specific PPAR γ -deficient mice develop increased adiposity and insulin resistance but respond to thiazolidinediones. *J. Clin. Invest.* **112**, 608–618.
- Pääsuke, R., Eimre, M., Piirsoo, A., Peet, N., Laada, L., Kadaja, L., Roosimaa, M., Pääsuke, M., Märtson, A., Seppet, E., et al.** (2016). Proliferation of human primary myoblasts is associated with altered energy metabolism in dependence on ageing in vivo and in vitro. *Oxid. Med. Cell. Longev.* **2016**,.
- Peoples, G. E., McLennan, P. L., Howe, P. R. C. and Groeller, H.** (2008). Fish oil reduces heart rate and oxygen consumption during exercise. *J. Cardiovasc. Pharmacol.* **52**, 540–547.
- Pepe, S. and McLennan, P. L.** (2002). Cardiac membrane fatty acid composition modulates myocardial oxygen consumption and postischemic recovery of contractile function. *Circulation* **105**, 2303–2308.
- Philpott, J. D., Witard, O. C. and Galloway, S. D. R.** (2018). Applications of omega-3 polyunsaturated fatty acid supplementation for sport performance. *Res. Sport. Med.* 1–19.
- Pierce, B. J. and McWilliams, S. R.** (2014). The fat of the matter: how dietary fatty acids can affect exercise performance. *Integr. Comp. Biol.* **54**, 903–912.
- Pierce, B. J., McWilliams, S. R., O'Connor, T. P., Place, A. R. and Guglielmo, C. G.** (2005). Effect of dietary fatty acid composition on depot fat and exercise performance in a migrating songbird, the red-eyed vireo. *J. Exp. Biol.* **208**, 1277–1285.
- Piersma, T.** (1998). Phenotypic Flexibility during Migration: Optimization of Organ Size Contingent on the Risks and Rewards of Fueling and Flight? *J. Avian Biol.* **29**, 511–520.
- Piersma, T., Gudmundsson, G. A. and Lilliendahl, K.** (2002). Rapid Changes in the Size of Different Functional Organ and Muscle Groups during Refueling in a Long-Distance Migrating Shorebird. *Physiol. Biochem. Zool.* **72**, 405–415.
- Porter, R. K., Hulbert, A. J. and Brand, M. D.** (1996). Allometry of mitochondrial proton leak: influence of membrane surface area and fatty acid composition. *Am. J. Physiol. Integr. Comp. Physiol.* **271**, R1550–R1560.
- Poulsen, L. la C., Siersbæk, M. and Mandrup, S.** (2012). PPARs: Fatty acid sensors controlling metabolism. *Semin. Cell Dev. Biol.* **23**, 631–639.
- Price, E. R.** (2010). Dietary lipid composition and avian migratory flight performance: Development of a theoretical framework for avian fat storage. *Comp. Biochem. Physiol. Part A* **157**, 297–309.

- Price, E. R. and Guglielmo, C. G.** (2009). The effect of muscle phospholipid fatty acid composition on exercise performance: a direct test in the migratory white-throated sparrow (*Zonotrichia albicollis*). *Am. J. Physiol. Regul. Integr. Comp. Physiol.* **297**, R775-82.
- Price, E. R., Krokfors, A. and Guglielmo, C. G.** (2008). Selective mobilization of fatty acids from adipose tissue in migratory birds. *J. Exp. Biol.* **211**, 29–34.
- Price, E. R., McFarlan, J. T. and Guglielmo, C. G.** (2010). Preparing for migration? The effects of photoperiod and exercise on muscle oxidative enzymes, lipid transporters, and phospholipids in white-crowned sparrows. *Physiol. Biochem. Zool.* **83**, 252–262.
- Price, E. R., Gerson, A. R., McFarlan, J. T., Guglielmo, C. G., McWilliams, S. R., Bauchinger, U., Zajac, D. M. and Cerasale, D. J.** (2011a). Migration- and exercise-induced changes to flight muscle size in migratory birds and association with IGF1 and myostatin mRNA expression. *J. Exp. Biol.* **214**, 2823–2831.
- Price, E. R., Staples, J. F., Milligan, C. L. and Guglielmo, C. G.** (2011b). Carnitine palmitoyl transferase activity and whole muscle oxidation rates vary with fatty acid substrate in avian flight muscles. *J. Comp. Physiol. B Biochem. Syst. Environ. Physiol.* **181**, 565–573.
- R Core Team** (2018). R: A Language and Environment for Statistical Computing. *R Foundation for Statistical Computing*, Vienna Austria. URL <https://www.R-project.org/>.
- Ramenofsky, M. and Wingfield, J. C.** (2006). Behavioral and physiological conflicts in migrants: The transition between migration and breeding. *J. Ornithol.* **147**, 135–145.
- Rehfeldt, C.** (2007). Satellite cell addition is/is not obligatory for skeletal muscle hypertrophy. *J. Appl. Physiol.* **103**, 1104–1106.
- Rosenblatt, J. D., Parry, D. J. and Partridge, T. A.** (1996). Phenotype of adult mouse muscle myoblasts reflects their fiber type of origin. *Differentiation* **60**, 39–45.
- Ruf, T., Valencak, T., Tataruch, F. and Arnold, W.** (2006). Running speed in mammals increases with muscle n-6 polyunsaturated fatty acid content. *PLoS One* **1**.
- Russell, A. P., Hesselink, M. K. C., Lo, S. K. and Patrick, S.** (2005). Transcription Factors With Acute Exercise. *FASEB J.* **20**, 1–20.
- Scanes, C. G. and Braun, E.** (2013). Avian metabolism: Its control and evolution. *Front. Biol. (Beijing)*. **8**, 134–159.
- Schmidt-Nielsen, K.** (1972). Locomotion: energy cost of swimming, flying, and running. *Science (80-)*. **177**, 222–228.
- Schmitz, G. and Ecker, J.** (2008). The opposing effects of n-3 and n-6 fatty acids. *Prog. Lipid Res.* **47**, 147–155.

- Seynnes, O. R., de Boer, M. and Narici, M. V.** (2006). Early skeletal muscle hypertrophy and architectural changes in response to high-intensity resistance training. *J. Appl. Physiol.* **102**, 368–373.
- Shahini, A., Vydiam, K., Choudhury, D., Rajabian, N., Nguyen, T., Lei, P. and Andreadis, S. T.** (2018). Efficient and high yield isolation of myoblasts from skeletal muscle. *Stem Cell Res.* **30**, 122–129.
- Shaw, A. K.** (2016). Drivers of animal migration and implications in changing environments. *Evol. Ecol.* **30**, 991–1007.
- Skip, M. M., Bauchinger, U., Goymann, W., Fusani, L., Cardinale, M., Alan, R. R. and McWilliams, S. R.** (2015). Migrating songbirds on stopover prepare for, and recover from, oxidative challenges posed by long-distance flight. *Ecol. Evol.* **5**, 3198–3209.
- Stanley, W. C., Khairallah, R. J. and Dabkowski, E. R.** (2012). Update on lipids and mitochondrial function: impact of dietary n-3 polyunsaturated fatty acids. *Curr. Opin. Clin. Nutr. Metab. Care* **15**, 122–126.
- Tajbakhsh, S.** (2009). Skeletal muscle stem cells in developmental versus regenerative myogenesis. *J. Intern. Med.* **266**, 372–389.
- Talbot, D. A., Duchamp, C., Rey, B., Hanuise, N., Rouanet, J. L., Sibille, B. and Brand, M. D.** (2004). Uncoupling protein and ATP/ADP carrier increase mitochondrial proton conductance after cold adaptation of king penguins. *J. Physiol.* **558**, 123–135.
- Toews, D. P. L., Brelsford, A., Grossen, C., Milá, B. and Irwin, D. E.** (2016). Genomic variation across the Yellow-rumped Warbler species complex. *Auk* **133**, 698–717.
- Tsipoura, N. and Burger, J.** (1999). Shorebird diet during spring migration stopover on Delaware Bay. *Condor* **101**, 635–644.
- Vágási, C. I., Pap, P. L., Vincze, O., Osváth, G., Erritzøe, J. and Møller, A. P.** (2016). Morphological Adaptations to Migration in Birds. *Evol. Biol.* **43**, 48–59.
- Vagner, M. and Santigosa, E.** (2011). Characterization and modulation of gene expression and enzymatic activity of delta-6 desaturase in teleosts: A review. *Aquaculture* **315**, 131–143.
- Vaillancourt, E., Prud'homme, S., Haman, F., Guglielmo, C. G. and Weber, J.-M.** (2005). Energetics of a long-distance migrant shorebird (*Philomachus pugnax*) during cold exposure and running. *J. Exp. Biol.* **208**, 317–25.
- Wahli, W. and Michalik, L.** (2012). PPARs at the crossroads of lipid signaling and inflammation. *Trends Endocrinol. Metab.* **23**, 351–363.
- Walsberg and Wolf** (1995). Variation in the respiratory quotient of birds and implications for indirect calorimetry using measurements of carbon dioxide production. *J. Exp. Biol.* **198**, 213–9.

- Wang, H., Hiatt, W. R., Barstow, T. J. and Brass, E. P.** (1999). Relationships between muscle mitochondrial DNA content, mitochondrial enzyme activity and oxidative capacity in man: Alterations with disease. *Eur. J. Appl. Physiol. Occup. Physiol.* **80**, 22–27.
- Wang, Y., Zhang, C., Yu, R. T., Cho, H. K., Nelson, M. C., Bayuga-Ocampo, C. R., Ham, J., Kang, H. and Evans, R. M.** (2004). Regulation of muscle fiber type and running endurance by PPAR δ . *PLoS Biol.* **2**, e294.
- Weber, J.-M.** (2011). Metabolic fuels: regulating fluxes to select mix. *J. Exp. Biol.* **214**, 286–294.
- Wickham, H.** (2016). *ggplot2: Elegant graphics for data analysis*. Springer-Verlag New York. <http://ggplot2.org>.
- Wickham, H., François, R., Henry, L. and Müller, K.** (2018). dplyr: A grammar of data manipulation. *R package version 0.7.7*. <https://CRAN.R-project.org/package=dplyr>.
- Wikelski, M., Tarlow, E. M., Raim, A., Diehl, R. H., Larkin, R. P. and Visser, G. H.** (2003). Costs of migration in free-flying songbirds. *Nature* **423**, 704.
- Willer, M., Daugaard, J. R., Storlien, L. H., Kiens, B., Helge, J. W. and Wu, B. J.** (2001). Training affects muscle phospholipid fatty acid composition in humans. *J. Appl. Physiol.* **90**, 670–677.
- Wu, B. J., Hulbert, A. J., Storlien, L. H. and Else, P. L.** (2004). Membrane lipids and sodium pumps of cattle and crocodiles: an experimental test of the membrane pacemaker theory of metabolism. *Am. J. Physiol. Integr. Comp. Physiol.* **287**, R633–R641.
- Xu, H. E., Kliewer, S. A., Montana, V. G., Moore, J. T., Willson, T. M., Plunket, K. D., Oplinger, J. A., McKee, D. D., Lambert, M. H., Gampe, R. T., et al.** (2002). Structural determinants of ligand binding selectivity between the peroxisome proliferator-activated receptors. *Proc. Natl. Acad. Sci.* **98**, 13919–13924.
- Xue, X., Hixson, S. M., Hori, T. S., Booman, M., Parrish, C. C., Anderson, D. M. and Rise, M. L.** (2015). Atlantic salmon (*Salmo salar*) liver transcriptome response to diets containing *Camelina sativa* products. *Comp. Biochem. Physiol. Part D* **14**, 1–15.
- Yablonka-Reuveni, Z. and Nameroff, M.** (1990). Temporal differences in desmin expression between myoblasts from embryonic and adult chicken skeletal muscle. *Differentiation* **45**, 21–28.
- Yaffe, D. and Saxel, O.** (1977). Serial passaging and differentiation of myogenic cells isolated from dystrophic mouse muscle. *Nature* **270**, 725–727.
- Yao, T. and Asayama, Y.** (2017). Animal-cell culture media: History, characteristics, and current issues. *Reprod. Med. Biol.* **16**, 99–117.

- Yépez, V. A., Kremer, L. S., Iuso, A., Gusic, M., Kopajtich, R., Koňářikova, E., Nadel, A., Wachutka, L., Prokisch, H. and Gagneur, J.** (2018). OCR-Stats: Robust estimation and statistical testing of mitochondrial respiration activities using Seahorse XF analyzer. *PLoS One* **13**, 1–18.
- Yoseph, B. and Soker, S.** (2015). Redefining the satellite cell as the motor of skeletal muscle regeneration. *J. Sab* **3**, 76–82.
- Zajac, D. M., Cerasale, D. J., Landman, S. and Guglielmo, C. G.** (2011). Behavioral and physiological effects of photoperiod-induced migratory state and leptin on *Zonotrichia albicollis*: II. Effects on fatty acid metabolism. *Gen. Comp. Endocrinol.* **174**, 269–275.
- Zammit, P. S., Relaix, F., Nagata, Y., Pérez Ruiz, A., Colline, C. A., Partridge, T. A. and Beauchamp, J. R.** (2006). Pax7 and myogenic progression in skeletal muscle satellite cells. *J. Cell Sci.* **119**, 1824–1832.
- Zhang, Y.** (2012). Roles of PGC-1 α /PPARs pathway in regulating insulin sensitivity in mouse skeletal muscle cells under prolonged hypoxia.
- Zhang, Y., King, M. O., Harmon, E., Eyster, K. and Swanson, D. L.** (2015). Migration-induced variation of fatty acid transporters and cellular metabolic intensity in passerine birds. *J. Comp. Physiol. B Biochem. Syst. Environ. Physiol.* **185**, 797–810.

Appendices

Appendix A

Summary of H-FABP knockdown experiments in yellow-rumped warbler and C₂C₁₂ myotubes.

The second objective of my thesis was to knockdown expression of the heart-type fatty acid binding protein (H-FABP) in a model of migratory bird muscle to determine its role in fatty acid oxidation in these birds. I was unsuccessful in knocking down expression of H-FABP in my avian model but did successfully silence expression in a mammalian skeletal muscle cell line. I will briefly summarize here the background and justification for this study, the methods I used to troubleshoot knockdowns in my bird model, the successful method optimized in a mammalian cell line, and future directions for this research.

Background

When flying, birds work at an estimated 80% of their maximal oxygen consumption capacity, and during migratory flights, birds maintain this sprinting pace for many hours or days (Guglielmo, 2010; McClelland, 2004). Migratory flights are fueled predominantly by lipids mobilized from discrete adipose stores that are built up before birds initiate flight (McWilliams et al., 2004). Lipids are the ideal macronutrient for fueling flight because they are more energy dense than proteins or carbohydrates (Jenni and Jenni-Eiermann, 1998). However, lipids are limited as an energy substrate in mammals due to the high cost of transport associated with their catabolism (McClelland, 2004). During the migratory period, birds upregulate their metabolisms and especially pathways associated with lipid transport and oxidation are highly upregulated (Banerjee and Chaturvedi, 2016; Dick, 2017). The heart-type fatty acid binding protein (H-FABP) is of interest because of the dramatic increase in expression of this protein in the flight muscles of some birds. H-FABP comprises up to 13% of total cytosolic protein in the muscle of migrant Western Sandpipers during migration relative to expression in the winter (Guglielmo et al., 2002). In mammals, the rate of transport of fatty acids limits the

rate of fatty acid oxidation. Consequently, the dramatic increases in expression of H-FABP in migrant birds may be critical to their ability to maintain the high rates of fatty acid transport required to sustain endurance flights. My aim was to knockdown expression of H-FABP using short interfering RNAs (siRNA) in skeletal muscle models of a terrestrial mammal and migratory bird to determine the role of this protein in the high metabolic rates maintained by flying birds.

Temporary knockdowns of mRNA and protein expression can be achieved using siRNAs in vertebrates. siRNAs are 19-21 bp long double-stranded oligonucleotides that selectively degrade complementary mRNAs through the RNA interference pathway in eukaryotes (Kim and Rossi, 2008). However, vertebrate cells do not take up siRNAs into the cytosol endogenously and they must be transfected into cells (Heidel et al., 2004; Shegokar et al., 2011). I attempted transfections using the polymer-based JetPRIME transfection reagent (Polyplus), lipid complex based Lipofectamine 3000, and Lipofectamine RNAiMax on primary yellow-rumped warbler (*Setophaga coronata coronata*) myotubes.

Transfection of Primary Avian Myotubes

I designed siRNAs following the criteria compiled by Fakhr et al. (2016) and the sequences used are listed in table A1. I was unable to elicit H-FABP knockdown in primary avian myotubes as measured by western blot using H-FABP targeted siRNAs (Table A1). Cell culture techniques were carried out as described in the methods of this thesis (see section 2.3) and adherent cell transfections were conducted four days after initiating differentiation to transfect myotubes.

Table A1. siRNA sequences designed following the criteria described by Fakhr et al. (2016). siRNA ID denotes a unique identifier name for siRNAs designed against C₂C₁₂ (*Mus musculus*) or yellow-rumped warbler (*Setophaga coronata coronata*) H-FABP or a scrambled sequence control (SCR).

Target Species	siRNA ID	siRNA Sequence
Mouse - C ₂ C ₁₂ (<i>Mus musculus</i>)	MMU _{si} 01_H-FABP	Sense: GGAGCUAGUUGACGGGAAA[dT][dT]
		Antisense: UUUCCCGUCAACUAGCUCC[dT][dT]
	MMU _{si} 02_SCR	Sense: GGAUGGAAACGGUAGAGCU[dT][dT]
		Antisense: AGCUCUACCGUUCCAUC[dT][dT]
Yellow-rumped warbler (<i>Setophaga coronata coronata</i> YRWA)	YRW _{Asi} 01_FABP3	Sense: GCACCUGGAAGCUGGUGGA[dT][dT]
		Antisense: UCCACCAGCUUCCAGGUGC[dT][dT]
	YRW _{Asi} 02_SCR	Sense: GGACGAGCUGCCGGAUAGU[dT][dT]
		Antisense: ACUAUCCGGCAGCUCGUCC[dT][dT]
	YRW _{Asi} 03_FABP3	Sense: UGGUGGACACCCAGAAUUU[dT][dT]
		Antisense: AAAUUCUGGGUGUCCACCA[dT][dT]

JetPRIME transfections were carried out closely following the manufacturer's instructions for siRNA transfections. Briefly, I plated satellite cells in 35 mm collagen-coated culture dishes and differentiated them for four days. To prepare the transfection mix, I diluted siRNAs in 200 μ L of jetprime buffer to final concentrations of 25, 50, 100, and 200 nM. I added 4 to 8 μ L of jetprime reagent to the transfection mix, vortexed it thoroughly and incubated for 15 min at room temperature. The transfection mix was then added directly to the cell media. Cells were incubated with transfection mix for 24 h at 38.5 °C in media with 10-20% serum content. I added fresh media at 24 h for collections at later timepoints. I collected total protein 24, 48, and 72 h following transfection.

I conducted Lipofectamine 3000 transfections closely following the manufacturer's instructions. I grew cells following the procedure described above and prepared transfection mixes with final siRNA concentrations of 25 to 100 nM. To make the transfection mix, I added 3.75 to 10 μ L of lipofectamine 3000 reagent to 250 μ L of

Opti-MEM medium and incubated with siRNAs for 15 min at room temperature. I added the transfection mix to cells in media and incubated for 24 to 48 h at 38.5 °C without changing media.

Lipofectamine RNAiMax transfections were similarly conducted to follow closely the manufacturer's instructions. Final siRNA concentrations of 50, to 200 nM were prepared using RNAiMax. I added 9 µL of RNAiMax transfection reagent to 300 µl of Opti-MEM medium with diluted siRNAs and incubated for 5 min at room temperature. I then added the transfection solution directly to cell media and incubated for 24 to 48 h at 38.5 °C. Additionally, I tested double transfections using RNAiMax wherein I followed the same protocol to prepare transfection mix to be added with fresh cell media 24 h after the first transfection was carried out. I conducted double transfections using 100 and 200 nM final concentration of siRNAs added at 0 and 24 h timepoints, collecting protein at 48 and 72 h.

Transfection of C₂C₁₂ myotubes

I differentiated C₂C₁₂ myoblasts for five days, following the methods described in section 2.3 of this thesis, before transfecting them with lipofectamine 3000 transfection reagent. Following the procedure described above, I used a final concentration of 35 nM siRNAs diluted with 7.5 µL of lipofectamine reagent in Opti-MEM. I collected total protein following methods described by Zhang (2012). Briefly, I washed cells in PBS and incubated them in cold RIPA buffer (50 mM Tris-HCl, 150 mM NaCl, 1 mM EDTA, 1% NP-40, 0.25% Na-deoxycholate, pH 7.4). I scraped cells from their dishes and transferred the lysed cells to 1.5 mL microtubes. I then sonicated suspended cell lysate, centrifuged the suspension at 12,500 ×g for 10 min at 4 °C, and transferred the supernatant to a fresh tube. Samples were stored at -20 °C before conducting SDS-PAGE and western blotting. I quantified total protein by conducting BCA assays as described in section 2.8 of this thesis. I prepared 20 µg of total protein in Laemmli buffer and heated for ~10 min at 75 °C and loaded samples into 15% polyacrylamide gels for SDS-PAGE. I ran electrophoresis at 150 V for ~60 min before transferring separated proteins onto PVDF membranes using Trans-Blot semi-dry transfer system (Bio-Rad). Following transfer,

membranes were washed in TBS-T for 10 min three times and blocked in 5% milk for 1 h at room temperature. I then added anti-H-FABP antibody to a final dilution of 1:1000 in 5% milk and incubated overnight at 4 °C (Invitrogen, CA# PA5-13461). Membranes were washed in TBS-T for 10 min, three times and incubated in TBS-T with 5% milk and 1:5000 anti-rabbit HRP secondary antibody for 1 h and imaged in a ChemiDoc (Bio-Rad) using ECL chemiluminescent substrate (GE Healthcare Life Sciences). Expression of H-FABP detected at ~14 kDA was normalized to total protein measured using Ponceau stain.

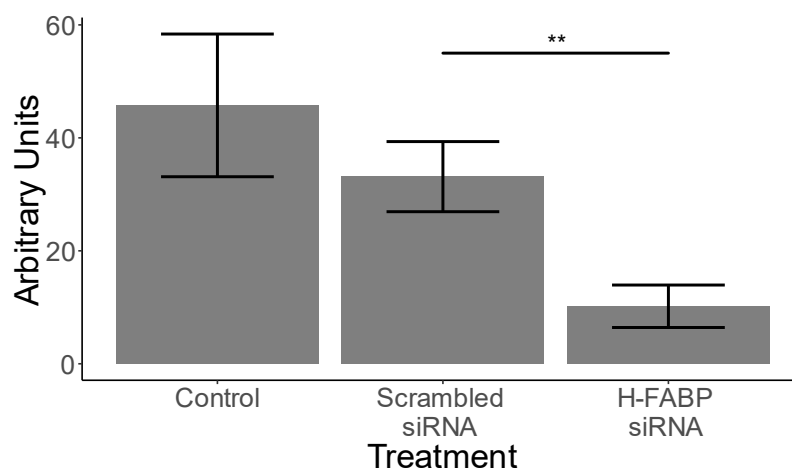


Figure A1. C₂C₁₂ cells exhibited ~40% knockdown in expression of H-FABP relative to the scrambled control. Protein expression was measured by western blotting and is represented in arbitrary optical density units. Error bars represent the standard deviation (n=3). This process indicates that the siRNAs and the transfection process I used is effective in C₂C₁₂ but not in yellow-rumped warbler cells.

Future Directions

Although I was unable to successfully knockdown expression of H-FABP in yellow-rumped warbler myotubes, continued advances in transfection technologies may permit simpler transfection strategies in these cells in the future. Furthermore, the mechanisms by which some transfection techniques induce the uptake of oligonucleotides in vertebrate cells is not fully understood (Paganin-Gioanni et al., 2011) and continuing

research in these fields will likely improve the application of these techniques more broadly. Additionally, alternative gene knockdown or knockout techniques may be more fruitful in these cells. The use of siRNAs to induce a transient and localized knockdown was desirable in my research for logistical and project planning purposes. However, other forms of gene expression manipulations (i.e. CRISPR, shRNA, plasmids) may be more successful in these cells than siRNA transfections. Researchers interested in conducting gene studies in yellow-rumped warblers or other migrant birds should consider this system but carefully plan transfection protocols and examine newly available materials for experiments.

References

- Banerjee, S. and Chaturvedi, C. M. (2016). Migratory preparation associated alterations in pectoralis muscle biochemistry and proteome in Palearctic-Indian emberizid migratory finch, red-headed bunting, *Emberiza bruniceps*. *Comp. Biochem. Physiol. - Part D Genomics Proteomics* 17, 9–25.
- Dick, M. F. (2017). The long haul: migratory flight preparation and performance in songbirds.
- Fakhr, E., Zare, F. and Teimoori-Toolabi, L. (2016). Precise and efficient siRNA design: a key point in competent gene silencing. *Cancer Gene Ther.* 23, 73–82.
- Guglielmo, C. G. (2010). Move that fatty acid: Fuel selection and transport in migratory birds and bats. *Integr. Comp. Biol.* 50, 336–345.
- Guglielmo, C. G., Haunerland, N. H., Hochachka, P. W. and Williams, T. D. (2002). Seasonal dynamics of flight muscle fatty acid binding protein and catabolic enzymes in a migratory shorebird. *Am. J. Physiol. Regul. Integr. Comp. Physiol.* 282, R1405-13.
- Heidel, J. D., Hu, S., Liu, X. F., Triche, T. J. and Davis, M. E. (2004). Lack of interferon response in animals to naked siRNAs. *Nat. Biotechnol.* 22, 1579–1582.
- Jenni, L. and Jenni-Eiermann, S. (1998). Fuel Supply and Metabolic Constraints in Migrating Birds. *J. Avian Biol.* 29, 521–528.
- Kim, D. H. and Rossi, J. J. (2008). RNAi mechanisms and applications. *Biotechniques* 44, 613–616.

McClelland, G. B. (2004). Fat to the fire: The regulation of lipid oxidation with exercise and environmental stress. *Comp. Biochem. Physiol. - B Biochem. Mol. Biol.* 139, 443–460.

Mewilliams, S. R., Guglielmo, C. G., Pierce, B., Klaassen, M. and Flying, M. (2004). Flying, Fasting, and Feeding in Birds during Migration : A Nutritional and Physiological Ecology Perspective. *J. Avian Biol.* 35, 377–393.


Paganin-Gioanni, A, Bellard, E., Escoffre, J. M., Rols, M. P., Teissié, J. and Golzio, M. (2011). Direct visualization at the single-cell level of siRNA electrotransfer into cancer cells. *Proc. Natl. Acad. Sci. U. S. A.* 108, 10443–10447.

Shegokar, R., Shaal, L. A. L. and Mishra, P. R. (2011). siRNA delivery: Challenges and role of carrier systems. *Pharmazie* 66, 313–318.

Zhang, Y. (2012). Roles of PGC-1 α /PPARs pathway in regulating insulin sensitivity in mouse skeletal muscle cells under prolonged hypoxia.

Appendix B

Environment and Climate Change Canada scientific capture permits issued to Dr. Christopher Guglielmo and Dr. Christy Morrisey.




CANADIAN WILDLIFE SERVICE - PERMIT
PERMIS - SERVICE CANADIEN DE LA FAUNE

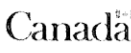
Permit to/for Permis de/pour <p style="text-align: center;">SCIENTIFIC</p>		Permit no. No de permis <p style="text-align: center;">CA 0256</p>	
Organization Organisation <p style="text-align: center;">University of Western Ontario</p>		Issued under section Délivré en vertu de l'article <p style="text-align: center;">19</p>	
Surname Nom de famille <p style="text-align: center;">Guglielmo</p>		Name Prénom <p style="text-align: center;">Christopher</p>	
		Department Département <p style="text-align: center;">Department of Biology</p>	
		of de <p style="text-align: center;">MIGRATORY BIRD REGULATIONS</p>	

Date of issue Date d'émission <p style="text-align: center;">August 15, 2015</p>	Date of expiry Date d'expiration <p style="text-align: center;">August 14, 2017</p>
---	--

Special Conditions - Conditions spéciales

1. Prior to any use of this permit the permittee will notify the Ontario Ministry of Natural Resources relative to collecting procedures, times and localities of collection. Landowner's permission must be obtained prior to collecting on private property.
2. Permit or a copy of the permit to be carried in the field by all collectors.
3. The permit holder is authorized to collect and to possess for scientific research purposes, migratory birds – to wit: Tree Swallow (*Tachycineta bicolor*) (take limit 20 per year), Black-throated Blue Warbler (*Setophaga caerulescens*) (take limit 60 per year), Western Sandpiper (*Calidris mauri*) (take limit 60 per year), White-throated Sparrow (*Zonotrichia albicollis*) (take limit 60 per year), Yellow-rumped Warbler (*Setophaga coronata*) (take limit 80 per year), Hermit Thrush (*Catharus guttatus*) (take limit 60 per year), Swainson's Thrush (*Catharus ustulatus*) (take limit 60 per year), American Robin (*Turdus migratorius*) (take limit 60 per year) and Ruby-throated Hummingbird (*Archilocus colubris*) (take limit 20 per year) – from locations in SW Ontario (Perth, Elgin, Middlesex, Haldimand, and Bruce Counties).
4. Western Sandpipers will be obtained under collection permit held by Dr. David Lank at Simon Fraser University in British Columbia and transported by air to Western University.
5. Capture, handling and housing procedures are to be performed according to the Animal Care Committee protocols of the University of Western Ontario. Samples not to be retained are to be disposed of by the approved laboratory waste management system of the University of Western Ontario.
6. All other birds are to be released into the wild by the conclusion of the study or otherwise be humanely euthanized.
7. Permit holder shall submit a written report, by January 31, of each year following, indicating the results of the study to the Canadian Wildlife Service, 867 Lakeshore Road, Burlington, ON., L7R 4A6.
8. Nominees to this permit are: Department of Biology faculty/staff as acting under the direction of the permittee.





**Environment
Canada**

**Environnement
Canada**

Canadian Wildlife
Service - PERMIT

PERMIS - Service Canadien
de la Faune

SCIENTIFIC PERMIT - TAKE

permit to / for *permis de / pour*

Saskatchewan

15-SK-SC004

in the province(s) *dans la/les province(s)*

permit no. *no. de permis*

Dr. Christy A. Morrissey

4. (1)

issued under section *délivré en vertu de l'article*

Migratory Birds Regulations

of *de*

01-May-2012 *amended:* 10-Apr-2017

date of issue *date d'émission*

01-May-2018

date of expiry *date d'expiration*

name and address *nom et adresse*

31-Jan-2018

Annual report due by

Special Conditions

1. The following authorization only is NOT VALID in 2017 and will be reinstated in 2018 with demonstration of animal care approval: The permit holder and his/her nominee(s) are authorized to either perform biopsies on, or collect and euthanize, a maximum of 3 individuals from up to 9 different species (maximum of 15 birds total per year) from the following list: Semipalmated Sandpiper, White-rumped Sandpiper, Stilt Sandpiper, Red-necked Phalarope, Wilson's Phalarope, American Avocet, Willet, Killdeer, and/or Dunlin. Birds may be collected from mist-nets or drop nets or captured using net guns. Biopsies may be conducted to sample liver and adipose tissue by use of a topical anaesthetic followed by making an incision which will be closed and the bird released after recovery. If required, some birds may be immediately euthanized by cervical dislocation or injection of T-61. Morphometric measurements of euthanized birds may be taken as well as blood, liver and adipose tissue samples. Collected tissues may be analyzed and used in cell culture experiments which will be carried out at the University of Saskatchewan.

Valid in 2017: The permit holder is also authorized to capture up to 20 Sanderlings. Capture must take place during spring migration utilizing mist nets or controlled drop nets. These birds will be transported to the Facility for Applied Avian Research at the University of Saskatchewan where the following activities are approved: screening for fat loads using non-invasive Magnetic Resonance Imaging and, taking of weekly weight measurements and blood sampling. Specimens may be transferred to Dr. Chris Guglielmo at University of Western if Dr. Guglielmo under proper provincial import and export permits as well as authorization from the Canadian Wildlife Service in Ontario Region.

All activities conducted under this permit will be carried out in accordance with animal care protocol #20120021. No activities authorized here are in addition to those authorized under Scientific Banding Permit #10268L.

All activities outside of those conducted at the University of Saskatchewan will take place at Chaplin Lake, Last Mountain Lake, Big Quill Lake, Little Quill Lake, and Clavet all located in the province of Saskatchewan.

2. Kristin Bianchini, Margaret Eng, Ella Lunny, Kirsty Gurney and Jessica Howell are nominees and are authorized to act on behalf of the permit holder. All individuals conducting work under this permit must have a signed copy of this permit on their person while working in the field and/or lab. Any changes to nominees during the duration of the permit must be reported to this office immediately by written communication.



- 3. The permit holder must provide Environment Canada with a detailed written report of all activities on or before the annual report date indicated above. In order to extend the permit for another year without reapplication, a request to do so must be submitted with the aforementioned report.**

Any changes to the nominee list along with up-to-date animal care submission and approval documents (where applicable) should be submitted at the same time if feasible or, at the latest, by one month prior to proceeding with permitted activities.

General Conditions

1. By signing this document you bind yourself to respect all terms and conditions of this permit.
2. Anyone carrying out work under the authority of this permit must have a signed copy of this permit while working in the field and/or lab and it shall be shown on request by a Game Officer or RCMP Officer.
3. This permit is NOT VALID in any Federal or Provincial Game Preserve or Bird Sanctuary or National or Provincial Park, National Wildlife Area, Wildlife Management Unit or other protected areas without authorization.
4. The issuance of this permit does not exempt the permit holder from compliance with all relevant Canadian, Provincial and Territorial Laws, and Regulations otherwise applicable nor does it exempt the permit holder from complying with applicable jurisdictional bylaws.
5. Animal care approval (where applicable) must be kept up-to-date in order for this permit to remain valid.
6. No Migratory Birds, eggs or parts thereof taken under the authority of this permit shall be killed for consumption, sold, traded or bartered except as provided by the terms of this permit.
7. It is recommended that the permit holder advise local RCMP and Conservation Officers of his/her field activities.
8. Unless otherwise stated, this permit does not authorize the possession, killing, taking, capturing and banding, or disturbing of species listed on Schedule 1 of the Species at Risk Act as threatened, endangered or extirpated.

I declare that I have read and understand this Permit, including all the conditions attached.

Appendix C

University of Western Ontario, Animal Use and Care Committee protocol approval letter. Protocol 2010-020 issued to Dr. Christopher Guglielmo.

Chris Guglielmo	
From:	[REDACTED]
Sent:	May-12-14 3:29 PM
To:	[REDACTED]
Cc:	[REDACTED]
Subject:	eSirius Notification - New Animal Use Protocol is APPROVED2010-216::5
[REDACTED]	
AUP Number:	2010-216
PI Name:	Guglielmo, Christopher
AUP Title:	Energetics, Fuel Use, Water Balance And Immunocompetence During Exercise In Migrating Birds
Approval Date:	05/12/2014
Official Notice of Animal Use Subcommittee (AUS) Approval: Your new Animal Use Protocol (AUP) entitled "Energetics, Fuel Use, Water Balance And Immunocompetence During Exercise In Migrating Birds" has been APPROVED by the Animal Use Subcommittee of the University Council on Animal Care. This approval, although valid for four years, and is subject to annual Protocol Renewal.2010-216::5	
<ol style="list-style-type: none">1. This AUP number must be indicated when ordering animals for this project.2. Animals for other projects may not be ordered under this AUP number.3. Purchases of animals other than through this system must be cleared through the ACVS office. Health certificates will be required.	
The holder of this Animal Use Protocol is responsible to ensure that all associated safety components (biosafety, radiation safety, general laboratory safety) comply with institutional safety standards and have received all necessary approvals. Please consult directly with your institutional safety officers.	
Submitted by: Copeman, Laura on behalf of the Animal Use Subcommittee University Council on Animal Care	
1	

Curriculum Vitae

Name: Kevin G. Young

Post-secondary Education and Degrees: Trent University
Peterborough, Ontario, Canada
2016 BSc.H.

Recognitions and Awards: Dean's Honour Role – Trent University
2013-2016

Travel Grant – Northern Scientific Training Program
2015 - \$3,500

Queen Elizabeth II Graduate Scholarship
2017-2018 - \$15,000

Conference Presentations: Young KG, CMG Vanderboor, TRH Regnault, CG Guglielmo (2019). The role of n-3 PUFA in migrant muscle: a comparative test of the natural doping hypothesis in vitro. *Comparative Physiology & Biochemistry Workshop*, Keene Ontario. Oral Presentation.

Young KG, CMG Vanderboor, TRH Regnault, CG Guglielmo (2018). Characterization of isolated muscle progenitor cells of Yellow-rumped warblers (*Setophaga coronata*) and Sanderlings (*Calidris alba*). *International Ornithological Congress*, Vancouver British Columbia. Poster Presentation.

Young KG, CMG Vanderboor, TRH Regnault, CG Guglielmo (2018). Method for the Isolation and Growth of Muscle Progenitor Cells of Yellow-rumped warblers (*Setophaga coronata*). *The Society for Integrative & Comparative Biology Annual Meeting*, San Francisco California. Poster Presentation.

Young KG, TRH Regnault, CG Guglielmo (2017). Silencing Cytosolic Fatty Acid Transport in a Migratory Bird. *Comparative Physiology & Biochemistry Workshop*, Keene Ontario. Oral Presentation.

Young KG, LV Kennedy, PA Smith, E Nol (2016). Does Camera Presence Affect Arctic-breeding Shorebird Nest Survival? *Ontario Biology Day*, Toronto Ontario. Oral Presentation.

**Related Work
Experience**

Teaching Assistant - Techniques in Physiology and Biochemistry
BIOL 3625
The University of Western Ontario
2019

Teaching Assistant – Animal Behaviour
BIOL 3436
The University of Western Ontario
2016-2017

Teaching Assistant – Analysis and Interpretation of Biological
Data
BIOL 2244
The University of Western Ontario
2017

Teaching Assistant – Scientific Methods in Biology
BIOL 2290
The University of Western Ontario
2016

Academic Assistant – Foundations of Cellular and Molecular
Biology
BIOL 1030
Trent University
2016

Academic Assistant – Microbiology
BIOL 3250
Trent University
2015